Functional constraints of *wtf* killer meiotic drivers

Authors:
Ananya Nidamangala Srinivasa[1,2], Samuel Campbell[1], Shriram Venkatesan[1], Nicole L. Nuckolls[1], Jeffrey J. Lange[1], Randal Halfmann[1,3], SaraH Zanders*[1,2]

[1]Stowers Institute for Medical Research, Kansas City, Missouri, United States of America
[2]Department of Cell Biology and Physiology, University of Kansas Medical Center, Kansas City, Kansas, United States of America
[3]Department of Biochemistry and Molecular Biology, University of Kansas Medical Center, Kansas City, Kansas, United States of America

*Corresponding Author
Email: sez@stowers.org

Abstract

Killer meiotic drivers are selfish DNA loci that sabotage the gametes that do not inherit them from a driver+/driver- heterozygote. These drivers often employ toxic proteins that target essential cellular functions to cause the destruction of driver- gametes. Identifying the mechanisms of drivers can expand our understanding of infertility and reveal novel insights about the cellular functions targeted by drivers. In this work, we explore the molecular mechanisms underlying the *wtf* family of killer meiotic drivers found in fission yeasts. Each *wtf* killer acts using a toxic Wtf^{poison} protein that can be neutralized by a corresponding $Wtf^{antidote}$ protein. The *wtf* genes are rapidly evolving and extremely diverse. Here we found that self-assembly of Wtf^{poison} proteins is broadly conserved and associated with toxicity across the gene family, despite minimal amino acid conservation. In addition, we found the toxicity of Wtf^{poison} assemblies can be modulated by protein tags designed to increase or decrease the extent of the Wtf^{poison} assembly, implicating assembly size in toxicity. We also identified a conserved, critical role for the specific co-assembly of the Wtf^{poison} and $Wtf^{antidote}$ proteins in promoting effective neutralization of Wtf^{poison} toxicity. Finally, we engineered *wtf* alleles that encode toxic Wtf^{poison} proteins that are not effectively neutralized by their corresponding $Wtf^{antidote}$ proteins. The possibility of such self-destructive alleles reveals functional constraints on *wtf* evolution and suggests similar alleles could be cryptic contributors to infertility in fission yeast populations. As rapidly evolving killer meiotic drivers are widespread in eukaryotes, analogous self-killing drive alleles could contribute to sporadic infertility in many lineages.

Introduction

Genomes often contain selfish DNA sequences that persist by promoting their own propagation into the next generation without providing an overall fitness benefit to the organism [1,2]. Killer meiotic drivers are one class of selfish sequences that act by preferentially destroying gametes that do not inherit the driver from a heterozygote [3]. This gamete destruction leads to biased, or sometimes, complete transmission of the driver+ genotype from driver+/driver- heterozygotes.

Killer meiotic drive systems generally decrease the fitness of the organism carrying the driver, both through their killing activities and through indirect mechanisms [4].

Distinct killer meiotic drive systems have repeatedly evolved in eukaryotes and drivers found in distinct species are generally not homologous [3,5–12]. Despite this, killer meiotic drivers fall into a limited number of mechanistic classes with shared themes [3,13,14]. Additionally, unrelated killer meiotic drivers have recurrently exploited conserved facets of cell physiology. This has enabled study of the killing and/or rescue activities of drive proteins outside of their endogenous species [5,11,15,16]. Overall, drivers represent unique tools that can be used to discover novel, unexpected insights into the exploited biological processes.

The *wtf* genes are a family of extremely diverse, rapidly evolving killer meiotic drivers found in multiple copies in most *Schizosaccharomyces* (fission yeast) species [17–22]. The *wtf* driver genes each produce a Wtf^{poison} and a $Wtf^{antidote}$ protein using distinct transcripts with overlapping coding sequences (Fig 1A) [15,17,23]. The amino acid sequences of the two proteins are largely identical, except the $Wtf^{antidote}$ proteins have an additional N-terminal domain of about 45 amino acids not found in the Wtf^{poison} (Fig 1A). All four developing spores (products of meiosis) are exposed to the Wtf^{poison}, but spores that inherit a compatible $Wtf^{antidote}$ can neutralize the poison and survive [22].

Little is known about the mechanism of toxicity of the Wtf^{poison} proteins. The general mechanism used by $Wtf^{antidote}$ proteins is better understood. The antidote-specific N-terminal domain is the most conserved region and includes targeting motifs (PY motifs) that are recognized by Rsp5/NEDD4 ubiquitin ligases which route the protein through the trans Golgi network to endosomes and, ultimately, to the vacuole (fungal lysosome; Fig 1B) [15,24]. When both proteins are present, the $Wtf^{antidote}$ co-assembles with the Wtf^{poison}, and the $Wtf^{antidote}$ thereby traffics the Wtf^{poison} to the vacuole [15,24]. This mechanism is similar to a non-homologous drive system recently described in rice, where an antidote protein rescues the gametes that inherit the drive locus from a toxic poison protein by co-trafficking the poison to the autophagosome [5].

In general, the poison protein encoded by one *wtf* gene is not compatible with (i.e., neutralized by) the antidotes of widely diverged *wtf* genes [17,19,25]. However, Wtf^{poison} proteins can be neutralized by $Wtf^{antidote}$ proteins encoded at different loci if the sequences are identical or highly similar (outside of the antidote-specific N-terminal domain; Fig 1A) [17,22,24,26]. Although the

examples are limited, similarity at the C-termini of the Wtf poison and antidote proteins may be particularly important for compatibility [15,25,26]. For example, the *wtf18-2* allele encodes an antidote protein that neutralizes the poison produced by the *wtf13* driver. The Wtf18-2^{antidote} and Wtf13^{antidote} proteins are highly similar overall (82% amino acid identity) and identical at their C-termini. Interestingly, the antidote encoded by the reference allele of *wtf18* is not identical to Wtf13^{poison} at the C-terminus and does not neutralize it. In addition, swapping one amino acid for two different amino acids in the C-terminus of Wtf18-2^{antidote} (D366NN mutation) to make it more like the reference Wtf18^{antidote} abolishes the protein's ability to neutralize Wtf13^{poison} [26]. Still, the rules governing poison and antidote compatibility are largely unknown.

While it is clear that a functional *wtf* driver kills about half the spores produced by *wtf*+/*wtf*- heterozygotes, the full impacts of *wtf* gene evolution on the fitness of populations is not clear. Because the *wtf* genes encode the poison and antidote proteins on overlapping coding sequences (Fig 1A), novel poisons can emerge simultaneously with their corresponding antidotes via mutation. This has been observed with a limited number of engineered *wtf* alleles, and one can observe evidence of this divergence in the diversity of extant *wtf* alleles in natural populations [15,19–21,26]. The natural alleles, however, represent a selected population and thus provide a biased sample of the novel *wtf* alleles generated by mutation and recombination. Novel alleles that generate functional drivers are predicted to be favored by the self-selection enabled by drive and be over-represented in natural populations. Conversely, alleles that generate a toxic poison without a compatible antidote would be expected to be under-represented in natural populations due to infertility caused by self-killing.

Major questions remain about the mechanism(s) of Wtf^{poison} toxicity and about the rules of Wtf^{poison} and Wtf^{antidote} compatibility. Our working model is that the toxicity of Wtf^{poison} proteins is tied to their self-assembly [15]. This assembly, however, has only been conclusively demonstrated for the Wtf4 proteins, encoded by the *wtf4* gene from the isolate of *S. pombe* known as *kambucha*. For Wtf^{antidote} function, a working model is that a similar homotypic assembly with the Wtf^{poison} is required to establish a physical connection between the proteins so that the poison is shuttled to the vacuole along with a ubiquitinated antidote [15,24]. The ubiquitination and trafficking of the Wtf antidotes to the vacuole has been demonstrated to be conserved between widely diverged Wtf^{antidote} proteins [19,24]. However, it is not clear if antidote co-assembly with a poison has a functional role in poison neutralization, or if it merely provides a physical link between the proteins to facilitate co-trafficking. It is also unclear if changes in the

100 coding sequence shared by the poison and antidote proteins of a given *wtf* can generate an
101 incompatible set of proteins, or if poisons will always be neutralized by sequence-matched
102 antidotes.
103
104 To test these models and to better understand the amino acid sequences that support the Wtf
105 protein functions, we analyzed a panel of natural and engineered Wtf proteins. We found that
106 both well-conserved and poorly-conserved amino acid sequences can contribute to protein
107 function. Our analyses revealed broad conservation of Wtf^{poison} self-assembly and suggest that
108 assembly size can affect Wtf^{poison} toxicity, analogous to several other self-assembling toxic
109 proteins [27–29]. This strongly implicates self-assembly as a critical parameter in Wtf^{poison}
110 toxicity. In addition, we found that specific co-assembly with the $Wtf^{antidote}$ is required for efficient
111 Wtf^{poison} neutralization via trafficking to the vacuole. Finally, our analyses identified multiple *wtf*
112 alleles that generate poison proteins that are not efficiently neutralized by their corresponding
113 antidotes. Such alleles are self-destructive and could contribute to sporadic infertility. This work
114 refines our understanding of the functional constraints of Wtf proteins, with important
115 evolutionary implications. More broadly, our observations offer insight into how functional
116 conservation can be maintained despite extreme amino acid sequence divergence and extends
117 our understanding of the limits of protein assembly trafficking mechanisms.
118
119 **Results**
120
121 **Wtf^{poison} protein self-assembly is broadly conserved.**
122 To test the models of Wtf protein functions and to understand how these functions could be
123 supported by extremely diverse protein sequences (e.g., <20% amino acid identity), we
124 generated a large panel of *wtf* variants that represent over 100 million years of divergence [19].
125 We reasoned that functionally important features of the proteins would be conserved in
126 functional variants (i.e. toxic Wtf^{poison} proteins), despite minimal amino acid conservation. Twelve
127 of the variants we assayed are wild-type or mutant alleles of *wtf* genes found in *S. octosporus*,
128 *S. osmophilus* or *S. cryophilus* (S1 Fig A-E). One of these genes, *S. octosporus wtf25*, has been
129 previously characterized and found to encode a functional meiotic driver in its endogenous
130 species ([19]; S1 Table). Four additional genes (*S. cryophilus wtf1*, *S. osmophilus wtf41*, and *S.*
131 *octosporus wtf61*) have been shown to encode functional Wtf^{poison} and $Wtf^{antidote}$ proteins in an
132 ectopic *Saccharomyces cerevisiae* assay system ([19]; S1 Table). The *S. cerevisiae* system
133 used to study Wtf proteins is well established and reflects phenotypes observed in the

134 endogenous fission yeast species [15,19,24]. Finally, we assayed a panel of new mutant alleles
135 of the previously characterized *wtf4* gene from the *S. kambucha* isolate of *S. pombe* [15,22,23]
136 (Fig 1 D).
137
138 Our initial model, based on Wtf4^{poison}, was that Wtf^{poison} toxicity is linked to the ability of a Wtf^{poison}
139 to self-assemble [15]. To test this idea, we assayed if other functional Wtf^{poison} proteins besides
140 wild-type Wtf4^{poison} also self-assemble. To do this, we used the Distributed Amphifluoric FRET
141 (DAmFRET) approach, in which proteins are tagged with the photoconvertible mEos3.1
142 fluorophore (referred to as mEos hereafter) and expressed in *S. cerevisiae*. A uniform fraction of
143 the green mEos population is photoconverted to its red form, and protein-protein interactions
144 are then detected as FRET (Fluorescence Resonance Energy Transfer) between the green and
145 red fluorophores within single cells. Monomeric mEos exhibits negligible FRET and is used as a
146 negative control (Fig 2A, B) [15,30].
147
148 We first tagged four toxic (*S. cryophilus* Wtf1^{poison}, *S. osmophilus* Wtf41^{poison}, and *S. octosporus*
149 Wtf25^{poison} and Wtf61^{poison}) and one non-toxic (*S. osmophilus* Wtf19^{poison}) Wtf^{poison} protein at the
150 C-terminus with mEos. The tagged proteins retained their toxic/non-toxic phenotypes when
151 expressed in *S. cerevisiae* using a galactose-inducible expression system (Fig 2C) [19]. The
152 assayed proteins all share less than 20% amino acid identity with Wtf4^{poison}, which we use as a
153 positive control (S1 Fig B). We found that all five newly tested Wtf^{poison}-mEos proteins, including
154 the nontoxic Wtf19^{poison}-mEos, exhibited self-assembly (Fig 2B). It is important to note, however,
155 that the data reported for Wtf25^{poison}-mEos are limited and we could not reliably assay that
156 protein via DAmFRET. This is because only living cells are considered in DAmFRET and cells
157 expressing Wtf25^{poison}-mEos generally die shortly after the fluorescent protein can be detected
158 (e.g. they die faster than cells expressing Wtf4^{poison}).
159
160 We also assayed DAmFRET in partial deletion alleles of *wtf4^{poison}-mEos* (S2 Fig, S3 Fig). Some
161 of these alleles are described in more detail below, but for this section we focused on exploring
162 the potential connection between assembly and toxicity. The two toxic mutant Wtf4^{poison} proteins
163 tested, Wtf4-ex5Δ^{poison}-mEos (S2 Fig A, D-F) and Wtf4Δ$^{20\text{-}poison}$-mEos (S3 Fig A-E) both
164 exhibited self-assembly. Of these two proteins, Wtf4Δ$^{20\text{-}poison}$-mEos is more like wild-type
165 Wtf4^{poison}-mEos, in both toxicity and degree of assembly (S2 Fig D-F; S3 Fig B-E). Most non-
166 toxic Wtf4 mutant proteins (Wtf4-TMD1Δ^{poison}-mEos, Wtf4-ex3Δ^{poison}-mEos, Wtf4-ex4Δ^{poison}-
167 mEos, Wtf4-ex6Δ^{poison}-mEos and Wtf4-consΔ^{poison}-mEos) exhibited reduced assembly compared

168 to the wild-type (S2 Fig A-E, S3 Fig A-D). We did, however, find one exceptional mutant protein,
169 Wtf4Δ$^{10\text{-poison}}$-mEos. This protein was not toxic but showed similar assembly to the wild-type
170 protein (S3 Fig A-D). We could not reliably assay the assembly of some alleles (Wtf4-
171 TMD2Δ^{poison}-mEos, Wtf4-TMD6Δ^{poison}-mEos and Wtf4-ex2Δ^{poison}-mEos) due to low fluorescence
172 signal (S2 Fig A-B, S6 Fig B).
173
174 These results show that Wtf^{poison} self-assembly is broadly conserved (over 100 million years)
175 and can be supported by a wide range of amino acid sequences (e.g., proteins sharing <20%
176 amino acid identity, S1 Fig B). Given the broad conservation of self-assembly, that all the toxic
177 alleles exhibited assembly, and that mutant alleles with reduced toxicity also exhibited reduced
178 assembly, our results strongly support an association between self-assembly and toxicity.
179 Importantly, our results also demonstrate that self-assembly alone is insufficient for Wtf^{poison}
180 toxicity, as we found several Wtf^{poison} proteins (Wtf19-mEos and Wtf4Δ$^{10\text{-poison}}$-mEos) that
181 assemble but are not toxic.
182
183 **Deletion alleles demonstrate that both conserved and non-conserved regions contribute**
184 **to Wtf4^{poison} self-assembly and toxicity.**
185 Our deletion mutants in *wtf4^{poison}* encompass both non-conserved and conserved sequences
186 allowing us to test the functional importance of both sequence types (Fig 1; [19-21]). Within *S.*
187 *pombe* Wtf proteins, there is one well conserved 29 base pair segment found at the beginning of
188 exon 3 (Fig 1B; [20]). The Wtf4-consΔ^{poison}-mEos protein lacks this domain and has disrupted
189 self-assembly and is non-toxic, indicating the conserved sequence has a functional role in both
190 Wtf4^{poison} assembly and toxicity (S2 Fig C-E).
191
192 We similarly found that several regions that are poorly conserved in Wtf proteins are functionally
193 important in Wtf4^{poison}. For example, exon 4 is not conserved within functional *wtf* genes, even
194 within *S. pombe* [19, 20, 25]. Still, our results demonstrate exon 4 is functionally important in
195 *wtf4* as the Wtf4-ex4Δ^{poison}-mEos protein has disrupted self-assembly and is not toxic (S2 FigA,
196 D-E). An additional variable feature of *wtf* genes is the number of predicted transmembrane
197 domains, which varies between four and eight within functional Wtf proteins (S5 Table, [80]).
198 The *wtf4* gene has 6 predicted transmembrane domains and we assayed individual deletions of
199 three (Wtf4-TMD1Δ^{poison}-mEos, Wtf4-TMD2Δ^{poison}-mEos and Wtf4-TMD6Δ^{poison}-mEos). All three
200 transmembrane deletions disrupted toxicity, indicating they are also functionally important (S2
201 Fig B, D-E).

202

203 An additional set of deletion mutants we queried in a poorly conserved region followed up on an
204 observation by Hu et al in one of the inaugural papers describing *wtf* drivers [17]. In that work,
205 Hu et al described 10 amino acid C-terminal truncations of two *wtf* genes known as *cw9* and
206 *cw27*. These mutant alleles both exhibited disrupted Wtf^{poison}, but not $Wtf^{antidote}$ activity,
207 implicating the C-terminus in Wtf^{poison} function. These proteins share 62% amino acid identity in
208 the C-terminal exon 6 with each other and, at most, 70% with Wtf4. We tested if a similar 10
209 amino acid truncation of *wtf4* would specifically disrupt $Wtf4^{poison}$ activity. This mutation gave us
210 the exceptional *wtf4-Δ*^{10} allele described above that encodes a non-toxic $Wtf4\Delta^{10\text{-poison}}$, that
211 surprisingly exhibits wild-type self-assembly (S3 Fig A-D). To expand our analyses beyond *wtf4*,
212 we also made 10 amino acid C-terminal truncations of *S. cryophilus* Wtf1*, S. osmophilus* Wtf41*,*
213 *S. octosporus* Wtf61 and Wtf25 poison. These proteins are all significantly smaller than Wtf4
214 (S1 Fig C). Surprisingly, we found that these additional truncated proteins all retained toxicity
215 (S3 Fig F-G) indicating the C-termini are not universally important for Wtf^{poison} toxicity.
216

217 We extended our deletion analyses of the C-terminus of Wtf4 poison and were surprised to find
218 that deleting ten more amino acids than the ten missing in the non-toxic $Wtf4\Delta^{10\text{-poison}}$ protein
219 restored toxicity. Specifically, the $Wtf4\Delta^{20\text{-poison}}$ protein exhibited robust self-assembly and near
220 wild-type levels of toxicity (S3 Fig A-D). A larger deletion of 29 amino acids, $Wtf4ex4\Delta^{poison}$,
221 showed reduced self-assembly and was not toxic (S3 Fig A-D).
222

223 Together, our results show that even non-conserved sequences can have context-dependent
224 importance within a Wtf^{poison} protein. Specifically, a feature (e.g. the residues encoded in exon 4,
225 or the last 10 amino acids of $Wtf4^{poison}$) can be functionally important in one Wtf^{poison} protein, but
226 be dispensable in another. This, combined with the lack of conservation within Wtf proteins,
227 suggests that the contextually important amino acids (like the last 10 of $Wtf4^{poison}$) do not have a
228 specific function, but can rather contribute to the overall properties of the protein that can be
229 complemented by changes elsewhere in the protein.
230

231 **Intracellular localization of mutant Wtf^{poison} proteins is correlated with toxicity.**
232 We identified self-assembly as one feature shared by functional Wtf^{poison} proteins and suspected
233 that intracellular localization could be another, since we previously found that the toxic *S.*
234 *octosporus* $Wtf25^{poison}$-mCherry exhibited similar localization to that of toxic $Wtf4^{poison}$ [19].
235 Specifically, both poisons show small puncta broadly distributed in the cytoplasm of *S.*

236 *cerevisiae* cells, with minor localization to what appears to be the endoplasmic reticulum (ER;
237 [15,19]). All functionally confirmed Wtf driver proteins have multiple predicted transmembrane
238 domains (S5 Table) and hence, this localization pattern may reflect the poison being trafficked
239 from the ER through the secretory pathway, through the Golgi and trans-Golgi network [24].
240
241 To test the hypothesis that a link exists between the intracellular distribution and toxicity of
242 Wtf^{poison} proteins, we imaged the wild-type Wtf^{poison}-mEos proteins described above in *S.*
243 *cerevisiae* cells. The localization of the *S. octosporus* Wtf25^{poison}-mEos was similar to the
244 previously described Wtf25^{poison}-mCherry described above (Fig 2D). The additional toxic Wtf^{poison}
245 proteins from *S. octosporus*, *S. osmophilus* and *S. cryophilus*, also exhibited dispersed puncta,
246 like the toxic Wtf4^{poison}-mEos control cells (Fig 2D). The nontoxic *S. osmophilus* Wtf19^{poison}-
247 mEos, however, showed a distinct localization pattern with strong signal enrichment in what
248 appears to be the ER (Fig 2D). These data are consistent with our hypothesis that there is a link
249 between intracellular distribution and toxicity with toxic Wtf^{poison} proteins exhibiting distributed
250 puncta.
251
252 To further test our hypothesis, we also assayed the localization of the mutant Wtf4^{poison} proteins
253 mentioned above (S2 Fig F, S3 Fig E). The most toxic mutant protein, Wtf4Δ^{20poison}-mEos,
254 localized in distributed puncta like wild-type (S3 Fig A-C, E). The less toxic Wtf4-ex5Δ^{poison}-
255 mEos protein also formed some distributed puncta, but also exhibited more ER-like localization
256 than wild-type (S2 Fig A, D, F). Most of the non-toxic mutant Wtf4^{poison} proteins (Wtf4-
257 TMD1Δ^{poison}-mEos, Wtf4-TMD2Δ^{poison}-mEos, Wtf4-ex2Δ^{poison}-mEos, Wtf4-ex3Δ^{poison}-mEos, Wtf4-
258 ex4Δ^{poison}-mEos, and Wtf4-consΔ^{poison}-mEos) were less dispersed and exhibited a largely ER-
259 like localization, similar to the non-toxic *S. osmophilus* Wtf19^{poison}-mEos (S2 Fig A-D, F, Fig 2C-
260 D). One additional non-toxic mutant, Wtf4-TMD6Δ^{poison}-mEos, localized to the vacuole,
261 reminiscent of Wtf^{antidote} protein localization (S2 Fig B, D, F). The non-toxic Wtf4-ex6Δ^{poison}-mEos
262 had a unique localization pattern that combined a diffuse distributed signal with some larger
263 protein assemblies (S3 Fig A-C, E). Finally, the non-toxic Wtf4Δ$^{10\text{-}poison}$-mEos localization was
264 indistinguishable from wild-type Wtf4^{poison}-mEos (S3 Fig A-C, E).
265
266 In summary, all the toxic Wtf^{poison} proteins show a distributed puncta localization pattern, like
267 Wtf4^{poison}. All except one non-toxic Wtf^{poison} protein showed a distinct localization pattern from
268 Wtf4^{poison}, most often with enhanced ER-like localization. These results parallel our DAmFRET
269 analyses where all toxic Wtf^{poison} proteins assemble and all the nontoxic proteins, except one,

270 show reduced or lack of assembly. In both cases, the exceptional protein is Wtf4Δ$^{10\text{-poison}}$, which
271 is non-toxic, but shows wild-type assembly and localization in cells. Despite the exception, our
272 results show that Wtf^{poison} self-assembly (assayed by DAmFRET) combined with cellular
273 localization patterns are good predictors of Wtf^{poison} protein toxicity (Fig 7A).
274
275 **Altering assembly properties of Wtf^{poison} proteins affects toxicity.**
276 To further test the model that the toxicity of Wtf^{poison} proteins is tied to their self-assembly, we
277 sought to alter the assembly properties of Wtf4^{poison} using tags. We first aimed to increase the
278 overall size of the Wtf4^{poison} assemblies. To do this, we employed a construct that contains the
279 human ferritin heavy chain protein (FTH1) fused to a nanobody that recognizes mEos
280 (mEosNB) (Kimbrough et al. forthcoming). The FTH1 domain self assembles to form a 24-mer
281 core and can form supramolecular clusters when fused to self-assembling proteins [31,32]. In
282 our assay, we expressed Wtf4^{poison}-mEos from a galactose inducible promoter and the mEosNB-
283 FTH1 from a doxycycline repressible promoter (Fig 3A, B). As expected, we found that
284 Wtf4^{poison}-mEos formed fewer and larger puncta inside cells in the presence of mEosNB-FTH1,
285 consistent with the mEosNB-FTH1 complexes bringing Wtf^{poison}-mEos assemblies into
286 supramolecular clusters (i.e., -Dox panels, Fig 3C). Expression of the mEosNB-FTH1 alone had
287 no effect on yeast growth (Fig 3D, panel (i)). While expression of the Wtf4^{poison}-mEos alone was
288 toxic, co-expression of the mEosNB-FTH1 and Wtf4^{poison}-mEos markedly suppressed the toxicity
289 of the Wtf4^{poison}-mEos (Fig 3D, compare panel (ii) to panel (iii)). We also observed the same
290 suppression of toxicity with four additional toxic Wtf^{poison}-mEos proteins in the presence of the
291 mEosNB-FTH1, indicating the effect was not specific to Wtf4^{poison} (Fig 3C-D). These results
292 indicate that these supramolecular Wtf^{poison} assemblies are non-toxic. This effect could be due to
293 altered intracellular localization and/or the reduced exposed surface area of the Wtf^{poison}
294 assemblies.
295
296 We next attempted to increase the solubility Wtf4^{poison} assemblies using a modified N-terminal
297 domain (NT*) tag derived from spidroins, a principal component of spider silk [33]. The NT* tag
298 can decrease protein aggregation, which is the role of the native domain in spiders [34–38]. We
299 added NT* to the N-terminus of the Wtf4^{poison}-mEos to generate NT*-Wtf4^{poison}-mEos (Fig 4A).
300 We found that this protein had a novel combination of assembly and localization not
301 represented in any of our other alleles. Specifically, the NT*-Wtf4^{poison}-mEos protein showed
302 less self-assembly than Wtf4^{poison}-mEos (Fig 4C), but the NT* tag did not visibly alter the
303 localization of the protein within cells (Fig 4E). Interestingly, the NT*-Wtf4^{poison}-mEos protein

304 showed increased toxicity in cells (Fig 4B). To test if the effects of the NT* tag were specific to
305 Wtf4^{poison} or more general, we also tagged *S. octosporus* Wtf25^{poison} with NT* to generate NT*-
306 Wtf25^{poison}-mEos (S4 Fig A). As with NT*-Wtf4^{poison}-mEos, we observed unaltered localization
307 and increased toxicity of the NT*-Wtf25^{poison}-mEos protein, relative to wild-type Wtf25^{poison}-mEos
308 (S4 Fig B, D). We could not, however, quantify NT*-Wtf25^{poison}-mEos assembly by DAmFRET
309 as the high toxicity prevented us from obtaining sufficient viable cells with mEos fluorescence
310 (S6 Fig E).
311
312 We also assayed how another solubility tag, the *E. coli* Maltose Binding Protein (MBP), affected
313 Wtf^{poison} toxicity [39–41]. The MBP-tagged Wtf4^{poison} (MBP-Wtf4^{poison}-mEos) had the same
314 phenotype as the NT*-tagged Wtf4^{poison} protein: decreased assembly, increased toxicity,
315 unaltered localization, relative to the wild-type protein (S5 Fig). The phenotype of the MBP-
316 tagged Wtf25^{poison} (MBP-Wtf25^{poison}-mEos) however, did not mirror that of the NT*-tagged
317 protein. Instead, we found that the MBP-Wtf25^{poison}-mEos protein showed reduced, but still high
318 toxicity. The MBP-Wtf25^{poison}-mEos protein also showed an altered, stronger endoplasmic
319 reticulum-like localization, as compared to the wild-type protein (S5 Fig A-C). This protein thus
320 adds to those described above in which we see more ER-like localization associated with
321 reduced Wtf^{poison} toxicity. The MBP-Wtf25^{poison}-mEos protein did exhibit self-assembly, but we
322 could not compare it the wild-type protein as high toxicity limited the viable cells we could assay
323 via DAmFRET (S5 Fig D, S6 Fig F).
324
325 The bulk of our experiments are consistent with a model where the assembly properties and the
326 distribution of Wtf^{poison} proteins within cells affects toxicity, with distributed, punctate assemblies
327 exhibiting more toxicity. Increasing Wtf^{poison} solubility (while maintaining assembly), increases
328 toxicity, unless localization is disrupted. Forcing Wtf^{poison} proteins into large, localized
329 assemblies, suppresses toxicity. The non-toxic Wtf4Δ$^{10\text{-}poison}$ protein that forms distributed
330 assemblies, however, undermines this simple model or at least indicates that there are
331 additional unidentified features that are essential for toxicity.
332
333 An additional possibility that we considered was that the expression levels of the Wtf^{poison}
334 proteins likely contributes to the phenotypes we observed, despite expressing all alleles from a
335 common vector backbone using a common promoter. To assay expression levels, we quantified
336 fluorescence of the mEos tags shared by all alleles. We did not use western blots as that
337 approach is challenging to apply to Wtf^{poison} proteins as they are toxic and highly hydrophobic

338 [15,23]. Instead, we looked at the acceptor (red form of mEos) fluorescence in live cells
339 analyzed in the DAmFRET experiments (S6 Fig; Data from Fig 2B, S2 Fig E, S3 Fig D, Fig 4C).
340 As expected, based on other studies [42–45], we observed significant fluorescent protein signal
341 heterogeneity within cells expressing the monomer mEos control and each Wtf^{poison} protein
342 tested (S6 Fig). We did not, however, find increased fluorescent signal in cells expressing the
343 most toxic proteins (as determined by growth assays). On the contrary, we tended to observe
344 less signal in the cells expressing the most toxic proteins (e.g., Wtf4^{poison} and NT*-Wtf4^{poison}).
345 These data support a model in which cells expressing the higher levels of toxic proteins are
346 more likely to be removed by death and are not quantified. As mentioned above, however, we
347 also observed low signal in the cells expressing the non-toxic Wtf4-ex2Δ^{poison}, Wtf4-TMD2Δ^{poison},
348 and Wtf4-TMD6Δ^{poison} alleles (S6 Fig). The low levels of Wtf4-TMD6Δ^{poison} could be due to its
349 degradation in the vacuole (S2 Fig F). For the other two alleles, it is formally possible the low
350 levels of these proteins in cells could contribute to their lack of toxicity.
351
352 **Limited modularity of the Wtf^{antidote}-specific domain.**
353 We next wanted to test which protein features affect Wtf4^{antidote} function (Fig 1A-B). As described
354 above, the Wtf4^{antidote} shares the resides encoded by exons 2-4 with the Wtf4^{poison} but has an
355 additional N-terminal domain encoded by exon 1. We hypothesized that the amino acids
356 encoded by exon 1 would be insufficient for function and that exons 2-6 would be required for
357 protein self-assembly as they comprise the Wtf4^{poison} protein, which self-assembles [15]. As
358 expected, we found that a protein consisting of only the exon 1-encoded residues linked to a
359 mEos tag (Wtf4 Exon1-mEos) could not self-assemble (S7 Fig A-B). The Wtf4 Exon1-mEos
360 protein was also not trafficked to the vacuole, despite this protein harboring two PY motifs that
361 promote ubiquitin-mediated trafficking of wild-type Wtf^{antidote} proteins [24] (S7 Fig E). Finally, the
362 Wtf4 Exon1-mEos protein could not rescue Wtf4^{poison} toxicity, which parallels recent results
363 using distinct Wtf proteins ((S7 Fig C, F) [24]). These results demonstrate that the antidote-
364 specific domain encoded by *wtf4* exon 1 is insufficient for antidote function.
365
366 To test if the exon 1 encoded domain was modular, we generated two mutants *wtf4^{poison}-ex1*
367 and *wtf4^{poison}-ex1^{int}*. The *wtf4^{poison}-ex1* allele moves the antidote-specific domain moved to the C-
368 terminus of the protein (S7 Fig A). The *wtf4^{poison}-ex1^{int}* allele moved exon 1 a more central region
369 of the protein (beginning of exon 4). This location is between the last two predicted
370 transmembrane domains and is not predicted to disrupt them (Figure 1B). We found that mEos
371 tagged versions of both Wtf4^{poison}-ex1 and Wtf4^{poison}-ex1^{int} proteins were both non-toxic and

372 trafficked to the vacuole, suggesting they retained at least some antidote functionality (S7 Fig D,
373 F). Only the Wtf4^{poison}-ex1, however, could neutralize the toxicity of Wtf4^{poison}-mCherry (S7 Fig D,
374 F). These results demonstrate that the domain encoded by exon 1 is at least partially modular,
375 but that a central location within the polypeptide can disrupt the Wtf^{antidote} protein's ability to
376 neutralize a Wtf^{poison}. We speculate this could be because extensive, continuous, amino acid
377 identity facilitates Wtf^{poison} and Wtf^{antidote} co-assembly.
378
379 **Wtf^{antidote} requires more than physical linkage to effectively traffic Wtf^{poison} to the vacuole**
380 We next wanted to determine if co-assembly serves merely to link Wtf^{poison} and Wtf^{antidote} proteins
381 to allow for co-trafficking, or if co-assembly serves a more nuanced role in neutralizing Wtf^{poison}
382 toxicity. To test this, we generated Wtf^{poison} and Wtf^{antidote} proteins that were physically linked, but
383 not co-assembled, by artificially tethering Wtf^{poison} proteins to diverged Wtf^{antidote} proteins, with
384 which they cannot co-assemble, using a combination of GFP and GFP-binding protein (GBP)
385 tags (Fig 5A, B; S8 Fig A, B).
386
387 We first tested if tethering Wtf4^{poison} to *S. octosporus* Wtf61^{antidote} could neutralize the toxic
388 Wtf4^{poison}. We generated Wtf4^{poison}-GBP-mCherry and Wtf61^{antidote}-GFP proteins and found the
389 tags did not disrupt protein function. Specifically, the Wtf4^{poison}-GBP-mCherry protein was toxic,
390 and could be rescued by Wtf4^{antidote} proteins, including Wtf4^{antidote}-GFP. Similarly, the
391 Wtf61^{antidote}-GFP protein was able to rescue Wtf61^{poison}-mCherry (Fig 5C). However, Wtf61^{antidote}-
392 GFP was not able to efficiently traffic Wtf4^{poison}-GBP-mCherry to the vacuole or neutralize its
393 toxicity (Fig 5C, D). This failure to rescue is not a failure of the GFP-GBP interaction to link the
394 proteins as we found that the Wtf61^{antidote}-GFP and Wtf4^{poison}-GBP-mCherry proteins largely co-
395 localized, which they did not do in the absence of the GBP tag (Fig 5D). Moreover, the
396 localization of the tethered Wtf61^{antidote}-GFP-Wtf4^{poison}-GBP-mCherry changed relative to the
397 individual proteins: the Wtf61^{antidote}-GFP no longer trafficked to the vacuole and Wtf4^{poison}-GBP-
398 mCherry was less distributed in cells. Effective GFP-GBP linkage is the most parsimonious
399 explanation of these observations. To test if our results were generalizable, we also analyzed a
400 widely diverged, independent pair of Wtf proteins (*S. octosporus* Wtf25^{poison} and *S. cryophilus*
401 Wtf1^{antidote}). Our results with this protein pair mirrored those described above suggesting that
402 specific antidote-poison co-assembly generally promotes proper antidote function (S8 Fig).
403
404 Given that the tethered Wtf61^{antidote}-GFP and Wtf4^{poison}-GBP-mCherry were often adjacent to
405 vacuoles and not totally distributed in cells, as occurs when trafficking of Wtf proteins is

406 disrupted [15], we suspected that the vacuolar targeting was still occurring, but blocked at a late
407 step in the process (e.g., vacuole entry). Consistent with this notion, the assemblies often co-
408 localized with the Rnq-1mCardinal protein, which is a prion protein that marks the insoluble
409 protein deposit (IPOD) [46–48] (Fig 5E). This result was surprising to us because with a different
410 expression system (β-estradiol induction) a considerable amount of the Wtf4^{poison}/Wtf4^{antidote} co-
411 assemblies accumulate at the IPOD are not toxic to cells [15]. It is unclear why GFP/GBP
412 mediated assemblies, but not Wtf/Wtf mediated co-assemblies, would be toxic at the IPOD, and
413 we speculate about this in the discussion.
414
415 Beyond the GFP/GBP tethering experiments, we made additional observations suggesting that
416 a specific nature of co-assembly with Wtf^{poison} is required for Wtf^{antidote} function. When
417 characterizing the toxic NT*-Wtf4^{poison} protein (with the NT* domain that increases solubility), we
418 found that this protein was not effectively rescued by wild-type Wtf4^{antidote}-mCherry (Fig 4D).
419 This drastic reduction in rescue (relative to that observed with the wild-type Wtf4^{poison}) is striking
420 given that the colocalization of NT*-Wtf4^{poison}-mEos with Wtf4^{antidote}-mCherry appears only mildly
421 reduced relative to that observed between wild-type Wtf4 proteins (Figure 4E, F). In addition,
422 the localization of the NT*-Wtf4^{poison}-mEos is altered in the presence of Wtf4^{antidote}-mCherry (it
423 becomes less distributed compared to wild type Wtf4 proteins; Fig 4E). These observations
424 suggest the NT*-Wtf4^{poison}-mEos and Wtf4^{antidote}-mCherry proteins interact, but are not efficiently
425 trafficked to the vacuole (Fig 4E). This is analogous to the GFP/GBP linked, but unassembled,
426 Wtf^{poison} and Wtf^{antidote} pairs described above. The effect of the NT* tag on Wtf^{poison}/Wtf^{antidote}
427 compatibility was not, however, universal. We did not observe strong disruption of
428 poison/antidote compatibility caused by the NT* tag on *S. octosporus* Wtf25^{poison} (NT*-Wtf25^{poison}
429 allele, S4 Fig), indicating that factors affecting poison/antidote compatibility can be context
430 dependent.
431
432 Together, our results demonstrate that a physical linkage is insufficient to ensure efficient
433 neutralization of a Wtf^{poison} protein's toxicity by a Wtf^{antidote}. Instead, specific co-assembly of the
434 proteins likely both links compatible Wtf^{poison} and Wtf^{antidote} proteins and facilitates their effective
435 co-trafficking into the vacuole.
436
437 **C-terminal region supports Wtf4^{antdiote} function**
438 As introduced above, Hu et al previously described mutant alleles of two *S. pombe wtf* genes
439 lacking the codons for the last 10 amino acids. Those mutants maintained Wtf^{antidote} activity [17].

440 To test if the C-terminal amino acids were generally dispensable for antidote function, we made
441 *wtf4*^{antidote} truncation alleles. We found that a 10 amino acid truncation of Wtf4, (Wtf4Δ$^{10\text{-antidote}}$-
442 mCherry) was slightly toxic to cells, as compared to the Wtf4^{antidote}-mCherry and empty vector
443 controls (S13 Fig A-B). A 20 amino acid truncation of the , Wtf4Δ$^{20\text{-antidote}}$-mCherry, showed even
444 more toxicity, although it was still considerably less than the toxicity observed with the Wtf4^{poison}-
445 mCherry. A 29 amino acid truncation, Wtf4-ex6Δ^{antidote}-mCherry, exhibited no toxicity (S13 fig A-
446 B). These results suggest that the C-terminal 20 amino acids of Wtf4^{antidote} play a role in limiting
447 the toxicity of the Wtf4^{antidote} protein.
448
449 We next tested if the truncation Wtf4^{antidote} proteins could rescue the toxicity of a wild-type
450 Wtf4^{poison}-mEos protein. Neither the Wtf4Δ$^{10\text{-antidote}}$-mCherry or Wtf4-ex6Δ^{antidote}-mCherry proteins
451 appreciably neutralized Wtf4^{poison}-mEos toxicity (S13 Fig A-B). The Wtf4Δ$^{20\text{-antidote}}$-mCherry
452 protein, however, rescued growth of cells expressing Wtf4^{poison}-mEos to a level comparable to
453 that observed in the cells expressing only Wtf4Δ$^{20\text{-antidote}}$-mCherry. So, despite the slight toxicity
454 of the Wtf4Δ$^{20\text{-antidote}}$-mCherry protein, it still retained some antidote function.
455
456 Interestingly, we were surprised to see that the other truncated antidotes Wtf4Δ$^{10\text{-antidote}}$-mCherry
457 and Wtf4-ex6Δ^{antidote}-mCherry could also partially rescue the toxicity of Wtf4Δ$^{20\text{-poison}}$-mEos
458 poison, although it was much less rescue compared to that of the wild-type Wtf4^{antidote}-mCherry
459 protein. This demonstrates that these truncated proteins retain some functionality.
460
461 Our results indicate that the C-terminus supports Wtf4^{antidote} function, but that some functionality
462 remains even in the absence of the last 29 amino acids. When considered in combination with
463 the results of Hu et al, [17], our combined results indicate that the importance of the C-terminus
464 is context dependent. Like our Wtf^{poison} results discussed earlier, these observations, combined
465 with the lack of conservation of Wtf proteins, suggests that Wtf^{antidote} function (outside of the
466 conserved PY motifs) relies on overall properties of the protein (e.g., lack of toxicity and ability
467 to co-assemble with a matching Wtf^{poison}), rather than any functional domain.
468
469 **Self-killing alleles that encode a functional Wtf^{poison} with an incompatible Wtf^{antidote}**
470 Because Wtf proteins are encoded on largely overlapping coding sequences, a change in the
471 shared coding sequence can simultaneously create a novel Wtf^{poison} protein and a matching
472 novel Wtf^{antidote} protein. Our engineered mutant alleles offered the opportunity to explore if

473 matching proteins are always compatible (i.e., if a novel toxic Wtf^{poison} protein is always
474 neutralized by its corresponding Wtf^{antidote} protein).
475
476 We therefore explored poison and antidote compatibility more broadly within the alleles we
477 generated. In many cases, the Wtf^{antidote} proteins were able to rescue their matching Wtf^{poison}
478 alleles (S1 Table). One class of mutants, however, created toxic Wtf^{poison} proteins that were not
479 rescued by the matching Wtf^{antidote}. In *wtf4*, these mutants changed a region of exon 6 that
480 encodes a 7 amino acid repeat found in variable numbers (0-84 base pairs of repeat sequence)
481 within *S. pombe wtf* genes (Figure 6A, B) [20]. The repeat region in *wtf4* encodes one complete
482 repeat plus three additional amino acids of the repeat (Figure 6C). We found that mutating this
483 region in Wtf4 by either scrambling the amino acid order (Wtf4-rep2^{sc}) or by replacing the ten
484 amino acids with alanine (Wtf4-rep2^{A} allele) generated toxic Wtf^{poison} proteins that were not
485 neutralized by their matching Wtf^{antidote} proteins (Figure 6D). The Wtf4-rep2$^{sc\text{-}antidote}$-mCherry and
486 Wtf4-rep2$^{A\text{-}antidote}$-mCherry proteins were both trafficked to the vacuole when expressed alone
487 but did not effectively co-traffic their corresponding Wtf^{poison} proteins (Figure 6E). The Wtf4-
488 rep2$^{sc\ antidote}$-mCherry and Wtf4-rep2$^{sc\ poison}$-mEos proteins showed decreased co-localization,
489 relative to wild-type proteins, suggesting the proteins had disrupted co-assembly (Figure 6E-F).
490 Alternatively, the Wtf4-rep2$^{A\ antidote}$-mCherry and Wtf4-rep2$^{A\ poison}$-mEos proteins colocalized (Fig
491 6F), but remained more distributed within cells relative to wild-type (Figure 6E). This distributed
492 localization is a change from the vacuolar localization of Wtf4-rep2$^{A\ antidote}$-mCherry alone,
493 further supporting that the Wtf4-rep2$^{A\ antidote}$-mCherry and Wtf4-rep2$^{A\ poison}$-mEos are interacting.
494 Therefore, the incompatibility of the Wtf4-rep2^{A} proteins adds additional support to our earlier
495 conclusion that a particular form of association is required between Wtf^{antidote} and Wtf^{poison}
496 proteins to ensure the poison is effectively trafficked to the vacuole and neutralized.
497
498 We also assayed the effects of deleting the repeat region of *wtf4* exon 6 alone (*wtf4-rep2Δ*
499 allele), or in combination with deleting another repetitive region found in exon 3 (*wtf4-rep1-2Δ*
500 allele; S9 Fig A) [20]. We found that the Wtf4-rep2Δ^{poison}-mEos protein is toxic but is only
501 partially rescued by Wtf4-rep2Δ^{antidote}-mCherry, relative to the rescue observed between wild-
502 type Wtf4 poison and antidote proteins (S9 Fig D). We found that the two Wtf4-rep2Δ proteins
503 exhibit decreased colocalization, relative to wild-type proteins, suggesting the limited rescue is
504 due to disrupted poison-antidote interaction (S9 Fig E-F). Interestingly, we found that the defect
505 in poison-antidote compatibility conferred by the deletion of the exon 6 repeats in the *wtf4-rep2Δ*
506 allele is partially suppressed by also deleting the repetitive region found in exon 3. Specifically,

507 the proteins encoded by the *wtf4-rep1-2Δ* allele, with both regions deleted, have near wild-type
508 phenotypes (S9 Fig A-F). We observed no defects in poison and antidote compatibility in the
509 proteins encoded by an allele (*wtf4-rep1Δ*) lacking only the repetitive region in exon 3 (S9 Fig A-
510 B, D-E).
511
512 Finally, we also tested if the novel mutations we made in this study in the exon 3 or C-terminal
513 repeats affected compatibility with wild-type Wtf proteins. In all cases tested, the repeat mutant
514 Wtf^{poison} proteins were not neutralized by their wild-type $Wtf^{antidote}$ counterparts and vice versa
515 (S10 Fig A-H). For example, Wtf4-rep1Δ^{poison}-mEos is not neutralized by Wtf4^{antidote}-mCherry and
516 Wtf4^{poison}-mEos is not neutralized by Wtf4-rep1$\Delta^{antidote}$-mCherry (S10 Fig B).
517
518 The repeats in exon 6, but not in exon 3, are broadly conserved in the *wtf* gene family [19]. We
519 also mutated the homologous region in *S. octosporus wtf25* and found analogous phenotypes
520 as those described above in *wtf4* (S11 Fig). Like *wtf4*, *S. octosporus wtf25* also encodes 10
521 amino acids in this C-terminal region (S11 Fig A-C). We generated the *S. octosporus wtf25-*
522 *rep2Δ* allele by swapping the endogenous codons for those of *wtf4*. We found that this allele
523 encoded an incompatible Wtf25-rep2$^{Sk\text{-}poison}$-mCherry and Wtf25-rep2$^{Sk\text{-}antidote}$-mEos pair (S11
524 Fig D). Surprisingly, the individual Wtf25-rep2^{Sk} proteins were compatible with Wtf25 proteins
525 (i.e., Wtf25-rep2$^{Sk\text{-}poison}$-mCherry was rescued by Wtf25^{antidote}-mEos and vice versa). We also
526 deleted the repeat region of *S. octosporus wtf25* (to generate the *wtf25-rep2Δ* allele) and again
527 found phenotypes similar to those observed in the analogous *wtf4* mutant (*wtf4-rep2Δ*) (S12 Fig
528 A-D). Specifically, the Wtf25-1^{antidote}-mCherry showed reduced rescue of the Wtf25-rep2Δ^{poison}-
529 mEos toxicity, relative to the wild-type Wtf25 protein pair (S12 Fig C).
530
531 Altogether, our results further support a critical role for the repeats in Wtf^{poison} and $Wtf^{antidote}$
532 compatibility and reveal that mutants in this domain can encode Wtf^{poison} proteins not neutralized
533 by the matching $Wtf^{antidote}$ proteins. Such alleles are important constraints on *wtf* gene evolution
534 as they would contribute to infertility via self-killing.
535
536 **Discussion**
537
538 **Protein assembly plays conserved roles in Wtf protein function.**
539 The mutant analyses provided in this work expands and supports a working model in which 1)
540 Wtf^{poison} toxicity is tied to the homotypic assembly of the proteins [15], 2) $Wtf^{antidote}$ proteins are

541 ubiquitinated and trafficked to the vacuole [15,24] and, 3) Wtf^{antidote} proteins co-assemble with
542 their matching Wtf^{poison} proteins and co-traffic them to the vacuole [15,26]. Recent work has
543 established that ubiquitin-mediated Wtf^{antidote} trafficking and co-trafficking with their
544 corresponding Wtf^{poison} proteins are conserved within the extremely diverse gene family [24]. It
545 was unclear, however, if homotypic protein assembly is a conserved feature of Wtf^{poison} or
546 Wtf^{antidote} protein function.
547
548 The results of this study support the model that homotypic protein assembly plays critical roles
549 in the function of Wtf^{poison} proteins. First, we observed that the ability to self-assemble was
550 conserved amongst functional (i.e., toxic) wild-type Wtf^{poison} proteins from four
551 *Schizosaccharomyces* species (Fig 2). Given that the functional proteins share as little as 20%
552 amino acid identity, these observations likely reflect conserved functional importance of self-
553 assembly. Our mutant analyses of Wtf4^{poison} proteins provided additional support for this model
554 in that all toxic mutant proteins self-assembled (S2 Fig, S3 Fig). Furthermore, we found that the
555 Wtf^{poison} toxicity could be modulated by altering the assembly properties of the protein with tags
556 (Fig 3, Fig 4, S4 Fig, S5 Fig). Together, our data suggest that Wtf^{poison} toxicity is tied to protein
557 assembly with distributed, small assemblies showing greater toxicity than localized, larger
558 assemblies (Fig 2-4, S2-5 Fig, Fig 7). The recent work of Zheng et al. (2023) suggests the
559 distributed assemblies may represent localization to the trans-Golgi network.
560
561 Still, it is important to note that the Wtf4Δ$^{10\ poison}$ allele was non-toxic, despite assembling into
562 small, distributed assemblies indistinguishable from those generated by the wild-type protein
563 (S3 Fig). This exceptional protein highlights that even if self-assembly is critical for Wtf^{poison}
564 toxicity, it is not the only factor required. In addition, this allele offers an opportunity for future
565 work to explore features that distinguish toxic from nontoxic protein assemblies.
566
567 Our results also support an expanded, more nuanced role for homotypic protein assembly and
568 trafficking in Wtf^{antidote} function. First, we found that the antidote-specific domain that contains
569 the PY motifs is insufficient to promote vacuole trafficking, suggesting some other features of
570 Wtf proteins are also required (S7 Fig). We posit protein self-assembly could contribute to this
571 function. For Wtf^{antidote} neutralization of a Wtf^{poison}, we initially assumed that co-assembly of
572 Wtf^{antidote} with Wtf^{poison} proteins served only to physically link the proteins, thus enabling the
573 Wtf^{antdiote} to traffic the Wtf^{poison} to the vacuole [24]. We found, however, that physical linkage
574 between a Wtf^{poison} and Wtf^{antidote} can be insufficient to ensure their co-trafficking to the vacuole

575 and neutralization of the Wtf^{poison}'s toxicity. We observed this insufficiency in experiments linking
576 two distinct pairs of non-matching Wtf^{poison} and Wtf^{antidote} proteins with GFP-GBP tags (Fig 5, S8
577 Fig). In addition, we found that the *wtf4-rep2^{A}* and *NT*-wtf4* alleles encode protein pairs in which
578 poison-antidote interaction appeared largely intact, but trafficking into the vacuole and poison
579 neutralization was disrupted (Fig 4, Fig 6). These experiments suggest that efficient co-
580 trafficking of Wtf^{poison}/ Wtf^{antidote} protein assemblies requires a particular conformation or strong
581 affinity between the interacting proteins not replicated in the ineffective Wtf^{poison}/Wtf^{antidote}
582 combinations mentioned above (Fig 7).
583
584 Moreover, our experiments surprisingly revealed that trafficking toxic Wtf assemblies to the
585 proper destination may not always be sufficient to ensure their neutralization. In previous work
586 using a different induction system than that employed here, we found that much of the trafficked
587 Wtf4^{poison}/Wtf4^{antidote} assemblies accumulated at the insoluble protein deposit (IPOD), in addition
588 to the vacuole [15] and the cells were viable. Similar, but generally smaller, assemblies can be
589 seen accumulating outside of the vacuole (likely the IPOD) in many of the viable cells we image
590 expressing Wtf^{antidote} proteins or compatible Wtf^{poison}/Wtf^{antidote} assemblies using the GAL
591 induction system employed in this study (e.g., Fig 6E panels expressing Wtf4^{antidote} and
592 Wtf4^{antidote}/Wtf4^{poison}). Similarly, Zheng et al found that vacuole localization was not essential for
593 Wtf^{poison} neutralization as they observed that trafficking to the endosome can be sufficient [24].
594 Here, however, we observed that Wtf4^{poison}-GBP/Wtf61^{antidote}-GFP assemblies (and likely the
595 Wtf25^{poison}-GBP/Wtf1^{antidote}-GFP assemblies) were trafficked to the IPOD, but were still toxic (Fig
596 5, S8 Fig, Fig 7). These results suggest that factors beyond localization, perhaps assembly
597 conformation, can also affect the toxicity of Wtf proteins.
598
599 **Commonalities between Wtf proteins and other self-assembling proteins.**
600 The Wtf proteins share broad parallels with other nonhomologous proteins that form
601 assemblies. For example, a sequence-independent common oligomeric property may underly
602 the toxicity of unrelated amyloid proteins [49]. While Wtf^{poison} proteins are related to each other,
603 their sequences are extremely diverged. We propose a common feature of their assembled
604 forms is likely responsible for their shared toxicity. Another feature Wtf proteins share with
605 several unrelated proteins is the capacity to form functional assemblies. Multiple amyloidogenic
606 proteins form functional amyloids that perform diverse biological functions, including long term
607 memory in flies [50], epigenetic inheritance in yeast [51] and biofilm formation in bacteria [52–
608 54]. Some functionally aggregating amyloids have also shown to be toxic at intermediate stages

609 of assembly, suggesting that protein toxicity could pose a risk in certain instances [55]. The co-
610 expression of Wtf^{antidote} with the toxic Wtf^{poison} results in a change in its localization and the
611 assembly properties of the Wtf^{poison}-Wtf^{antidote} complex. This suggests that protein-protein
612 interaction within a pair of corresponding Wtf proteins is similar to functional aggregation. While
613 the outcome of functional Wtf protein assembly is different (i.e., successful drive), the delicate
614 interplay between toxic and non-toxic protein assemblies is similar to functionally aggregating
615 amyloids.
616
617 The use of E3 ubiquitin ligases to direct protein trafficking is an additional theme Wtf proteins
618 share with other self-assembling proteins acting in diverse cell signaling processes, including
619 immune response [56,57], prion disease [58] and other neurodegenerative disorders [59–65]. In
620 multiple cases, ubiquitination of a key protein results in its aggregation, differential trafficking to
621 specific intracellular locations or degradation, suggesting that this is a common mechanism for
622 enabling downstream signaling processes. Additionally, a lack of ubiquitination by the ligase
623 often results in toxic aggregates [58,61,64] or reduced functionality of the key protein [56,57],
624 which are very reminiscent of the Wtf^{poison}/Wtf^{antidote} assemblies discussed above.
625
626 **Rapidly evolving coding sequence repeats can affect Wtf^{poison}-Wtf^{antidote} compatibility.**
627 Most *S. pombe wtf* genes contain varying copy numbers of a sequence repeat in exon 3 [20].
628 The potential role of the exon 3 repeats was unclear, but all functionally validated *S. pombe wtf*
629 drivers contain the exon 3 repeats (S5 Table). One *wtf* gene (*wtf23* from the CBS5557 strain)
630 that lacks the exon 3 repeats has been tested in *S. pombe* and failed to cause drive in two strain
631 backgrounds, although it was not determined if the encoded proteins were non-functional or if
632 the driver was effectively suppressed [20,25]. Previous work also found that a mismatch of
633 repeat numbers in exon 3 between a Wtf13^{poison} (five repeats) and Wtf18-2^{antidote} (four repeats)
634 could still produce a compatible poison and antidote pair. In this work, we found that deleting the
635 exon 3 repeats in *wtf4* (*wtf4-rep1Δ* allele) produced a functional, compatible Wtf^{poison} and
636 Wtf^{antidote} pair. The Wtf4-rep1Δ^{poison}, however, was not neutralized by the wild-type Wtf4^{antidote},
637 which has two repeats (S10 Fig B). This indicates that the exon 3 repeats can affect Wtf^{poison}
638 and Wtf^{antidote} compatibility in a context dependent fashion.
639
640 Many *S. pombe wtf* genes also contain a sequence repeat in exon 6 [20]. Repeats homologous
641 to those found in *S. pombe* exon 6 can also be found in the C-termini of many genes in *S.*
642 *octosporus* and *S. osmophilus* [19]. All functionally validated drivers contain repeats in *S.*

643 *octosporus*, but one functional *S. pombe* driver (*wtf35* from FY29033) lacks the repeats (S5
644 Table) [19,25]. Previous work demonstrated that a mismatch in the number of exon 6 repeats
645 could affect Wtf^{poison} and Wtf^{antidote} compatibility in *S. pombe* Wtf proteins [15,26]. This current
646 work extends previous work by showing with additional alleles of *wtf4* and novel alleles of *S.*
647 *octosporus wtf25* that copy number mismatches in this region disrupt Wtf^{poison} and Wtf^{antidote}
648 compatibility.
649
650 Overall, our results support the model that the rapid copy number evolution of the repeats found
651 in *wtf* genes contributes to rapid innovation of novel Wtf^{poison} and Wtf^{antidote} pairs [19,20]. These
652 highly evolvable sequences have likely contributed to the long-term evolutionary success of *wtf*
653 drivers, as generating novel alleles allows frequent generation of novel drivers likely to be
654 heterozygous (and thus drive) in crosses. Frequent driver turnover may also complicate the
655 evolution of drive suppressors that are not other *wtf* genes. Still, this work reveals that these
656 hypermutable regions come with a burden as they contain the potential to generate self-killing
657 alleles, which are discussed below.
658
659 **Wtf fitness landscape likely includes self-killing alleles.**
660 Our analyses of mutations in the repeats found in exon 6 of *S. pombe* genes revealed a novel
661 self-killing phenotype in which a *wtf* allele can encode a toxic Wtf^{poison} that is not effectively
662 neutralized by its corresponding Wtf^{antidote}. Such an allele is expected to lead to a dominant loss
663 of fertility, analogous to mutations where the antidote protein expression or function is disrupted
664 [17,22,24]. This phenotype was strongest in mutants that changed the sequence of the repeats
665 (i.e., *wtf4-rep2^{sc}*, *wtf4-rep2^{A}* and *wtf25-rep^{Sk}*). These mutations are rather dramatic and have a
666 low probability of arising spontaneously in nature.
667
668 A weaker version of the self-killing phenotype was, however, also observed in mutations that
669 deleted the repeats. Interestingly, the deleterious effects of removing the exon 6 repeats in *wtf4*
670 (*wtf4-rep2Δ* allele) could be suppressed by also deleting the exon 3 repeats (*wtf4-rep1-2Δ*
671 allele) (S9 Fig D). This suppression, in addition to the one functional driver known to lack the
672 exon 6 repeats, shows that changes in other regions of the protein can compensate for the
673 missing repeats. Still, the existence of *wtf* genes without the repeats, and extensive gene
674 conversion within the family, suggests that novel deleterious repeat deletion mutations are likely
675 to arise recurrently in natural populations [19–21].
676

677 We may have also fortuitously sampled one largely self-killing allele from a natural population
678 that did not have disrupted repeats, suggesting there are multiple paths to generating such
679 alleles. The *wtf41* gene from *S. osmophilus* encodes a toxic Wtf41^{poison} that is not efficiently
680 neutralized by the corresponding Wtf41^{antidote} protein (S14 Fig, [19]). All together, we propose
681 self-killing *wtf* alleles could contribute to recurrent, spontaneous sub-fertility or infertility. We
682 propose this spontaneous sub-fertility could be a persistent burden on the population fitness of
683 all *Schizosaccharomyces* species carrying *wtf* drivers.
684
685 **Rapid evolution and the risk of self-killing alleles.**
686
687 Beyond *wtf* genes, there are many known killer meiotic drivers [3,5,6,8,9,11]. There are also
688 likely many more yet to be discovered, given their accelerated pace of discovery in recent years.
689 Although the genes causing drive in different systems are not homologous, they often share
690 mechanistic and evolutionary themes [13,14,66]. Those themes include production of
691 poisons/killer elements and rapid evolution. The *wtf* genes have illustrated that high evolvability,
692 via nonallelic gene conversion and mutable coding sequence repeats, can facilitate the
693 evolutionary success of meiotic drivers [19,21,67]. This work reveals that rapid evolution of killer
694 elements also presents the risk of generating self-killing alleles. There is no reason to suppose
695 such risks would be specific to the *wtf* killers. Instead, we posit that such self-killing alleles may
696 be a widespread source of recurrent, spontaneous infertility in eukaryotes.
697
698 **Materials and Methods**
699
700 **Cloning**
701
702 We confirmed all the vectors described in this study by Sanger sequencing or by Nanopore
703 sequencing via Plasmidsaurus. Find the specifics for the yeast strains used in this study are
704 listed in S2 Table, plasmids are in S3 Table and the oligos are in S4 Table.
705
706 ***S. cerevisiae* vectors:**
707
708 *Generation of a Gal-inducible GFP vector to tag alleles:* We amplified GFP-ADH1 terminator
709 from a previously published plasmid, pSZB464 [15] with oligos 3744+3743. We digested this
710 product with SacI and SpeI and cloned it into pDK20 [68] to generate pSZB1528. We then

711 isolated the Gal promoter-GFP-ADH1T after digestion with SacI and KpnI, and cloned it into a
712 SacI-KpnI digested pRS316 [69] to generate pSZB1540.
713
714 *Generation of a Gal-inducible mCherry vector to tag alleles:* We amplified mCherry-ADH1
715 terminator from pFA6a-mCherry-kanMX6 [70] with oligos 3745+3743. We digested this product
716 with SacI and SpeI and cloned it into pDK20 [68] to generate pSZB1526. We then isolated the
717 Gal promoter-mCherry-ADH1T after digestion with SacI and KpnI, and cloned it into a SacI-KpnI
718 digested pRS314 [69] to generate pSZB1537.
719
720 *Generation of a Gal-inducible mEos3.1 vector to tag alleles:* We digested V08 [30] with SacI and
721 KpnI to release the fragment with Gal promoter- 4x(EAAAR) linker-mEos3.1. We then cloned
722 this into SacI-KpnI digested pRS316 [69] to generate pSZB1460.
723
724 *Generation of a monomer mEos3.1 in an ARS/CEN plasmid:* We cut out Gal-monomer
725 mEos3.1-cyc1T from RHX0935 [30] with SacI and KpnI, and cloned into SacI, KpnI cut pRS316
726 [69] to generate pSZB1514.
727
728 *Generation of Gal-inducible wtf alleles:*
729
730 *S. kambucha wtf4 exon 1:* The gene consisting of 136 base pairs that makes up exon 1 of *S.*
731 *kambucha wtf4* was synthesized and cloned into pSZB1460 by IDT to generate pSZB1552.
732
733 *S. kambucha wtf4-rep1Δ :* We deleted 66 base pairs (bases 313-378 of poison coding
734 sequence) that make up the exon 3 coding sequence repeats in *S. kambucha wtf4*^{poison} and
735 cloned it into pSZB1460 to generate pSZB1565. We repeated the same deletion in *S.*
736 *kambucha wtf4*^{antidote} (bases 439-504 of antidote coding sequence) and this construct was
737 synthesized and cloned it into pSZB1537 by IDT to generate pSZB1736.
738
739 *S. kambucha wtf4-rep2Δ :* We deleted 30 base pairs (bases 802-831 of poison coding
740 sequence) that make up the exon 6 repeats in *S. kambucha wtf4* and this construct was
741 synthesized and cloned it into pSZB1460 to generate pSZB1566 by IDT. To construct the
742 mutant antidote, we deleted bases 928-957 of the antidote coding sequence and this construct
743 was synthesized and cloned it into pSZB1537 by IDT generate pSZB1737.
744

745 *S. kambucha wtf4-rep1-2Δ* : We deleted 66 base pairs (bases 313-378 of poison coding
746 sequence) and 30 base pairs (bases 802-831 of poison coding sequence) to delete both the
747 exon 3 and 6 coding sequence repeats in *S. kambucha wtf4.* This construct was then
748 synthesized and cloned into pSZB1460 to generate pSZB1670. To construct the mutant
749 antidote, we deleted 66 base pairs (bases 439-504 of antidote coding sequence) and 33 base
750 pairs (bases 928-957 of antidote coding sequence) and this construct was synthesized and
751 cloned it into pSZB1537 by IDT generate pSZB1738.
752
753 *S. kambucha wtf4-rep2^{sc}:* We randomly scrambled the 10 amino acids that make up the exon 6
754 coding sequence repeats in *S. kambucha wtf4^{poison}*, and then reordered the codons to match the
755 amino acids. We then replaced the wild-type 30 base pairs with the scrambled 30 base pairs
756 (TTTGGGAGAGCGAGAGGGATAGGTAATATA) and this construct was synthesized and
757 cloned into pSZB1460 to generate pSZB1742. To construct the mutant antidote, we replaced
758 the exon 6 coding sequence repeats with the same scrambled 30 base pairs, and this construct
759 was synthesized and cloned into pSZB1537 by IDT to generate pSZB1740.
760
761 *S. kambucha wtf4-rep2^{A}:* We replaced the 30 base pairs that make up the exon 6 coding
762 sequence repeats with alanine codons (GCAGCGGCTGCCGCTGCAGCTGCCGCAGCG) in *S.*
763 *kambucha wtf4^{poison}* and this construct was synthesized and was cloned into pSZB1460 to
764 generate pSZB1743. To construct the mutant antidote, we replaced the exon 6 coding
765 sequence repeats with the same alanine codons, and this construct was synthesized and
766 cloned into pSZB1537 by IDT to generate pSZB1741.
767
768 *S. kambucha wtf4^{poison}-ex1^{int}*: We inserted exon 1 in between exons 3 and 4 of *S. kambucha*
769 *wtf4^{poison}* and this construct was synthesized and cloned into pSZB1460 by IDT to generate
770 pSZB1616. To maintain the in-frame codons, we inserted exon 1 at 541 base pairs of the poison
771 coding sequence, which is one base pair before exon 3 ends.
772
773 *S. kambucha wtf4^{poison}-ex1$^{in(PY\rightarrow PA)}$*: We mutated the two PY motifs within exon 1 in *S. kambucha*
774 *wtf4^{poison}-ex1^{int}* to PA (637-670 base pairs mutated from TAC to GCC; 670-673 base pairs
775 mutated from TAC to GCC) and this construct was synthesized and cloned into pSZB1460 by
776 IDT to generate pSZB1922.
777

778 *S. kambucha wtf4^{poison}-ex1:* We inserted exon 1 before the stop codon of *S. kambucha wtf4^{poison}*
779 coding sequence and this construct was synthesized and cloned into pSZB1460 by IDT to
780 generate pSZB1555.
781
782 *S. kambucha wtf4-TMD1Δ*: We used TMHMM2.0 [71,72] to predict transmembrane topology
783 (see S6 Table for a detailed description). With these predictions as guidance, we deleted the
784 first predicted transmembrane domain (bases 121-186 of poison coding sequence) from in *S.*
785 *kambucha wtf4^{poison}* and this construct was synthesized and cloned into pSZB1460 by IDT to
786 generate pSZB1561.
787
788 *S. kambucha wtf4-TMD2Δ:* We deleted the second predicted transmembrane domain (bases
789 232-291 of poison coding sequence) of *S. kambucha wtf4^{poison}* coding sequence and this
790 construct was synthesized and cloned into pSZB1460 by IDT to generate pSZB1562.
791
792 *S. kambucha wtf4-TMD6Δ:* We deleted the sixth predicted transmembrane domain (bases 580-
793 648 of poison coding sequence) of *S. kambucha wtf4^{poison}* coding sequence and this construct
794 was synthesized and cloned into pSZB1460 by IDT to generate pSZB1563.
795
796 *S. kambucha wtf4-ex2Δ*: We deleted exon 2 (bases 11-283) of *S. kambucha wtf4^{poison}* coding
797 sequence and this construct was synthesized and cloned into pSZB1460 by IDT to generate
798 pSZB1556.
799
800 *S. kambucha wtf4-ex3Δ:* We deleted exon 3 (bases 284-541) of *S. kambucha wtf4^{poison}* coding
801 sequence and this construct was synthesized and cloned into pSZB1460 by IDT to generate
802 pSZB1557.
803
804 *S. kambucha wtf4- ex4Δ :* We deleted exon 4 (bases 542-733) of *S. kambucha wtf4^{poison}* coding
805 sequence and this construct was synthesized and cloned into pSZB1460 by IDT to generate
806 pSZB1558.
807
808 *S. kambucha wtf4-ex5Δ:* We deleted exon 5 (bases 734-796) of *S. kambucha wtf4^{poison}* coding
809 sequence and this construct was synthesized and cloned into pSZB1460 by IDT to generate
810 pSZB1559.
811

812 *S. kambucha wtf4-ex6Δ :* We deleted exon 6 (bases 797-885) of *S. kambucha wtf4*^{poison} coding
813 sequence and this construct was synthesized and cloned into pSZB1460 by IDT to generate
814 pSZB1560. To construct the mutant antidote, we deleted exon 6 and this construct was
815 synthesized and cloned into pSZB1537 by IDT to generate pSZB1899.
816
817 *S. kambucha wtf4-consΔ :* From previous analysis of *S. pombe wtf* genes, a conserved region
818 within exon 3 was identified [20]. This conserved region within exon 3 was 29 base pairs long
819 (bases 284-312) in *S. kambucha wtf4*^{poison} coding sequence. To maintain in-frame codons, we
820 included one base pair upstream the conserved region, and made a 30 base pairs deletion
821 (bases 283-312) in *S. kambucha wtf4*^{poison} coding sequence and this construct was synthesized
822 and cloned into pSZB1460 by IDT to generate pSZB1617.
823
824 *S. kambucha wtf4-Δ*$^{10\text{-}poison}$*-mEos:* We amplified a 10 amino acid truncated poison from
825 pSZB464 [15] with oligos 3183+3186 and cloned this into V08 [30] via Golden Gate assembly
826 (New England Biolabs) to generate pSZB1402. We digested this with SacI and KpnI and cloned
827 the insert into SacI, KpnI digested pRS316 [69] to generate pSZB1505.
828
829 *S. kambucha wtf4-Δ*$^{10\text{-}antidote}$*-mCherry:* We amplified 10 amino acid truncated antidote from
830 pSZB708 [15] with oligos 1402+3138, and mCherry-cyc1T from pSZB708 [15] with oligos
831 3139+2170. We then stitched these pieces with oligos 1402+2170. We cut this fragment with
832 XhoI, BamHI and cloned this into XhoI, BamHI cut pDK20 [68] to generate pSZB1416. We cut
833 this plasmid with KpnI and XhoI and cloned the insert into KpnI, XhoI cut pRS314 [69] to
834 generate pSZB1550.
835
836 *S. kambucha wtf4-Δ*$^{20\text{-}poison}$*-mEos:* We amplified 20 amino acid truncated poison from pSZB464
837 [15] with oligos 3183+3282 and cloned this into V08 [30][30] via Golden Gate assembly (New
838 England Biolabs) to generate pSZB1444. We digested this with SacI and KpnI and cloned the
839 insert into SacI, KpnI digested pRS316 [69] to generate pSZB1507.
840
841 *S. kambucha wtf4-Δ*$^{20\text{-}antidote}$*-mCherry:* We amplified 20 amino acid truncated antidote from
842 pSZB708 [15] with oligos 1402+3829. We digested this fragment with XhoI and BamHI and
843 cloned the insert into XhoI, BamHI cut pSZB1537 to generate pSZB1567.
844

845 *S. kambucha wtf4^{poison}-mCherry:* We amplified *S. kambucha wtf4^{poison}-mCherry-cyc1T* from
846 pSZB708 [15] with oligos 2625+964. This product was cut with BamHI and XhoI and cloned into
847 BamHI, XhoI cut pDK20 [68] to generate pSZB1374. We cut this plasmid with KpnI and XhoI
848 and cloned the insert into KpnI, XhoI cut pRS314 [69] to generate pSZB1381.
849
850 *S. kambucha wtf4^{poison}-mEos:* We digested RHX1389 [15] with KpnI, SacI and ligated the insert
851 with KpnI, SacI cut pRS316 [69] to generate pSZB1455. This plasmid had the start site of the
852 poison mutated to TAG, which was then corrected to ATG by GenScript to generate pSZB1476.
853
854 *S. kambucha wtf4^{poison}-GBP-mCherry:* We added the GFP-binding protein sequence from
855 Addgene plasmid #89068 [73] at the end of *S. kambucha wtf4^{poison}* and this construct was
856 synthesized and cloned into pSZB1537 by IDT to generate pSZB1748.
857
858 *S. kambucha NT*-wtf4^{poison}-mEos*: We added the mutated N-terminal domain (D40K, K65D)
859 from the flagelliform spidroin 1A variant 1 from *Trichonephila clavipes*, NT* [33,34], followed by
860 a TEV cleavage site (ENLYFQS) [74] at the N-terminus of *S. kambucha wtf4^{poison}* coding
861 sequence, which was synthesized and cloned into pSZB1460 by IDT to generate pSZB1900.
862
863 *S. kambucha MBP-wtf4^{poison}-mEos*: We added the *S. cerevisiae* codon-optimized *E. coli* Maltose
864 Binding Protein (MBP) coding sequence [75,76] followed by a 4X(GGGS)-GG linker to the N-
865 terminus of *S. kambucha wtf4^{poison}* coding sequence, which was synthesized and cloned into
866 pSZB1460 by IDT to generate pSZB1949.
867
868 *S. kambucha wtf4^{antidote}-GFP*: We ordered *S. kambucha wtf4^{antidote}* which was synthesized and
869 cloned into pSZB1540 by IDT to generate pSZB1874.
870
871 *S. kambucha wtf4^{antidote}-mCherry*: We amplified *S. kambucha wtf4^{antidote}-mCherry-cyc1T* from
872 pSZB1005 [15] with oligos 1402+2170. This product was digested with BamHI and XhoI and
873 cloned into BamHI, XhoI cut pDK20 [68] to generate pSZB1699. This plasmid was digested with
874 KpnI, XhoI and ligated with KpnI, XhoI cut pRS314 [69] to generate pSZB1774.
875
876 *S. kambucha wtf4^{antidote}-mEos*: We digested pSZB1120 (7) with KpnI, SacI and ligated the insert
877 into KpnI, SacI cut pRS316 [69] to generate pSZB1453. This plasmid had the start site of the

878 antidote mutated to TAG, which was then corrected to ATG by GenScript to generate
879 pSZB1477.
880
881 *S. octosporus wtf25^{poison}-mEos:* We amplified *S. octosporus wtf25^{poison}* from pSZB1353 [19] with
882 oligos 3841+3840 and cloned this into V08 [30] via Golden Gate assembly (New England
883 Biolabs) to generate pSZB1548. We digested this with SacI and KpnI and cloned the insert into
884 SacI, KpnI digested pRS316 [69] to generate pSZB1585.
885
886 *S. octosporus wtf25^{poison}-mCherry:* We ordered *S. octosporus wtf25^{poison}* coding sequence was
887 synthesized and cloned into pSZB1537 by IDT to generate pSZB1807.
888
889 *S. octosporus wtf25^{poison}-GBP-mCherry:* We added the GFP-binding protein sequence from
890 Addgene plasmid #89068 [73] at the end of *S. octosporus wtf25^{poison}* coding sequence and this
891 construct was synthesized and cloned into pSZB1537 by IDT to generate pSZB1868.
892
893 *S. octosporus wtf25^{antidote}-mCherry:* We ordered *S. octosporus wtf25^{antidote}* coding sequence was
894 synthesized and cloned into pSZB1537 by IDT to generate pSZB1746.
895
896 *S. octosporus wtf25^{antidote}-mEos:* We ordered *S. octosporus wtf25^{antidote}* coding sequence was
897 synthesized and cloned into pSZB1460 by IDT to generate pSZB1806.
898
899 *S. octosporus wtf25^{antidote}-mEos in pRS314*: We amplified *S. octosporus wtf25^{antidote}* from
900 pSZB1347 [19] with oligos 3839+3840. This insert was cloned into V08 [30] via Golden Gate
901 cloning (New England Biolabs) to generate pSZB1593. We digested this with KpnI, SacI and
902 cloned the insert into pRS314 [69] to generate pSZB1598.
903
904 *S. octosporus wtf25^{antidote}-GFP:* We ordered *S. octosporus wtf25^{antidote}* coding sequence was
905 synthesized and cloned into pSZB1540 by IDT to generate pSZB1869.
906
907 *S. octosporus wtf25-repΔ:* We deleted 30 base pairs (bases 505-534) that make up the exon 4
908 repeats in *S. octosporus wtf25^{poison}* and was synthesized and cloned into pSZB1460 by IDT to
909 generate pSZB1687. To construct the mutant antidote, we deleted bases 640-669 of the
910 antidote coding sequence and this construct was synthesized and cloned it into pSZB1540 by
911 IDT generate pSZB1739.

912

913 *S. octosporus wtf25-rep^{Sk}:* To swap the coding sequence repeats between *S. kambucha wtf4*
914 exon 6 and *S. octosporus wtf25* exon 4, we replaced the 30 base pairs from *wtf25*
915 (ATAGGAAACGGTGCACGGCATAGGAAAT) with 30 base pairs from *wtf4*
916 (ATAGGGAATATAGGGAGAGCGTTTAGAGGT) in *S. octosporus wtf25*. The mutant poison
917 was synthesized and cloned into pSZB1537 by IDT to generate pSZB1732. The mutant antidote
918 was synthesized and cloned into pSZB1460 by IDT to generate pSZB1731.
919

920 *S. octosporus wtf25Δ$^{10\text{-}poison}$-mEos:* We amplified a 10 amino acid C-terminal truncated
921 *wtf25^{poison}* from pSZB1353 [19] with oligos 4173+4174 and cloned this into V08 [30] via Golden
922 Gate assembly (New England Biolabs) to generate pSZB1675. We then cut out the tagged
923 poison with SacI and KpnI, and ligated it with cut pRS316 [69] to generate pSZB1694.
924

925 *S. octosporus NT*-wtf25^{poison}:* We added the mutated N-terminal domain (D40K, K65D) from the
926 flagelliform spidroin 1A variant 1 from *Trichonephila clavipes*, NT* [33,34], followed by a TEV
927 cleavage site (ENLYFQS) [74] at the N-terminus of *S. octosporus wtf25^{poison}* coding sequence,
928 which was synthesized and cloned into pSZB1460 by IDT to generate pSZB1927.
929

930 *S. octosporus MBP-wtf25^{poison}-mEos*: We added the *S. cerevisiae* codon-optimized *E. coli*
931 Maltose Binding Protein (MBP) coding sequence [75,76] followed by a 4X(GGGS)-GG linker to
932 the N-terminus of *S. octosporus wtf25^{poison}* coding sequence, which was synthesized and cloned
933 into pSZB1460 by IDT to generate pSZB1950.
934

935 *S. octosporus wtf61^{poison}-mEos:* We amplified *S. osmophilus wtf61^{poison}* from pSZB1040 [19] with
936 oligos 3837+3838 and cloned this into V08 [30] via Golden Gate assembly (New England
937 Biolabs) to generate pSZB1569. We digested this with SacI and KpnI and cloned the insert into
938 SacI, KpnI digested pRS314 [69] to generate pSZB1583.
939

940 *S. octosporus wtf61^{poison}-mCherry:* We amplified *S. osmophilus wtf61^{poison}* from pSZB1040 [19]
941 with oligos 4193+4194. We digested this product with XhoI, BamHI and cloned this into XhoI,
942 BamHI cut pSZB1537 to generate pSZB1706.
943

944 *S. octosporus wtf61^{antidote}-GFP:* We amplified *S. osmophilus wtf61^{antidote}* from pSZB1095 [19] with
945 oligos 4192+4194. We digested this product with XhoI, BamHI and cloned this into with XhoI,
946 BamHI cut pSZB1540 to generate pSZB1708.
947
948 *S. octosporus wtf61^{antidote}-mEos:* We amplified *S. osmophilus wtf61^{antidote}* from pSZB1095 [19]
949 with oligos 3836+3837 and cloned into V08 [30] via Golden Gate assembly (New England
950 Biolabs) to generate pSZB1645. We then digested pSZB1645 with KpnI and SacI and ligated it
951 with KpnI, BamHI cut pRS314 to generate pSZB1647.
952
953 *S. cryophilus wtf1^{poison}-mEos*: We amplified *S. cryophilus wtf1^{poison}* from pSZB1122 [19] with
954 oligos 3844+3843 and cloned this into V08 [30] via Golden Gate assembly (New England
955 Biolabs) to generate pSZB1544. We digested this with SacI and KpnI and cloned the insert into
956 SacI, KpnI digested pRS316 [69] to generate pSZB1575.
957
958 *S. cryophilus wtf1^{poison}-mCherry*: We ordered *S. cryophilus wtf1^{poison}* which was synthesized and
959 cloned into pSZB1537 by IDT to generate pSZB1870.
960
961 *S. cryophilus wtf1^{antidote}-mEos*: We amplified *S. cryophilus wtf1^{antidote}* from pSZB1192 [19] with
962 oligos 3843+3842 and cloned this into V08 [30] via Golden Gate assembly (New England
963 Biolabs) to generate pSZB1605. We digested this with SacI and KpnI and cloned the insert into
964 SacI, KpnI digested pRS314 [69] to generate pSZB1612.
965
966 *S. cryophilus wtf1^{antidote}-GFP*: We ordered *S. cryophilus wtf1^{antidote}* which was synthesized and
967 cloned into pSZB1540 by IDT to generate pSZB1871.
968
969 *S. cryophilus wtf1Δ$^{10\text{-}poison}$:* We amplified a 10 amino acid C-terminal truncated *wtf1^{poison}* from
970 pSZB1122 [19] and oligos 4177+4178 and cloned this into V08 [30] via Golden Gate assembly
971 (New England Biolabs) to generate pSZB1673. We then cut out the tagged poison with SacI,
972 KpnI and cloned into cut pRS316 [69] to generate pSZB1692.
973
974 *S. osmophilus wtf41^{poison}-mEos:* We cloned *S. osmophilus wtf41^{poison}* from pSZB1327 [19] with
975 oligos 3361+3362 and cloned this into V08 [30] via Golden Gate assembly (New England
976 Biolabs) to generate pSZB1533. We then cut out the tagged poison with SacI, KpnI and cloned
977 into cut pRS316 [69] to generate pSZB1581.

978

979 *S. osmophilus wtf41Δ$^{10\text{-}poison}$-mEos:* We cloned C-terminus 10 amino acid truncated *S.*
980 *osmophilus wtf41^{poison}* from pSZB1325 [19] with oligos 4175+4176 and cloned this into V08 [30]
981 via Golden Gate assembly (New England Biolabs) to generate pSZB1676. We then cut out the
982 tagged poison with SacI, KpnI and cloned into cut pRS316 [69] to generate pSZB1696.
983

984 *S. osmophilus wtf41^{antidote}-mEos:* We amplified *S. osmophilus wtf41^{antidote}* from pSZB1325 [19]
985 with oligos 3832+3362 and cloned this into V08 [30] via Golden Gate assembly (New England
986 Biolabs) to generate pSZB1599. We then cut out the tagged poison with SacI, KpnI and cloned
987 into cut pRS314 [69] to generate pSZB1607.
988

989 *S. osmophilus wtf19^{poison}-mEos:* We amplified *S. osmophilus wtf19^{poison}* from pSZB1324 [19] with
990 oligos 3835+3834 and cloned this into V08 [30] via Golden Gate assembly (New England
991 Biolabs) to generate pSZB1546. We then cut out the tagged poison with SacI, KpnI and cloned
992 into cut pRS316 [69] to generate pSZB1579.
993

994 **Strain construction**
995

996 *S. cerevisiae strains with Galactose and β-estradiol inducible systems:*
997

998 We used the previously published strain, SZY1637 [15] and an independently constructed
999 isolate of SZY1637, SZY1639 or SZY5807, to construct the strains in this study by transforming
1000 in the appropriate vectors. These strains have the lexA-ER-haB42 transcription factor integrated
1001 at *HIS3* [77]. In general, we used a protocol, modified from [78], to transform the vectors into
1002 these strains. Briefly, we incubated a mixture of 266μL of PLATE solution, 50μL of boiled
1003 salmon sperm DNA, 30μL of water, 1-4μL of vector DNA and a match-head sized amount of
1004 yeast at 30°C overnight and plated on selective media on the following day to select for
1005 transformants. We used Synthetic Complete (SC) media (Yeast Nitrogen Base from VWR
1006 #291940 and SC Supplement mix from SunSci) with the appropriate dropouts of the selective
1007 components to maintain vectors in the strains as in [15]. In some cases, transformants did not
1008 express the construct when induced. To ensure proper testing of genotypes, we screened
1009 multiple transformants via cytometry or microscopy to ensure that strains express the
1010 fluorescently tagged construct(s).
1011

1012 *Construction of S. cerevisiae strain with mEosNB-FTH1:*
1013
1014 We mated RHY3171 (Kimbrough et al, forthcoming) to BY4741 [79] to obtain progeny that did
1015 not have the *pGal-WHI5::hphMX* construct, which resulted in the generation of SZY6594. This
1016 strain had the *hoΔ::natMX::tTa{Off}tet07^mEosNB-(G4s)3-FTH1* construct, and did not undergo
1017 cell cycle arrest when induced with Galactose.
1018
1019 **Spot assays**
1020
1021 For spot assays, we first grew the strains for each experiment in the appropriate SC dropout
1022 media overnight at 30°C. The next day, we measured the OD600 of each strain, and normalized
1023 the OD of all the strains to an OD of ~1. We then serially diluted these normalized cultures 10-
1024 fold (up to the dilution of 10^{-5}) in water and plated 5μL of each dilution on both SC dropout
1025 media and SC Galactose dropout media. We imaged the plates post 72h of growth at 30°C,
1026 except in the case of Fig 4B and S4 Fig B C, where plates were grown for an additional day at
1027 30°C to clearly visualize differences in poison toxicity.
1028
1029 For the spot assays presented in Fig 3D, we first grew the strains in 5mL SC-URA (uracil) media
1030 overnight at 30°C. The next day, we pelleted overnight cultures and resuspended in 1mL of
1031 sterile water. We then used 100μL of this as the first in the dilution series. This was diluted 5-
1032 fold, up to eleven dilutions in order to observe the toxicity/suppression clearly. We plated 5μL of
1033 each dilution on SC-URA media, SC Galactose-URA media and SC Galactose-URA media with
1034 40mg/L Doxycycline (Calbiochem #324385). We imaged the plates post 72h of growth at 30°C.
1035
1036 For the spot assays presented in S5 Fig B, we first grew the strains in 5mL SC-TRP-URA media
1037 overnight at 30°C. The next day, we pelleted overnight cultures and resuspended in 1mL of
1038 sterile water. We then used 100μL of this as the first in the dilution series. This was diluted 5-
1039 fold, up to 11 dilutions in order to observe the toxicity/suppression clearly. We plated 5μL of
1040 each dilution on SC-TRP-URA media and SC Galactose-TRP-URA media. We imaged the
1041 plates post 72h of growth at 30°C.
1042
1043 **Microscopy**
1044

1045 The appropriate strains for each experiment were first grown in 5mL of the appropriate SC
1046 dropout media overnight at 30°C. The next day, we inoculated 3mL of SC Raffinose dropout
1047 media with 1mL of the saturated overnight cultures and let them grow overnight at 30°C. On the
1048 following day, we pelleted the cultures and resuspended the cells in 3mL SC Galactose dropout
1049 media and incubated at 30°C. Cells were induced for 4-6 hours on SC Galactose dropout
1050 media, and then imaged on a Zeiss LSM 980 confocal microscope which consisted of an Axio
1051 Observer Z1 base, through a 40x C-Apochromat (NA = 1.2) water immersion objective. The
1052 GFP and mCherry tagged proteins were excited at 488 and 561 nm, respectively. Emission was
1053 collected in channel mode onto a GaAsP detector in photon counting mode through a 491-544
1054 nm bandpass for GFP and a 570-632 nm bandpass for mCherry. Transmitted light was also
1055 collected. Image fields of view were zoomed optically to a ~26 µm square with 512 pixels in
1056 each dimension.
1057
1058 For imaging cells expressing *S. octosporus* Wtf61^{antidote}-GFP, *S. kambucha* Wtf4^{poison}-GBP-mCh
1059 and Rnq1-mCardinal, we first grew cells in SC-Trp-Ura-Leu media. The next day, we inoculated
1060 3mL of SC Raffinose-Trp-Ura-Leu media with 1mL of the saturated overnight cultures and let
1061 them grow overnight at 30°C. The following day, we pelleted the cultures and resuspended the
1062 cells in 3mL SC Galactose-Trp-Ura-Leu + 500nM β-estradiol (VWR, # #AAAL03801-03) media
1063 and incubated at 30°C. Cells were induced for 4 hours and then imaged as described above,
1064 except that we also excited mCardinal tagged proteins at 640nm and collected the emission on
1065 channel mode onto a 650-700 nm bandpass detector of the Zeiss LSM 980 confocal microscope.
1066
1067 **Spectral unmixing for mEosNB-FTH1 strains**
1068
1069 For imaging the mEosNB-FTH1 strains, we first grew the strains in 5mL SC-URA+40mg/L
1070 Doxycycline. The next day, we inoculated 3mL of both SC Raffinose-URA and SC Raffinose-
1071 URA+40mg/L Doxycycline media with 1mL of the saturated overnight cultures and let them
1072 grow overnight at 30°C. The following day, we pelleted the cultures and resuspended the cells
1073 in 3mL of both SC Galactose-URA and SC Galactose-URA+40mg/L Doxycycline and incubated
1074 at 30°C. The rest of the methodology was as described in the section above.
1075
1076 The background fluorescence for strains constructed with SZY6594 had high autofluorescence
1077 in the GFP channel. To distinguish autofluorescence from true mEos signal, we spectrally

1078 unmixed the images. First, we captured spectral images with the lambda mode on the dectector
1079 of the Zeiss LSM 980 confocal microscope (same settings as above), exciting the cells at 488
1080 nm and collecting emission over the entire visual spectrum, We then made reference spectra for
1081 mEos and autofluorescence from control cells, and then spectrally unmixed images using an in-
1082 house written plugin on ImageJ (https://research.stowers.org/imagejplugins/). The data
1083 presented in Figure 3C has transmitted light images collected on the channel mode with GFP
1084 excitation, and the spectrally unmixed images collected on lambda mode.
1085
1086 **Image analysis to quantify colocalization of mEos and mCherry signals in tagged**
1087 **constructs**
1088
1089 Cell regions of interest (ROIs) were found based on the transmitted light only using Cellpose
1090 (https://www.cellpose.org/) in Python using the "cyto" model and a diameter of 200. Pixels from
1091 these ROIs were then background subtracted using an average background signal from an ROI
1092 placed away from any cell. The Scipy Pearson Correlation for each cell ROI was then calculated
1093 for all pixels in each cell. Dead cells and aberrant ROIs were hand filtered out using Fiji
1094 (https://fiji.sc/). Find the raw data for these analyses in S1 Data.
1095
1096 **DAmFRET**
1097
1098 We performed the analysis similar to the methods in [15], with a few exceptions. We grew the
1099 strains in the same method described for microscopy, however, we induced the cells for 5-6
1100 hours. We then photoconverted the cells post induction for 5 minutes, using the OmniCure
1101 S2000 Elite UV lamp for photoconversion. The total power over 5 minutes of exposure amounts
1102 to 12.048 J/cm^2. The sample collection and data analysis were similar to methods described in
1103 [15] with a few exceptions. We included an empty vector strain in each experiment to effectively
1104 exclude auto fluorescent cell populations. All the cells for each experiment were induced at the
1105 same time, for the same amount of time, and were grown in the same 96-well plate. Three
1106 technical replicates were included for each sample.
1107
1108 There was only one fluorescent population that was independent of expression level for each
1109 construct analyzed. In order to clearly visualize AmFRET values across the cells expressing
1110 different constructs, we analyzed cells above a certain Acceptor fluorescence intensity threshold
1111 set for each experiment. For each set of experimental data, the median of the poison AmFRET

1112 values was calculated. The difference of this median value from 1 was then added to all the
1113 datasets within an experiment. For visualizing the results of the DAmFRET experiments, plots of
1114 AmFRET values were generated using GraphPad Prism 10 (Version 10.2.3 (347)).
1115
1116 Statistical analysis for the DAmFRET experiments involved pooling the technical replicates and
1117 performing pairwise t-tests comparing these values to either the wild-type Wtf4^{poison}-mEos
1118 dataset, or the monomer dataset. For each DAmFRET experiment, we then did a multiple
1119 sampling correction (Bonferroni correction) by dividing the p value cutoff (0.05) by the number of
1120 tests performed. Find the raw data and statistical analysis for each DAmFRET experiment in S2
1121 Data.
1122
1123 We used GraphPad Prism 10 (Version 10.2.3 (347)) to visualize acceptor fluorescence intensity
1124 values of live cells expressing the relevant Wtf^{poison} constructs. Three technical replicates of
1125 each isolate were plotted, with the median included. Find the raw data for this analysis in S2
1126 Data.
1127
1128 **Figure legends**
1129
1130 **Figure 1. Features of *wtf4* and mutant alleles.**
1131 **A.** A cartoon of *S. kambucha wtf4* coding sequence (CDS). Wtf4^{antidote} coding sequence is
1132 shown in magenta, which includes exons 1-6. The Wtf4^{poison} coding sequence is shown in cyan,
1133 which includes 21 base pairs from intron 1 (in grey), and exons 2-6. **B.** Features of Wtf4^{antidote}
1134 and Wtf4^{poison} proteins. Row 1 shows predicted secondary structure domains and functional
1135 motifs, including PY motifs (in mustard) and predicted transmembrane domains (in red). Row 2
1136 shows the coding sequence repeats in exon 3 and exon 6. Row 3 highlights a well-conserved
1137 region 9 amino acids long. Row 4 is the normalized hydrophobicity of the Wtf4 proteins from
1138 ProtScale, with the Kyle and Doolittle Hydropathy scale [80]. The higher the number on the
1139 scale, the higher the hydrophobicity of the amino acid. See S5 and S6 Tables for detailed
1140 descriptions. **C.** Percentage amino acid identity of Wtf^{antidotes} from 33 *wtf* driver genes from four
1141 isolates of *S. pombe* [20]. The antidote sequences were aligned using Geneious Prime
1142 (2023.0.4) and the percentage amino acid identity is depicted as a heatmap, with yellow being
1143 100% identity. *S. kambucha wtf4* CDS is shown below for comparison, with the exons labeled
1144 corresponding to the consensus. Labeled areas within exons 3 and 6, where identity is low,
1145 represent the expansion and contraction of the coding sequence repeats of different *wtf* genes.

1146 **D.** Cartoon of *wtf4* mutants constructed in this study. Each mutant category was constructed
1147 based on a specific feature mentioned above. The categories are depicted with a wild type *wtf4*
1148 allele at the top. See S1 Table for a comprehensive overview of the alleles and their
1149 phenotypes.
1150
1151 **Figure 2. Extremely diverged toxic Wtf^{poison} proteins exhibit similar self-assembly and**
1152 **intracellular localization**.
1153 **A**. Cartoon illustrating the Distributed Amphifluoric FRET (DAmFRET) assay (modified from
1154 [30]). AmFRET values for individual cells were calculated by dividing the acceptor fluorescence
1155 by the FRET fluorescence, both measured via cytometry. **B.** Combined AmFRET values for
1156 three technical replicates of the specified Wtf^{poison}-mEos proteins and monomer-mEos (negative
1157 control). X^{P} represents the WtfX poison proteins tested here. The median is indicated with a
1158 solid line and the bars represent the interquartile range. For easier comparison, the values were
1159 normalized so that Wtf4^{poison} had a median of 1 in each experiment. The data shown here here
1160 does not include outliers. See S2 Data for the complete dataset and p-values. Statistical
1161 significance: *p<0.01; t-tests with Bonferroni correction. **C.** A spot assay of cells serially diluted
1162 and plated on SC-TRP-URA and SC Gal-TRP-URA plates. Each strain carries an empty [*TRP1*]
1163 plasmid, and either an empty [*URA3*] plasmid (EV) or the indicated *wtf^{poison}-mEos* allele under
1164 the control of a galactose-inducible promoter. The plates were grown at 30•C for 3 days. **D.**
1165 Representative images of the same strains depicted in C were induced in galactose media for 4
1166 hours at 30•C to express the indicated mEos-tagged proteins. The images are not at the same
1167 brightness and contrast settings to clearly show localization of tagged proteins. Yellow arrows
1168 indicate endoplasmic reticulum-like localization. TL is transmitted light, and the scale bar is 4
1169 µm.
1170
1171 **Figure 3. Increasing poison assembly with tags suppresses Wtf^{poison} toxicity.**
1172 **A.** A cartoon of the constructs used in this experiment (C-D). The mEosNB-FTH1 construct was
1173 integrated into the genome and is under the control of a doxycycline-repressible promoter.
1174 mEosNB is a nanobody that binds mEos. The *wtf^{poison}* alleles are carried on a [*URA3*] plasmid
1175 and are under the control of a galactose-inducible promoter. **B.** Cartoon of the constructs
1176 expressed on each medium used: SC-Ura, SC Galactose-Ura + 40 mg/L doxycycline, and SC
1177 Galactose-Ura. FTH1 is a 24-mer, but is depicted as an 8-mer core. **C.** Representative images
1178 of cells induced with galactose media (with or without 40mg/L Doxycycline) for 4 hours at 30•C
1179 to express the indicated Wtf^{poison}mEos proteins. The cells induced without Doxycycline (-Dox)

1180 also express mEosNB-FTH1. This strain background exhibits high autofluorescence, so we
1181 spectrally unmixed the signal to remove autofluorescence (See Methods). The images are not
1182 at the same brightness and contrast settings to clearly show localization of tagged proteins. TL
1183 is transmitted light, and the scale bar is 4 µm. **D.** A spot assay of cells carrying the constructs
1184 illustrated in A-C serially diluted on SC-Ura, SC Galactose-Ura + 40mg/L Doxycycline and SC
1185 Galactose-Ura plates and grown at 30•C for 3 days. Each strain carries either an empty [*URA3*]
1186 plasmid (EV) or the indicated *wtf*^{poison}*-mEos* allele. These media induce the expression of
1187 mEosNB-FTH1 (i), the indicated Wtf^{poison}-mEos protein (ii), or both (iii), respectively. The
1188 horizontal break in the image of each plate is due to rearrangements of the images to facilitate
1189 easy comparison. All strains within a panel were grown on the same plates (i.e., one SC-TRP-
1190 URA or SC Gal-TRP-URA or SC Gal-TRP-URA + 40mg/L Doxycycline plate).
1191
1192 **Figure 4. Reducing Wtf4^{poison} assembly with NT* tag increases toxicity and affects its**
1193 **rescue by Wtf4^{antidote}.**
1194 **A.** Cartoon of alleles used in this experiment (B-F). The NT* tag has a general anti-aggregation
1195 property [33]. **B.** A spot assay of cells serially diluted and plated on SC-TRP-URA and SC Gal-
1196 TRP-URA plates and grown at 30•C for 4 days. Each strain carries both a [*URA3*] and a [*TRP1*]
1197 plasmid. The plasmids are either empty (EV) or carry the indicated *wtf4* alleles under the control
1198 of galactose-inducible promoters. The horizontal break in the image for each plate is due to a
1199 rearrangement of the image to facilitate easy comparison. All strains were grown on the same
1200 plates (i.e., one SC-TRP-URA or SC Gal-TRP-URA plate). **C.** AmFRET values for three
1201 technical replicates of the specified Wtf4^{poison}-mEos alleles and monomer-mEos (negative
1202 control). The median is indicated with a solid line and the bars represent the interquartile range.
1203 For easier comparison, the values were normalized so that Wtf4^{poison} had a median of 1 in each
1204 experiment. Since Wtf4-20^{poison}-mEos cells were very low in number, we pooled two biological
1205 replicates (n=6 technical replicates). The data shown here does not include outliers. See S2
1206 Data for the complete dataset and p-values. Statistical significance: *$p<0.025$, t-tests with
1207 Bonferroni correction. **D.** A spot assay of cells serially diluted and plated on SC-TRP-URA and
1208 SC Gal-TRP-URA plates and grown at 30•C for 3 days. Each strain carries both a [*URA3*] and a
1209 [*TRP1*] plasmid. The plasmids are either empty (EV) or carry the indicated *wtf4* alleles under the
1210 control of galactose-inducible promoters. All strains were grown on the same plates (i.e., one
1211 SC-TRP-URA or SC Gal-TRP-URA plate). **E.** Representative images of the same strains
1212 depicted in D were induced with galactose media for 4 hours at 30•C to express the indicated
1213 Wtf4^{poison}-mEos proteins and/or Wtf4^{antidote}-mCherry. The images are not at the same brightness

1214 and contrast settings to clearly show localization of tagged proteins. 4^P indicates $Wtf4^{poison}$, 4^A
1215 indicates $Wtf4^{antidote}$, TL is transmitted light, and the scale bar is 4 µm. **F**. Pearson's Correlation
1216 between mCherry and mEos signal in cells from E expressing the specified proteins. N>100, ***
1217 p<0.001, t-test.
1218
1219 **Figure 5. Effective neutralization of $Wtf4^{poison}$ requires more than a physical connection to**
1220 **a $Wtf^{antidote}$.**
1221 **A.** Cartoon of constructs used in this experiment. *S. kambucha wtf4^{poison}* was tagged at the C-
1222 terminus with either mCherry or GBP-mCherry (GBP: GFP-binding protein). *S. kambucha*
1223 *wtf4^{antidote}* was tagged with mEos or GFP. *S. octosporus wtf61^{antidote}* was tagged with GFP. *S.*
1224 *octosporus wtf61^{poison}* was tagged with mCherry. **B.** Experimental set up and summary of the
1225 results shown in C and D. In a matching Wtf protein pair (top), poison-antidote interaction and
1226 rescue of poison toxicity is observed. In the mismatched pair (bottom), interaction between GFP
1227 and GBP results in a forced interaction between the poison and the antidote (shown in D). This
1228 interaction is insufficient to rescue the mismatched poison (shown in C). **C.** Spot assay of cells
1229 serially diluted and plated on SC-TRP-URA and SC Gal-TRP-URA plates and grown at 30•C for
1230 3 days. Each strain carries both a [*URA3*] and a [*TRP1*] plasmid. The plasmids are either empty
1231 (EV) or carry the indicated *wtf* alleles under the control of galactose-inducible promoters. The
1232 horizontal break in the image of each plate is due to rearrangements of the images to facilitate
1233 easy comparison. All strains within a panel were grown on the same plates (i.e., one SC-TRP-
1234 URA or SC Gal-TRP-URA plate). **D.** Representative images of the same strains shown in C
1235 were induced in galactose for 4 hours at 30•C to express the indicated Wtf proteins. **E.**
1236 Representative images of cells induced with galactose and 500 nM β-estradiol for 4 hours at
1237 30•C to produce the indicated proteins. Rnq1-mCardinal marks the insoluble protein deposit
1238 (IPOD) that is associated with the vacuole [46–48]. In D-E, the images are not at the same
1239 brightness and contrast settings to clearly show localization of tagged proteins. 4^P indicates
1240 $Wtf4^{poison}$, 4^A indicates $Wtf4^{antidote}$, 61^P indicates $Wtf61^{poison}$, 61^A indicates $Wtf61^{antidote}$, TL is
1241 transmitted light, and the scale bar is 4 µm.
1242
1243 **Figure 6. Modification of *wtf4* exon 6 CDS repeats can disrupt antidote rescue.**
1244 **A.** Cartoon of two coding sequence repeat mutants of *S. kambucha wtf4*. **B**. Logo representing
1245 the amino acids encoded by the repeats found in exon 6 of *S. pombe wtf* genes from [20]. **C.**
1246 The amino acids encoded by the exon 6 repeats in *S. kambucha wtf4* and the *wtf4-rep2^{sc}* and
1247 *wtf4-rep2^{A}* mutant alleles. **D.** Spot assay of cells serially diluted and plated on SC-TRP-URA

1248 and SC Gal-TRP-URA plates and grown at 30•C for 3 days. Each strain carries both a [*URA3*]
1249 and a [*TRP1*] plasmid. The plasmids are either empty (EV) or carry the indicated *wtf4* alleles
1250 under the control of galactose-inducible promoters. The horizontal breaks in the image of each
1251 plate are due to rearrangements of the images to facilitate easy comparison. All strains within a
1252 panel were grown on the same plates (i.e., one SC-TRP-URA or SC Gal-TRP-URA plate). **E.**
1253 Representative images the same strains depicted in D were induced in galactose for 4 hours at
1254 30•C to express the indicated Wtf proteins. The images are not at the same brightness and
1255 contrast settings to clearly show localization of tagged proteins. The arrows in the TL panels
1256 highlight vacuoles. 4^{P} indicates $Wtf4^{poison}$, 4^{A} indicates $Wtf4^{antidote}$, TL indicates transmitted light,
1257 and the scale bar is 4 µm. **F**. Pearson's Correlation between mEos and mCherry signal in cells
1258 expressing the specified constructs from E. N>100, ***p<0.001, t-test.
1259
1260 **Figure 7. Analyses of Wtf proteins reveal additional functional constraints.**
1261 **A.** A dispersed Wtf^{poison} localization and poison-poison assembly can be observed across
1262 diverged species, and are associated with Wtf^{poison} toxicity. However, assembly and/or
1263 localization alone are insufficient to cause toxicity. In multiple examples of non-toxic proteins (an
1264 example is included in each panel), we observe either an endoplasmic reticulum-like localization
1265 or vacuolar localization. **B.** Modulating Wtf^{poison} assembly with exogenous tags affects its
1266 toxicity. While increasing Wtf^{poison} assembly via tethering to mEosNB-FTH1 suppresses toxicity,
1267 increasing solubility with NT* (or MBP in the case of *S. kambucha* $Wtf4^{poison}$*)* increases the
1268 toxicity. **C.** Multiple modalities of ineffective antidote rescue. Effective rescue of a Wtf^{poison} by the
1269 corresponding $Wtf^{antidote}$ (e.g., Wtf4 proteins) is supported by specific co-assembly and vacuolar
1270 localization. Artificial tethering of a mismatched Wtf^{poison} and $Wtf^{antidote}$ does not result in effective
1271 rescue. Disruption of poison-antidote co-localization (e.g., Wtf4-rep2^{sc} proteins) or vacuolar
1272 targeting of co-localized poison-antidote proteins (e.g., Wtf4-rep2^{A} proteins) also results in
1273 ineffective rescue.
1274
1275 **Supplemental Information**
1276
1277 **S1 Figure. Wtf proteins share limited amino acid identity but have common features**
1278 **A.** A cartoon of *S. octosporus wtf25* coding sequence (CDS). $Wtf25^{antidote}$ coding sequence is
1279 shown in purple, which includes exons 1-5. The $Wtf4^{poison}$ coding sequence is shown in navy,
1280 which begins at the 27th base pair of exon 2 and extends through exon 5. Row 4 depicts the
1281 predicted transmembrane domains (in red) and PY motif (in mustard). Row 5 depicts the CDS

1282 repeats found in exon 4 (in cobalt). Row 6 depicts the normalized hydrophobicity of Wtf25
1283 proteins from ProtScale, with the Kyle and Doolittle Hydropathy scale [80]. The higher the
1284 number on the scale, the higher the hydrophobicity of the amino acid. See S5 and S6 Tables for
1285 more detailed descriptions. **B.** Pairwise amino acid identity of the 6 $Wtf^{antidote}$ proteins shown.
1286 The amino acid sequences were aligned using Geneious Prime (2023.0.4), and the percentage
1287 amino acid identity is depicted as a heatmap, with yellow being 100% identity. **C.** Depiction of
1288 CDS repeats and lengths of 6 *$wtf^{antidote}$* CDSs. The CDS repeats found in exon 6 of *S. kambucha*
1289 *wtf4* are homologous to those found in exon 4 of the other *wtf* genes [19]. The scale bar
1290 represents 108 base pairs (bp). **D-E.** *S. octosporus wtf25* (**D**), *S. cryophilus wtf1*, and *S.*
1291 *osmophilus wtf41* (**E**) mutants constructed in this study. The categories have their respective
1292 wild type allele shown on top. See S1 Table for a comprehensive overview of the alleles and
1293 their phenotypes.
1294
1295 **S2 Figure. Deletion mutants affect $Wtf4^{poison}$ toxicity, self-assembly and localization.**
1296 Cartoon of *S. kambucha wtf4* exon deletion mutants (**A**), predicted transmembrane domain
1297 (TMD) deletion mutants (**B**) and a mutant that deletes a 9 amino acid conserved region encoded
1298 in exon 3 (**C**). **D.** A spot assay of cells serially diluted and plated on SC-LEU-URA and SC Gal-
1299 LEU-URA plates and grown at 30•C for 3 days. Each strain carries an empty [*LEU2*] plasmid,
1300 and either an empty [*URA3*] plasmid (EV) or the indicated *$wtf4^{poison}$-mEos* alleles under the
1301 control of a galactose-inducible promoter. The horizontal break in the image for each plate is
1302 due to rearrangement of the image to facilitate easy comparison. All strains were grown on the
1303 same plates (i.e., one SC-LEU-URA or SC Gal-LEU-URA plate). **E.** AmFRET values for three
1304 technical replicates of the specified $Wtf4^{poison}$-mEos proteins and monomer-mEos (negative
1305 control). The median is indicated with a solid line and the bars represent the interquartile range.
1306 For easier comparison, the values were normalized so that $Wtf4^{poison}$ had a median of 1 in each
1307 experiment. The data shown here does not include outliers. See S2 Data for the complete
1308 dataset and p-values. Statistical significance: *$p<0.008$, **$p<0.0008$, t-tests between the means
1309 of each replicate, with Bonferroni correction. **F.** Representative images of the same strains
1310 depicted in D were induced in galactose media for 4 hours at 30•C to express the indicated
1311 mEos-tagged proteins. The images are not at the same brightness and contrast settings to
1312 clearly show localization of tagged proteins. Yellow arrows indicate endoplasmic reticulum-like
1313 localization. 4^{P} indicates $Wtf4^{poison}$, TL is transmitted light, and the scale bar is 4 µm.
1314
1315 **S3 Figure. C-terminal truncations have inconsistent effects on Wtf^{poison} protein toxicity.**

1316 **A.** Cartoon of C-terminal truncation mutants of *S. kambucha wtf4*. **B.** Cartoon illustrating the
1317 amino acids lost with the C-terminal truncation alleles of *wtf4*. The amino acids comprising the
1318 exon 6 coding sequence repeats are highlighted in pink. **C.** A spot assay of cells serially diluted
1319 and plated on SC-TRP-URA and SC Gal-TRP-URA plates and grown at 30•C for 3 days. Each
1320 strain carries both an empty [*TRP1*] plasmid (EV) and a [*URA3*] plasmid that is either empty or
1321 carries the indicated *wtf4^{poison}-mEos* allele under the control of a galactose inducible promoter.
1322 **D.** AmFRET values for three technical replicates of the specified Wtf4^{poison}-mEos alleles and
1323 monomer-mEos (negative control). The median is indicated with a solid line and the bars
1324 represent the interquartile range. For easier comparison, the values were normalized so that
1325 Wtf4^{poison} had a median of 1 in each experiment. The data shown here does not include outliers.
1326 See S2 Data for the complete dataset and p-values. Statistical significance: *p<0.0125, t-test
1327 with Bonferroni correction. **E.** Representative images of the same strains depicted in C were
1328 induced with galactose media for 4 hours at 30•C to express the indicated mEos-tagged
1329 proteins. The images are not at the same brightness and contrast settings to clearly show
1330 localization of tagged proteins. 4^{P} indicates Wtf4^{poison}, TL is transmitted light, and the scale bar is
1331 4 µm. **F.** Cartoons of C-terminal truncation mutants of *S. cryophilus wtf1* (*wtf1-Δ^{10}*), *S.*
1332 *osmophilus wtf41* (*wtf41-Δ^{10}*), and *S. octosporus wtf25* (*wtf25-Δ^{10}*). **G.** Spot assays of cells
1333 serially diluted and plated on SC-URA and SC Gal-URA plates and grown at 30•C for 3 days.
1334 Each strain carries both an empty [*TRP1*] plasmid (EV) and an empty [*URA3*] plasmid (EV), or
1335 the indicated *wtf^{poison}-mEos* allele under the control of a galactose-inducible promoter. The
1336 horizontal breaks in the images for each plate are due to rearrangements of the image to
1337 facilitate easy comparison. All strains were grown on the same plates (i.e., one SC-TRP-URA or
1338 SC Gal-TRP-URA plate).
1339
1340 **S4 Figure**. **Reducing assembly with NT* tag increases Wtf25^{poison} toxicity.**
1341 **A.** Cartoon of alleles used in this experiment (B-E). The NT* tag has a general anti-aggregation
1342 property [33]. **B-C.** Spot assays of cells serially diluted on SC-TRP-URA and SC Gal-TRP-URA
1343 plates and grown at 30•C for 4 days. Each strain carries both a [*URA3*] and a [*TRP1*] plasmid.
1344 The plasmids are either empty (EV) or carry the indicated *wtf25* alleles under the control of
1345 galactose-inducible promoters. In B, the horizontal break in the image of each plate is due to a
1346 rearrangement of the image to facilitate easy comparison. All strains within a panel were grown
1347 on the same plates (i.e., one SC-TRP-URA or SC Gal-TRP-URA plate for panel B). **D.**
1348 Representative images of the same strains shown in C were induced with galactose media for 4
1349 hours at 30•C to express the indicated Wtf25^{poison}-mEos proteins and/or Wtf25^{antidote}-mCherry.

1350 The images are not at the same brightness and contrast settings to clearly show localization of
1351 tagged proteins. 25^{P} indicates $Wtf25^{poison}$, 25^{A} indicates $Wtf25^{antidote}$, TL is transmitted light, and
1352 the scale bar is 4 µm. **E**. Pearson's Correlation between mCherry and mEos signal in cells from
1353 D expressing the specified proteins. N>100, p>0.05, t-test.
1354
1355 **S5 Figure. Reducing Wtf^{poison} assembly with MBP tag affects toxicity.**
1356 **A.** Cartoon of alleles used in this experiment (B-C). MBP is the *E. coli* Maltose Binding Protein
1357 [75]. **B.** Spot assay of cells serially diluted and plated on SC-TRP-URA and SC Gal-TRP-URA
1358 plates and grown at 30•C for 4 days. Each strain carries both an empty [*TRP1*] plasmid and a
1359 [*URA3*] plasmid that is either empty (EV) or carries the indicated *wtf^{poison}-mEos* allele under the
1360 control of a galactose-inducible promoter. The horizontal break in the image of each plate is due
1361 to rearrangement of the image to facilitate easy comparison. All strains were grown on the same
1362 plates (i.e., one SC Gal-TRP-URA plate or SC-Trp-Ura). **C.** Representative images of the same
1363 strains depicted in B induced with galactose media for 4 hours at 30•C to express the indicated
1364 mEos-tagged proteins. The images are not at the same brightness and contrast settings to
1365 clearly show localization of tagged proteins. Yellow arrows indicate endoplasmic reticulum-like
1366 localization. 4^{P} indicates $Wtf4^{poison}$, 25^{P} indicates $Wtf25^{poison}$, TL is transmitted light, and the
1367 scale bar is 4 µm. **D.** AmFRET values for three technical replicates of the specified Wtf^{poison}-
1368 mEos alleles and monomer-mEos (negative control). The median is indicated with a solid line
1369 and the bars represent the interquartile range. For easier comparison, the values were
1370 normalized so that $Wtf4^{poison}$ had a median of 1 in each experiment. The data shown does not
1371 include outliers. See S2 Data for the complete dataset and p-values. Statistical significance:
1372 *p<0.016, t-test with Bonferroni correction.
1373
1374 **S6 Figure. The fluorescence signal intensity of expressed Wtf^{poison} proteins does not**
1375 **correlate with toxicity.**
1376 **A-F** Acceptor fluorescence intensity (in arbitrary units, a.u.) of similarly sized live cells across all
1377 Wtf DAmFRET experiments in this study, with the line indicating the median of the population.
1378 Data represented here is from the following experiments: A corresponds to Fig 2B, B
1379 corresponds to S2 Fig E, C corresponds to S3 Fig D, D corresponds to Fig 4C, E corresponds
1380 alleles in S4 Fig, and F corresponds to S5 Fig D. The Y-axis is scaled to a log10 scale. The data
1381 are color coded, with toxic poisons in teal, and non-toxic alleles in orange.
1382
1383 **S7 Figure. Limited modularity of the $Wtf4^{antidote}$-specific domain.**

1384 **A.** Cartoon of *wtf4*^{antidote} exon 1 and mutants that relocate, or both relocate and mutate the exon.
1385 **B.** AmFRET values for three technical replicates of the specified mEos-tagged proteins and
1386 monomer-mEos (negative control). The median is indicated with a solid line and the bars
1387 represent 1.5 times the interquartile range. For easier comparison, the values were normalized
1388 so that Wtf4^{poison} had a median of 1 in each experiment. The data shown does not include
1389 outliers. See S2 Data for the complete dataset and p-values. Statistical significance: *$p<0.0125$,
1390 t-tests with Bonferroni correction. **C-D.** Spot assays of cells serially diluted on SC-TRP-URA and
1391 SC Gal-TRP-URA plates and grown at 30•C for 3 days. Each strain carries both a [*URA3*] and a
1392 [*TRP1*] plasmid. The plasmids are either empty (EV) or carry the indicated *wtf4* alleles under the
1393 control of galactose-inducible promoters. The horizontal breaks in the images of each plate in
1394 panels C and E are due to rearrangements of the images to facilitate easy comparison. All
1395 strains within a panel were grown on the same plates (i.e., one SC-TRP-URA or SC Gal-TRP-
1396 URA plate for panel C). **E.** Representative images of the same strains shown in C induced with
1397 galactose media for 4 hours at 30•C to express the Wtf4^{poison}-mEos, Wtf4 exon1-mCherry, or
1398 both proteins. **F.** Representative images of the same strains shown in D were induced with
1399 galactose media for 4 hours at 30•C to the indicated *wtf4* alleles. In E-F, arrows in the
1400 transmitted light images indicate vacuoles. The images are not at the same brightness and
1401 contrast settings to clearly show localization of the tagged proteins. 4^{P} indicates Wtf4^{poison}, 4^{A}
1402 indicates Wtf4^{antidote}, Ex1 is Wtf4 exon1, TL is transmitted light, and the scale bar is 4 µm.
1403
1404 **S8 Figure. Effective neutralization of Wtf25^{poison} requires more than a physical connection**
1405 **to a Wtf^{antidote}.**
1406 **A.** Cartoon of constructs used in this experiment. *S. octosporus* Wtf25^{poison} was tagged at the C-
1407 terminus with either mCherry or GBP-mCherry (GBP: GFP-binding protein). *S. octosporus*
1408 Wtf25^{antidote} was tagged with mEos or GFP. *S. cryophilus* Wtf1^{antidote} was tagged with GFP. *S.*
1409 *cryophilus* Wtf1^{poison} was tagged with mCherry. **B.** Experimental set up and summary of the
1410 results shown in C and D. In a matching Wtf protein pair (top), poison-antidote interaction and
1411 rescue of poison toxicity is observed. In the mismatched pair (bottom), interaction between GFP
1412 and GBP results in a forced interaction between the poison and the antidote (shown in D). This
1413 interaction is insufficient to rescue the mismatched poison (shown in C). **C.** Spot assay of cells
1414 serially diluted and plated on SC-TRP-URA and SC Gal-TRP-URA plates and grown at 30•C for
1415 3 days. Each strain carries both a [*URA3*] and a [*TRP1*] plasmid. The plasmids are either empty
1416 (EV) or carry the indicated *wtf* alleles under the control of galactose-inducible promoters. The
1417 horizontal breaks in the images of each plate are due to rearrangements of the image to

1418 facilitate easy comparison. All strains within a panel were grown on the same plates (i.e., one
1419 SC-TRP-URA or SC Gal-TRP-URA plate). **D.** Representative images the strains depicted in C
1420 were induced in galactose for 4 hours at 30•C to express the indicated Wtf proteins. The images
1421 are not at the same brightness and contrast settings to clearly show localization of tagged
1422 proteins. 25^{P} indicates $Wtf25^{poison}$, 25^{A}- indicates $Wtf25^{antidote}$, 1^{P} indicates $Wtf1^{poison}$, 1^{A} indicates
1423 $Wtf1^{antidote}$, TL indicates transmitted light, and the scale bar is 4 µm.
1424
1425 **S9 Figure. *wtf4* coding sequence repeats are dispensable, but can affect antidote rescue.**
1426 **A.** Cartoon of exon 3 and exon 6 coding sequence repeat deletion mutants of *S. kambucha*
1427 *wtf4*. **B-C.** Logo for amino acids encoded by the repeats found in exon 3 (B) and exon 6 (C) of
1428 *S. pombe wtf* genes from [20]. The sequence of the amino acids encoded in each repeat region
1429 in *S. kambucha wtf4* is shown below each logo. **D.** Spot assay of cells serially diluted and plated
1430 on SC-TRP-URA and SC Gal-TRP-URA plates and grown at 30•C for 3 days. Each strain
1431 carries both a [*URA3*] and a [*TRP1*] plasmid. The plasmids are either empty (EV) or carry the
1432 indicated *wtf4* alleles under the control of galactose-inducible promoters. The horizontal break in
1433 the image of each plate is due to rearrangements of the images to facilitate easy comparison.
1434 All strains within a panel were grown on the same plates (i.e., one SC-TRP-URA or SC Gal-
1435 TRP-URA plate). **E.** Representative images of the same strains as depicted in D were induced
1436 in galactose for 4 hours at 30•C to express the indicated Wtf4 proteins. The images are not at
1437 the same brightness and contrast settings to clearly show localization of tagged proteins. The
1438 arrows in the TL panels highlight vacuoles. 4^{P} indicates $Wtf4^{poison}$, 4^{A} indicates $Wtf4^{antidote}$, TL
1439 indicates transmitted light, and the scale bar is 4 µm. **F**. Pearson's Correlation between mEos
1440 and mCherry signal in cells expressing the specified constructs from E. N>100, ***p<0.001, t-
1441 test.
1442
1443 **S10 Figure. Coding sequence repeat mutants do not interact with wildtype Wtf4 proteins**
1444 **functionally.**
1445 **A.** Cartoon of coding sequence repeat mutants of *S. kambucha wtf4.* **B-H.** Spot assays of cells
1446 serially diluted on SC-TRP-URA and SC Gal-TRP-URA plates and grown at 30•C for 3 days.
1447 Each strain carries both a [*URA3*] and a [*TRP1*] plasmid. The plasmids are either empty (EV) or
1448 carry the indicated *wtf4* alleles under the control of galactose-inducible promoters. The
1449 horizontal breaks in the images in within a panel are due to rearrangements of the images to
1450 facilitate easy comparison. All strains within a panel were grown on the same plates (i.e., one
1451 SC-TRP-URA or SC Gal-TRP-URA plate in panel B).

1452

1453 **S11 Figure. Swapping *wtf* CDS repeats across species affects Wtf25 antidote rescue.**
1454 **A.** Cartoon of a coding sequence repeat mutant of *S. octosporus wtf25*. **B**. Logo representing
1455 the amino acids encoded by the repeats found in exon 4 of *S. octosporus wtf* genes from [19].
1456 **C.** The amino acids encoded by the exon 4 repeats of *S. octosporus wtf25* and by the exon 6
1457 repeats of *S. kambucha wtf4*. **D.** Spot assay of cells serially diluted and plated on SC-TRP-URA
1458 and SC Gal-TRP-URA plates and grown at 30•C for 3 days. Each strain carries both a [*URA3*]
1459 and a [*TRP1*] plasmid. The plasmids are either empty (EV) or carry the indicated *wtf25* alleles
1460 under the control of galactose-inducible promoters. The horizontal breaks in the images are due
1461 to rearrangements of the images to facilitate easy comparison. All strains within a panel were
1462 grown on the same plates (i.e., one SC-TRP-URA or SC Gal-TRP-URA plate). **E.**
1463 Representative images of the same strains depicted in D were induced in galactose for 4 hours
1464 at 30•C to express the indicated Wtf25 proteins. The images are not at the same brightness and
1465 contrast settings to clearly show localization of tagged proteins. The arrows in the TL panel
1466 highlight vacuoles. Yellow arrows indicate endoplasmic reticulum-like localization. 25^{P} indicates
1467 $Wtf25^{poison}$, 25^{A} indicates $Wtf25^{antidote}$, TL indicates transmitted light, and the scale bar is 4 µm.
1468

1469 **S12 Figure. *S. octosporus wtf25* coding sequence repeats are functionally dispensable**
1470 **for poison toxicity but promote antidote rescue.**
1471 **A.** Cartoon of *S. octosporus wtf25* exon 4 coding sequence repeat deletion mutant. **B.** Logo for
1472 the amino acids encoded by the repeats found in exon 4 of *S. octosporus wtf* genes from [19] **C.**
1473 Spot assay of cells serially diluted and plated on SC-TRP-URA and SC Gal-TRP-URA plates
1474 and grown at 30•C for 4 days. Each strain carries both a [*URA3*] and a [*TRP1*] plasmid. The
1475 plasmids are either empty (EV) or carry the indicated *wtf25* alleles under the control of
1476 galactose-inducible promoters. The horizontal breaks in the images are due to rearrangements
1477 of the images to facilitate easy comparison. All strains within a panel were grown on the same
1478 plates (i.e., one SC-TRP-URA or SC Gal-TRP-URA plate). **D.** Representative images the same
1479 strains depicted in C were induced in galactose for 4 hours at 30•C to express the indicated
1480 Wtf25 proteins. The images are not at the same brightness and contrast settings to clearly show
1481 localization of tagged proteins. The arrows in the TL panels highlight vacuoles. Yellow arrows
1482 indicate endoplasmic reticulum-like localization. 25^{P} indicates $Wtf25^{poison}$, 25^{A} indicates
1483 $Wtf25^{antidote}$, TL indicates transmitted light, and the scale bar is 4 µm.
1484

1485 **S13 Figure. Idiosyncratic poison and antidote compatibility between wild-type and**
1486 **truncation alleles of *wtf4*.**
1487 **A.** Cartoon of *S. kambucha wtf4* C-terminal truncation mutants. **B.** Spot assay of cells serially
1488 diluted and plated on SC-TRP-URA and SC Gal-TRP-URA plates and grown at 30•C for 3 days.
1489 Each strain carries both a [*URA3*] and a [*TRP1*] plasmid. The plasmids are either empty (EV) or
1490 carry the indicated *wtf4* alleles under the control of galactose-inducible promoters. The
1491 horizontal breaks in the images are due to rearrangements of the images to facilitate easy
1492 comparison. All strains within a panel were grown on the same plates (i.e., one SC-TRP-URA or
1493 SC Gal-TRP-URA plate). **C.** Representative images the strains depicted in B were induced in
1494 galactose for 4 hours at 30•C to express the indicated Wtf4 proteins. The images are not at the
1495 same brightness and contrast settings to clearly show localization of tagged proteins. The
1496 arrows in the TL panels highlight vacuoles. 4^{P} indicates $Wtf4^{poison}$, 4^{A} indicates $Wtf4^{antidote}$, TL
1497 indicates transmitted light, and the scale bar is 4 µm.
1498
1499 **S14 Figure. C-terminus truncation alleles of diverged Wtf^{poison}s are rescued by their**
1500 **corresponding wild type $Wtf^{antidote}$s.**
1501 **A.** Cartoon of *S. cryophilus wtf1*, *S. osmophilus wtf41*, and *S. octosporus wtf25* C-terminal
1502 truncation mutants. **B-D.** Spot assays of cells serially diluted on SC-TRP-URA and SC Gal-TRP-
1503 URA plates and grown at 30•C for 3 days. Each strain carries both a [*URA3*] and a [*TRP1*]
1504 plasmid. The plasmids are either empty (EV) or carry the indicated
1505 *wtf* alleles under the control of galactose-inducible promoters. The horizontal breaks in the
1506 images within a panel are due to rearrangements of the images to facilitate easy comparison.
1507 All strains within a panel were grown on the same plates (i.e., one SC-TRP-URA or SC Gal-
1508 TRP-URA plate).
1509
1510 **S1 Table. Overview of *wtf* alleles and their phenotypes in this study**. Columns 1-2 describe
1511 the allele names and their construction. Columns 3-4 describe the toxicity of the poison and
1512 antidote proteins encoded by the corresponding allele. Column 5 notes if the mutant antidote
1513 can rescue the corresponding poison allele. Column 6-7 note if the specific antidote allele can
1514 rescue the wild-type poison (Column 6), or if the specific poison can be rescued by the wild-type
1515 antidote (Column 7). Column 9 notes if the corresponding antidote can rescue other poison
1516 alleles. Column 10 notes the AmFRET values are comparable to the wild-type $Wtf4^{poison}$-mEos
1517 or monomer-mEos. Finally, column 11 notes the figures/supplemental figures where these

1518 alleles can be found. Rows are separated based on the wild-type allele that the mutants were
1519 constructed from, where applicable. ND indicates that the specified experiment was not done.
1520
1521 **S2 Table. Yeast strains used in this study.** Column 1 is the figure where these strains were
1522 used, Column 2 is the name of the yeast strain and column 3 is the genotype of the strain. If the
1523 strain was constructed in this study, column 4 has the details on how the strain was constructed.
1524 If the strain was constructed in another study, column 5 notes the references for the same.
1525
1526 **S3 Table. Plasmids used in this study.** Column 1 denotes if the plasmids were used for strain
1527 construction or cloning, and the specific wild-type alleles that the plasmids correspond to.
1528 Column 2 is the name of the plasmid and column 3 is a short description of the plasmid. If the
1529 plasmid was not constructed in this study, column 4 references the studies the plasmids were
1530 constructed in.
1531
1532 **S4 Table. Oligos used in this study.** Column 1 denotes the name of the oligo and column 2
1533 has the sequence of the oligos. If the oligo was not constructed in this study, column 3
1534 references the studies the oligos were used in.
1535
1536 **S5 Table. Overview of features across *wtf* driver genes.** Column 1 denotes the *wtf* driver
1537 gene, and columns 2-8 describe specific features of each gene and their encoded proteins.
1538 Column 2 notes if the gene has been shown to drive in fission yeast or been shown to encode
1539 for functional Wtf poison and antidote proteins in *S. cerevisiae*. Column 3 notes the number of
1540 exons in the gene, and column 4 notes the size of the $Wtf^{antidote}$ protein in amino acids. If the
1541 antidote sequence had a predicted coiled-coil domain, column 4 notes the size and location in
1542 the antidote protein as described in [15]. Column 5 notes the numbers of PY motifs (L/PPXY;
1543 [24]) in exon 1. While some $Wtf^{antidote}$ proteins also have an additional PY motif in exon 2, we
1544 didn't include that information here since those motifs are shared by the corresponding poison
1545 proteins as well. Column 6 notes the number of predicted transmembrane domains predicted by
1546 TMHMM2.0 [71,72]. Column 7 notes the length of the exon 3 coding sequence repeats (if
1547 present) in amino acids. Column 8 notes the length of the exon 4/6 coding sequence repeats (if
1548 present) in amino acids. NA (not applicable) here indicates that the repeats were not present in
1549 the Wtf protein. Column 8 mentions the reference(s) where these genes/encoded proteins were
1550 characterized.
1551

1552 **S6 Table. Overview of predicted transmembrane domains of Wtf^{antidote} proteins.** The
1553 results from the TMHMM2.0 [71,72] analysis of Wtf^{antidote} proteins encoded by *wtf* driver genes in
1554 S5 table are detailed here. Find the specific results of the analyses, including the number of
1555 amino acids in the predicted transmembrane domains, probability of the N-terminal being
1556 internal to the membrane (N-in), the specific location and the length of the predicted
1557 transmembrane domains.
1558
1559 **S1 Data. Raw Data for Pearson's Correlation tests performed in this study.** Each sheet
1560 contains the raw data for the Pearson's Correlation tests and the statistical analysis
1561 corresponding to the tests performed in Fig 4F, S4 Fig E, Fig 6F and S9 Fig F respectively. See
1562 Methods for how this analysis was performed.
1563
1564 **S2 Data. Raw Data for AmFRET plots presented in this study.** Each sheet contains the raw
1565 data and the statistical analysis for the AmFRET plots of different Wtf^{poison}-mEos proteins,
1566 Wtf4^{antidote}-mEos, *S. kambucha wtf4* Exon1-mEos and monomer-mEos proteins in Fig 2B, S2
1567 Fig E, S3 Fig D, Fig 4C, S5 Fig, S6 Fig D and S7 Fig B respectively. The corresponding raw
1568 data for the Acceptor fluorescence intensity presented in S6 Fig for each of these experiments
1569 are found next to the relevant AmFRET data. See Methods for how this analysis was performed.
1570
1571 **Acknowledgements**
1572 We thank the members of the Zanders lab, the Halfmann lab and the Core facilities at Stowers
1573 Institute for their help and guidance throughout the stages of development of this paper. We
1574 thank the reviewers for their constructive comments that have improved the paper.
1575
1576 **Data Availability**
1577 All relevant data are within the manuscript and the Supporting Information Files. Additional raw
1578 data and images can be found at the Stowers Original Data Repository at
1579 http://www.stowers.org/research/publications/libpb-2486. Instructions for accessing data from
1580 the Stowers original data repository via FTP can be found at
1581 https://www.stowers.org/research/publications/odr#ftp.
1582
1583 **Funding**
1584 This work was supported by The Stowers Institute for Medical Research (SEZ, RHN); National
1585 Institutes of Health (NIH) R35 GM151982-01 and DP2 GM132936 (SEZ); and the Eunice

Kennedy Shriver National Institute of Child Health & Human Development of the NIH under Award Number F31HD097974 (NLN). The funders had no role in study design, data collection and analysis, or manuscript preparation. The content is solely the responsibility of the authors and does not necessarily represent the official views of the funders.

Competing interests

I have read the journal's policy, and the authors of this manuscript have the following competing interests: NLN, SEZ: Inventor on patent application based on *wtf* meiotic drivers. Patent application serial 62/491,107. The other authors declare that no competing interests exist.

References

[1] Burt A, Trivers R. Genes in Conflict. Harvard University Press; 2006. https://doi.org/10.2307/J.CTVJHZRC6.

[2] Sandler L, Novitski E. Meiotic Drive as an Evolutionary Force. Am Nat 1957;91:105–10.

[3] Bravo Núñez MA, Nuckolls NL, Zanders SE. Genetic Villains: Killer Meiotic Drivers. Trends in Genetics 2018;34:424–33. https://doi.org/10.1016/j.tig.2018.02.003.

[4] Zanders SE, Unckless RL. Fertility Costs of Meiotic Drivers. Current Biology 2019;29:R512–20. https://doi.org/10.1016/j.cub.2019.03.046.

[5] Wang C, Wang J, Lu J, Wang H, Wu C, Xiong Y, et al. A natural gene drive system confers reproductive isolation in rice. Cell 2023;186:3577–92. https://doi.org/10.1016/j.cell.2023.06.023.

[6] Xie Y, Shen R, Chen L, Liu YG. Molecular mechanisms of hybrid sterility in rice. Sci China Life Sci 2019;62:737–43. https://doi.org/10.1007/S11427-019-9531-7.

[7] Li J, Zhou J, Zhang Y, Yang Y, Pu Q, Tao D. New Insights into the Nature of Interspecific Hybrid Sterility in Rice. Front Plant Sci 2020;11. https://doi.org/10.3389/FPLS.2020.555572.

[8] Myint ZM, Koide Y, Takanishi W, Ikegaya T, Kwan C, Hikichi K, et al. OlCHR, encoding a chromatin remodeling factor, is a killer causing hybrid sterility between rice species *Oryza sativa* and *O. longistaminata*. IScience 2024;27. https://doi.org/10.1016/J.ISCI.2024.109761.

[9] Saupe SJ, Johannesson H. On the Mechanistic Basis of Killer Meiotic Drive in Fungi. Annu Rev Microbiol 2022; 76:305–23. https://doi.org/10.1146/ANNUREV-MICRO-041320-113730.

[10] Simon M, Durand S, Ricou A, Vrielynck N, Mayjonade B, Gouzy J, et al. APOK3, a pollen killer antidote in *Arabidopsis thaliana*. Genetics 2022;221. https://doi.org/10.1093/GENETICS/IYAC089.

[11] Wang D, Wang H, Xu X, Wang M, Wang Y, Chen H, et al. Two complementary genes in a presence-absence variation contribute to *indica-japonica* reproductive isolation in rice. Nat Commun 2023;14. https://doi.org/10.1038/S41467-023-40189-X.

[12] You S, Zhao Z, Yu X, Zhu S, Wang J, Lei D, et al. A toxin-antidote system contributes to interspecific reproductive isolation in rice. Nat Commun 2023;14. https://doi.org/10.1038/S41467-023-43015-6.

[13] Courret C, Wei X, Larracuente AM. New perspectives on the causes and consequences of male meiotic drive. Curr Opin Genet Dev 2023;83. https://doi.org/10.1016/J.GDE.2023.102111.

[14] Lai EC, Vogan AA. Proliferation and dissemination of killer meiotic drive loci. Curr Opin Genet Dev 2023;82. https://doi.org/10.1016/J.GDE.2023.102100.

[15] Nuckolls NL, Mok AC, Lange JJ, Yi K, Kandola TS, Hunn AM, et al. The *wtf4* meiotic driver utilizes controlled protein aggregation to generate selective cell death. Elife 2020; 9:1–35. https://doi.org/10.7554/eLife.55694.

[16] Urquhart AS, Gardiner DM. A Natural Fungal Gene Drive Enacts Killing via DNA Disruption. MBio 2023;14. https://doi.org/10.1128/MBIO.03173-22.

[17] Hu W, Jiang Z Di, Suo F, Zheng JX, He WZ, Du LL. A large gene family in fission yeast encodes spore killers that subvert Mendel's law. Elife 2017;6. https://doi.org/10.7554/ELIFE.26057.

[18] Brysch-Herzberg M, Jia GS, Sipiczki M, Seidel M, Li W, Assali I, et al. *Schizosaccharomyces lindneri* sp. nov., a fission yeast occurring in honey. Yeast 2023; 40:237–53. https://doi.org/10.1002/YEA.3857.

[19] De Carvalho M, Jia GS, Nidamangala Srinivasa A, Billmyre RB, Xu YH, Lange JJ, et al. The *wtf* meiotic driver gene family has unexpectedly persisted for over 100 million years. Elife 2022;11. https://doi.org/10.7554/eLife.81149.

[20] Eickbush MT, Young JM, Zanders SE. Killer meiotic drive and dynamic evolution of the *wtf* gene family. Mol Biol Evol 2019; 36:1201–14. https://doi.org/10.1093/molbev/msz052.

[21] Xu Y-H, Suo F, Zhang X-R, Du T-Y, Hua Y, Jia G-S, et al. Evolutionary modes of *wtf* meiotic driver genes in *Schizosaccharomyces pombe*. BioRxiv 2024:2024.05.30.596636. https://doi.org/10.1101/2024.05.30.596636.

[22] Nuckolls NL, Núñez MAB, Eickbush MT, Young JM, Lange JJ, Yu JS, et al. *wtf* genes are prolific dual poison-antidote meiotic drivers. Elife 2017;6. https://doi.org/10.7554/ELIFE.26033.

[23] Nuckolls NL, Nidamangala Srinivasa A, Mok AC, Helston RM, Núñez MAB, Lange JJ, et al. *S. pombe wtf* drivers use dual transcriptional regulation and selective protein exclusion from spores to cause meiotic drive. PLoS Genet 2022;18. https://doi.org/10.1371/JOURNAL.PGEN.1009847.

[24] Zheng JX, Du TY, Shao GC, Ma ZH, Jiang Z Di, Hu W, et al. Ubiquitination-mediated Golgi-to-endosome sorting determines the toxin-antidote duality of fission yeast *wtf* meiotic drivers. Nat Commun 2023;14. https://doi.org/10.1038/S41467-023-44151-9.

[25] Bravo Nuñez MA, Sabbarini IM, Eickbush MT, Liang Y, Lange JJ, Kent AM, et al. Dramatically diverse *Schizosaccharomyces pombe wtf* meiotic drivers all display high gamete-killing efficiency. PLoS Genet 2020;16. https://doi.org/10.1371/journal.pgen.1008350.

[26] Bravo Núñez MA, Lange JJ, Sarah ZE. A suppressor of a *wtf* poison-antidote meiotic driver acts via mimicry of the driver's antidote. PLoS Genet 2018;14. https://doi.org/10.1371/journal.pgen.1007836.

1671 [27] Mannini B, Mulvihill E, Sgromo C, Cascella R, Khodarahmi R, Ramazzotti M, et al.
1672 Toxicity of protein oligomers is rationalized by a function combining size and surface
1673 hydrophobicity. ACS Chem Biol 2014; 9:2309–17.
1674 https://doi.org/10.1021/CB500505M/SUPPL_FILE/CB500505M_SI_001.PDF.
1675 [28] Ries HM, Nussbaum-Krammer C. Shape matters: The complex relationship between
1676 aggregation and toxicity in protein-misfolding diseases. Essays Biochem 2016; 60:181–
1677 90. https://doi.org/10.1042/EBC20160008.
1678 [29] Bucciantini M, Giannoni E, Chiti F, Baroni F, Taddei N, Ramponi G, et al. Inherent
1679 toxicity of aggregates implies a common mechanism for protein misfolding diseases.
1680 Nature 2002 416:6880 2002; 416:507–11. https://doi.org/10.1038/416507a.
1681 [30] Khan T, Kandola TS, Wu J, Venkatesan S, Ketter E, Lange JJ, et al. Quantifying
1682 Nucleation In Vivo Reveals the Physical Basis of Prion-like Phase Behavior. Mol Cell
1683 2018; 71:155-168.e7. https://doi.org/10.1016/j.molcel.2018.06.016.
1684 [31] Bellapadrona G, Elbaum M. Supramolecular Protein Assemblies in the Nucleus of Human
1685 Cells. Angewandte Chemie International Edition 2014; 53:1534–7.
1686 https://doi.org/10.1002/ANIE.201309163.
1687 [32] Bracha D, Walls MT, Wei MT, Zhu L, Kurian M, Avalos JL, et al. Mapping Local and
1688 Global Liquid Phase Behavior in Living Cells Using Photo-Oligomerizable Seeds. Cell
1689 2018; 175:1467-1480.e13. https://doi.org/10.1016/J.CELL.2018.10.048.
1690 [33] Schellhaus AK, Xu S, Gierisch ME, Vornberger J, Johansson J, Dantuma NP. A spider
1691 silk-derived solubility domain inhibits nuclear and cytosolic protein aggregation in human
1692 cells. Communications Biology 2022 5:1 2022; 5:1–8. https://doi.org/10.1038/s42003-
1693 022-03442-5.
1694 [34] Kronqvist N, Sarr M, Lindqvist A, Nordling K, Otikovs M, Venturi L, et al. Efficient
1695 protein production inspired by how spiders make silk. Nat Commun 2017;8.
1696 https://doi.org/10.1038/NCOMMS15504.
1697 [35] Askarieh G, Hedhammar M, Nordling K, Saenz A, Casals C, Rising A, et al. Self-
1698 assembly of spider silk proteins is controlled by a pH-sensitive relay. Nature 2010
1699 465:7295 2010; 465:236–8. https://doi.org/10.1038/nature08962.
1700 [36] Abelein A, Chen G, Kitoka K, Aleksis R, Oleskovs F, Sarr M, et al. High-yield Production
1701 of Amyloid-β Peptide Enabled by a Customized Spider Silk Domain. Scientific Reports
1702 2020 10:1 2020; 10:1–10. https://doi.org/10.1038/s41598-019-57143-x.
1703 [37] Jaudzems K, Askarieh G, Landreh M, Nordling K, Hedhammar M, Jörnvall H, et al. pH-
1704 Dependent Dimerization of Spider Silk N-Terminal Domain Requires Relocation of a
1705 Wedged Tryptophan Side Chain. J Mol Biol 2012; 422:477–87.
1706 https://doi.org/10.1016/J.JMB.2012.06.004.
1707 [38] Andersson M, Chen G, Otikovs M, Landreh M, Nordling K, Kronqvist N, et al. Carbonic
1708 Anhydrase Generates CO2 and H+ That Drive Spider Silk Formation Via Opposite
1709 Effects on the Terminal Domains. PLoS Biol 2014;12: e1001921.
1710 https://doi.org/10.1371/JOURNAL.PBIO.1001921.
1711 [39] Brumbaugh-Reed EH, Aoki K, Toettcher JE, Toettcher J. Rapid and reversible dissolution
1712 of biomolecular condensates using light-controlled recruitment of a solubility tag.
1713 BioRxiv 2024:2024.01.16.575860. https://doi.org/10.1101/2024.01.16.575860.
1714 [40] Raran-Kurussi S, Keefe K, Waugh DS. Positional effects of fusion partners on the yield
1715 and solubility of MBP fusion proteins. Protein Expr Purif 2015; 110:159.
1716 https://doi.org/10.1016/J.PEP.2015.03.004.

1717 [41] Raran-Kurussi S, Sharwanlal SB, Balasubramanian D, Mote KR. A comparison between
1718 MBP- and NT* as N-terminal fusion partner for recombinant protein production in E. coli.
1719 Protein Expr Purif 2022; 189:105991. https://doi.org/10.1016/J.PEP.2021.105991.
1720 [42] Blake WJ, Kærn M, Cantor CR, Collins JJ. Noise in eukaryotic gene expression. Nature
1721 2003 422:6932 2003; 422:633–7. https://doi.org/10.1038/nature01546.
1722 [43] Elowitz MB, Levine AJ, Siggia ED, Swain PS. Stochastic gene expression in a single cell.
1723 Science (1979) 2002; 297:1183–6. https://doi.org/10.1126/SCIENCE.1070919/
1724 [44] Ozbudak EM, Thattai M, Kurtser I, Grossman AD, Van Oudenaarden A. Regulation of
1725 noise in the expression of a single gene 2002. https://doi.org/10.1038/ng869.
1726 [45] Nordholt N, Van Heerden J, Kort R, Bruggeman FJ. Effects of growth rate and promoter
1727 activity on single-cell protein expression. Scientific Reports 2017 7:1 2017; 7:1–11.
1728 https://doi.org/10.1038/s41598-017-05871-3.
1729 [46] Rothe S, Prakash A, Tyedmers J. The Insoluble Protein Deposit (IPOD) in Yeast. Front
1730 Mol Neurosci 2018; 11:385163. https://doi.org/10.3389/FNMOL.2018.00237/
1731 [47] Tyedmers J, Treusch S, Dong J, McCaffery JM, Bevis B, Lindquist S. Prion induction
1732 involves an ancient system for the sequestration of aggregated proteins and heritable
1733 changes in prion fragmentation. Proc Natl Acad Sci U S A 2010; 107:8633–8.
1734 https://doi.org/10.1073/PNAS.1003895107/
1735 [48] Kaganovich D, Kopito R, Frydman J. Misfolded proteins partition between two distinct
1736 quality control compartments. Nature 2008 454:7208 2008; 454:1088–95.
1737 https://doi.org/10.1038/nature07195.
1738 [49] Kayed R, Head E, Thompson JL, McIntire TM, Milton SC, Cotman CW, et al. Common
1739 structure of soluble amyloid oligomers implies common mechanism of pathogenesis.
1740 Science (1979) 2003; 300:486–9. https://doi.org/10.1126/SCIENCE.1079469/
1741 [50] Majumdar A, Cesario WC, White-Grindley E, Jiang H, Ren F, Khan MR, et al. Critical
1742 role of amyloid-like oligomers of *Drosophila* Orb2 in the persistence of memory. Cell
1743 2012; 148:515–29. https://doi.org/10.1016/J.CELL.2012.01.004.
1744 [51] Alberti S, Halfmann R, King O, Kapila A, Lindquist S. A systematic survey identifies
1745 prions and illuminates sequence features of prionogenic proteins. Cell 2009; 137:146.
1746 https://doi.org/10.1016/J.CELL.2009.02.044.
1747 [52] Perov S, Lidor O, Salinas N, Golan N, Tayeb-Fligelman E, Deshmukh M, et al. Structural
1748 Insights into Curli CsgA Cross-β Fibril Architecture Inspire Repurposing of Anti-amyloid
1749 Compounds as Anti-biofilm Agents. PLoS Pathog 2019;15.
1750 https://doi.org/10.1371/JOURNAL.PPAT.1007978.
1751 [53] Yan Z, Yin M, Chen J, Li X. Assembly and substrate recognition of curli biogenesis
1752 system. Nature Communications 2020 11:1 2020; 11:1–10.
1753 https://doi.org/10.1038/s41467-019-14145-7.
1754 [54] Sheng J, Olrichs NK, Gadella BM, Kaloyanova D V., Bernd Helms J. Regulation of
1755 Functional Protein Aggregation by Multiple Factors: Implications for the Amyloidogenic
1756 Behavior of the CAP Superfamily Proteins. Int J Mol Sci 2020; 21:1–23.
1757 https://doi.org/10.3390/IJMS21186530.
1758 [55] Jackson MP, Hewitt EW. Why Are Functional Amyloids Non-Toxic in Humans?
1759 Biomolecules 2017;7. https://doi.org/10.3390/BIOM7040071.
1760 [56] Kong L, Sui C, Chen T, Zhang L, Zhao W, Zheng Y, et al. The ubiquitin E3 ligase
1761 TRIM10 promotes STING aggregation and activation in the Golgi apparatus. Cell Rep
1762 2023;42. https://doi.org/10.1016/j.celrep.2023.112306.

1763 [57] Liu B, Zhang M, Chu H, Zhang H, Wu H, Song G, et al. The ubiquitin E3 ligase TRIM31
1764 promotes aggregation and activation of the signaling adaptor MAVS through Lys63-
1765 linked polyubiquitination. Nat Immunol 2017; 18:214–24. https://doi.org/10.1038/ni.3641.
1766 [58] Masperone L, Codrich M, Persichetti F, Gustincich S, Zucchelli S, Legname G. The E3
1767 Ubiquitin Ligase TRAF6 Interacts with the Cellular Prion Protein and Modulates Its
1768 Solubility and Recruitment to Cytoplasmic p62/SQSTM1-Positive Aggresome-Like
1769 Structures. Mol Neurobiol 2022; 59:1577–88. https://doi.org/10.1007/S12035-021-02666-
1770 6/
1771 [59] Zhang ZY, Harischandra DS, Wang R, Ghaisas S, Zhao JY, McMonagle TP, et al.
1772 TRIM11 protects against tauopathies and is down-regulated in Alzheimer's disease.
1773 Science (1979) 2023;381. https://doi.org/10.1126/science.add6696.
1774 [60] Davidson JM, Wu SSL, Rayner SL, Cheng F, Duncan K, Russo C, et al. The E3 Ubiquitin
1775 Ligase SCF Cyclin F Promotes Sequestosome-1/p62 Insolubility and Foci Formation and
1776 is Dysregulated in ALS and FTD Pathogenesis. Mol Neurobiol 2023; 60:5034–54.
1777 https://doi.org/10.1007/s12035-023-03355-2.
1778 [61] Watabe K, Kato Y, Sakuma M, Murata M, Niida-Kawaguchi M, Takemura T, et al. Praja1
1779 RING-finger E3 ubiquitin ligase suppresses neuronal cytoplasmic TDP-43 aggregate
1780 formation. Neuropathology 2020; 40:570–86. https://doi.org/10.1111/neup.12694.
1781 [62] Won SY, Park JJ, You ST, Hyeun JA, Kim HK, Jin BK, et al. p21-activated kinase 4
1782 controls the aggregation of α-synuclein by reducing the monomeric and aggregated forms
1783 of α-synuclein: involvement of the E3 ubiquitin ligase NEDD4-1. Cell Death Dis 2022;13.
1784 https://doi.org/10.1038/s41419-022-05030-1.
1785 [63] Watabe K, Niida-Kawaguchi M, Tada M, Kato Y, Murata M, Tanji K, et al. Praja1 RING-
1786 finger E3 ubiquitin ligase is a common suppressor of neurodegenerative disease-
1787 associated protein aggregation. Neuropathology 2022; 42:488–504.
1788 https://doi.org/10.1111/neup.12840.
1789 [64] Nadel CM, Thwin AC, Callahan M, Lee K, Connelly E, Craik CS, et al. The E3 Ubiquitin
1790 Ligase, CHIP/STUB1, Inhibits Aggregation of Phosphorylated Proteoforms of
1791 Microtubule-associated Protein Tau (MAPT). J Mol Biol 2023;435.
1792 https://doi.org/10.1016/j.jmb.2023.168026.
1793 [65] Yan C, Gong L, Chen L, Xu M, Abou-Hamdan H, Tang M, et al. PHB2 (prohibitin 2)
1794 promotes PINK1-PRKN/Parkin-dependent mitophagy by the PARL-PGAM5-PINK1 axis
1795 2020. https://doi.org/10.1080/15548627.2019.1628520.
1796 [66] Lindholm AK, Dyer KA, Firman RC, Fishman L, Forstmeier W, Holman L, et al. The
1797 Ecology and Evolutionary Dynamics of Meiotic Drive. Trends Ecol Evol 2016; 31:315–
1798 26. https://doi.org/10.1016/j.tree.2016.02.001.
1799 [67] Hernández JFL, Rubinstein BY, Unckless RL, Zanders SE. Modeling the Evolution of
1800 Populations with Multiple Killer Meiotic Drivers. BioRxiv 2023:2023.09.28.560003.
1801 https://doi.org/10.1101/2023.09.28.560003.
1802 [68] Dasgupta SK, Jain S, Kaushal D, Tyagi AK. Expression Systems for Study of
1803 Mycobacterial Gene Regulation and Development of Recombinant BCG Vaccines.
1804 Biochem Biophys Res Commun 1998; 246:797–804.
1805 https://doi.org/10.1006/BBRC.1998.8724.
1806 [69] Sikorski RS, Hieter P. A system of shuttle vectors and yeast host strains designed for
1807 efficient manipulation of DNA in Saccharomyces cerevisiae. Genetics 1989; 122:19–27.
1808 https://doi.org/10.1093/GENETICS/122.1.19.

1809 [70] Snaith HA, Samejima I, Sawin KE. Multistep and multimode cortical anchoring of tea1p
1810 at cell tips in fission yeast. EMBO J 2005; 24:3690.
1811 https://doi.org/10.1038/SJ.EMBOJ.7600838.
1812 [71] Sonnhammer ELL, Von Heijne G, Krogh A. A hidden Markov model for predicting
1813 transmembrane helices in protein sequences. AAAI Press; 1998.
1814 [72] Krogh A, Larsson B, Von Heijne G, Sonnhammer ELL. Predicting transmembrane protein
1815 topology with a hidden Markov model: Application to complete genomes. J Mol Biol
1816 2001; 305:567–80. https://doi.org/10.1006/jmbi.2000.4315.
1817 [73] Chen Y hui, Wang G yuan, Hao H chao, Chao C jiang, Wang Y, Jin Q wen. Facile
1818 manipulation of protein localization in fission yeast through binding of GFP-binding
1819 protein to GFP. J Cell Sci 2017; 130:1003–15. https://doi.org/10.1242/JCS.198457.
1820 [74] Sanchez MI, Ting AY. Directed evolution improves the catalytic efficiency of TEV
1821 protease. Nature Methods 2019 17:2 2019; 17:167–74. https://doi.org/10.1038/s41592-
1822 019-0665-7.
1823 [75] Kapust RB, Waugh DS. *Escherichia coli* maltose-binding protein is uncommonly
1824 effective at promoting the solubility of polypeptides to which it is fused. Protein Sci 1999;
1825 8:1668. https://doi.org/10.1110/PS.8.8.1668.
1826 [76] Fox JD, Routzahn KM, Bucher MH, Waugh DS. Maltodextrin-binding proteins from
1827 diverse bacteria and archaea are potent solubility enhancers. FEBS Lett 2003; 537:53–7.
1828 https://doi.org/10.1016/S0014-5793(03)00070-X.
1829 [77] Ottoz DSM, Rudolf F, Stelling J. Inducible, tightly regulated and growth condition-
1830 independent transcription factor in *Saccharomyces cerevisiae*. Nucleic Acids Res 2014;42.
1831 https://doi.org/10.1093/nar/gku616.
1832 [78] R Elble. A simple and efficient procedure for transformation of yeasts. Biotechniques
1833 1992.
1834 [79] Winston F, Dollard C, Ricupero-Hovasse SL. Construction of a set of convenient
1835 *Saccharomyces cerevisiae* strains that are isogenic to S288C. Yeast 1995;11:53–5.
1836 https://doi.org/10.1002/YEA.320110107.
1837 [80] Gasteiger E, Hoogland C, Gattiker A, Duvaud S, Wilkins MR, Appel RD, et al. Protein
1838 Identification and Analysis Tools on the ExPASy Server. The Proteomics Protocols
1839 Handbook 2005:571–607. https://doi.org/10.1385/1-59259-890-0:571.
1840

Figure 1

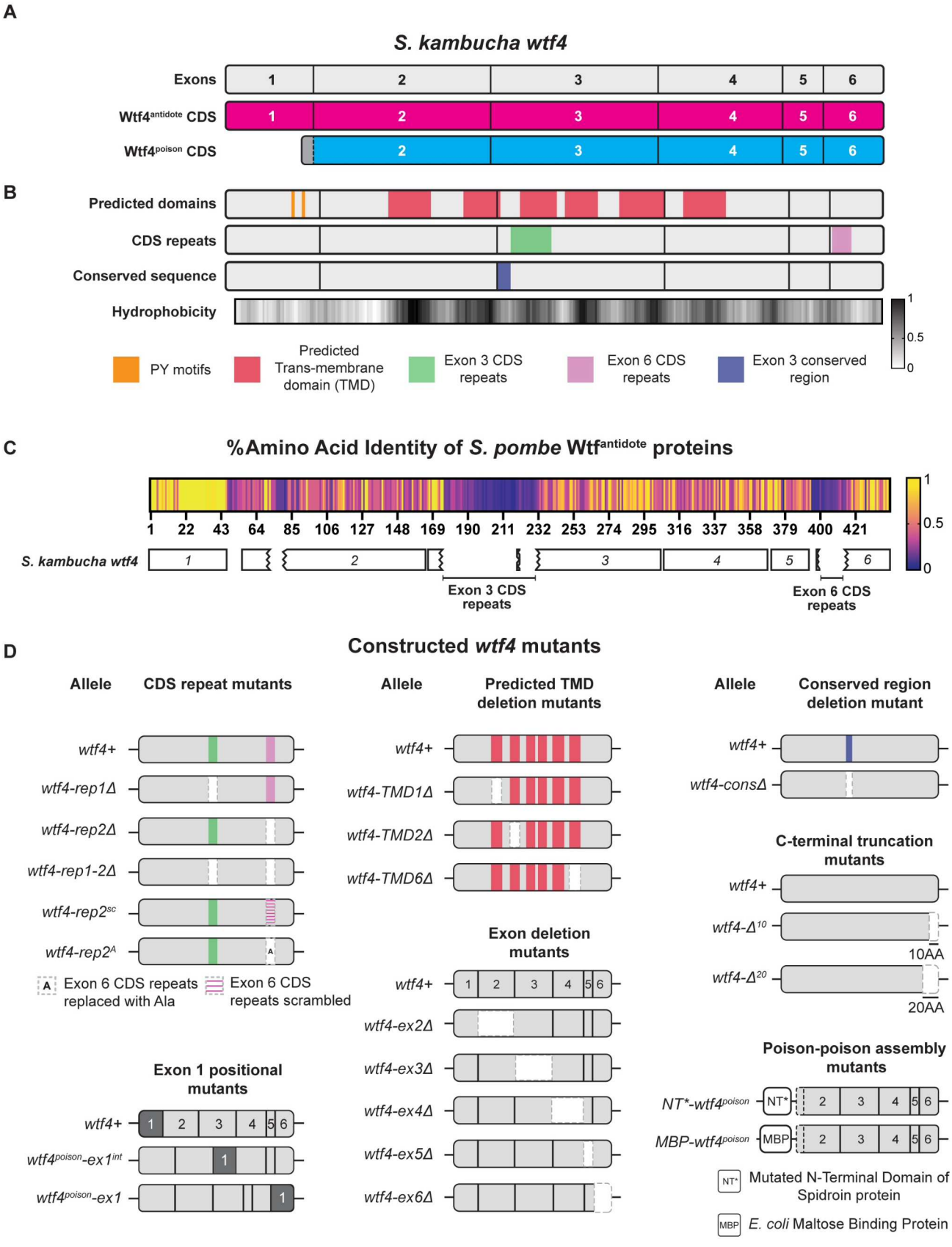
A
S. kambucha wtf4
Exons
1
2
3
4
5
6
Wtf4antidote CDS
Wtf4poison CDS
B
Predicted domains
CDS repeats
Conserved sequence
Hydrophobicity
1
0.5
0
PY motifs
Predicted Trans-membrane domain (TMD)
Exon 3 CDS repeats
Exon 6 CDS repeats
Exon 3 conserved region
C
%Amino Acid Identity of S. pombe Wtfantidote proteins
1 22 43 64 85 106 127 148 169 190 211 232 253 274 295 316 337 358 379 400 421
S. kambucha wtf4
Exon 3 CDS repeats
Exon 6 CDS repeats
D
Constructed wtf4 mutants
Allele
CDS repeat mutants
wtf4+
wtf4-rep1Δ
wtf4-rep2Δ
wtf4-rep1-2Δ
wtf4-rep2sc
wtf4-rep2A
Exon 6 CDS repeats replaced with Ala
Exon 6 CDS repeats scrambled
Exon 1 positional mutants
wtf4poison-ex1int
wtf4poison-ex1
Predicted TMD deletion mutants
wtf4-TMD1Δ
wtf4-TMD2Δ
wtf4-TMD6Δ
Exon deletion mutants
wtf4-ex2Δ
wtf4-ex3Δ
wtf4-ex4Δ
wtf4-ex5Δ
wtf4-ex6Δ
Conserved region deletion mutant
wtf4-consΔ
C-terminal truncation mutants
wtf4-Δ10
10AA
wtf4-Δ20
20AA
Poison-poison assembly mutants
NT*-wtf4poison
MBP-wtf4poison
NT*
MBP
Mutated N-Terminal Domain of Spidroin protein
E. coli Maltose Binding Protein

Figure 2

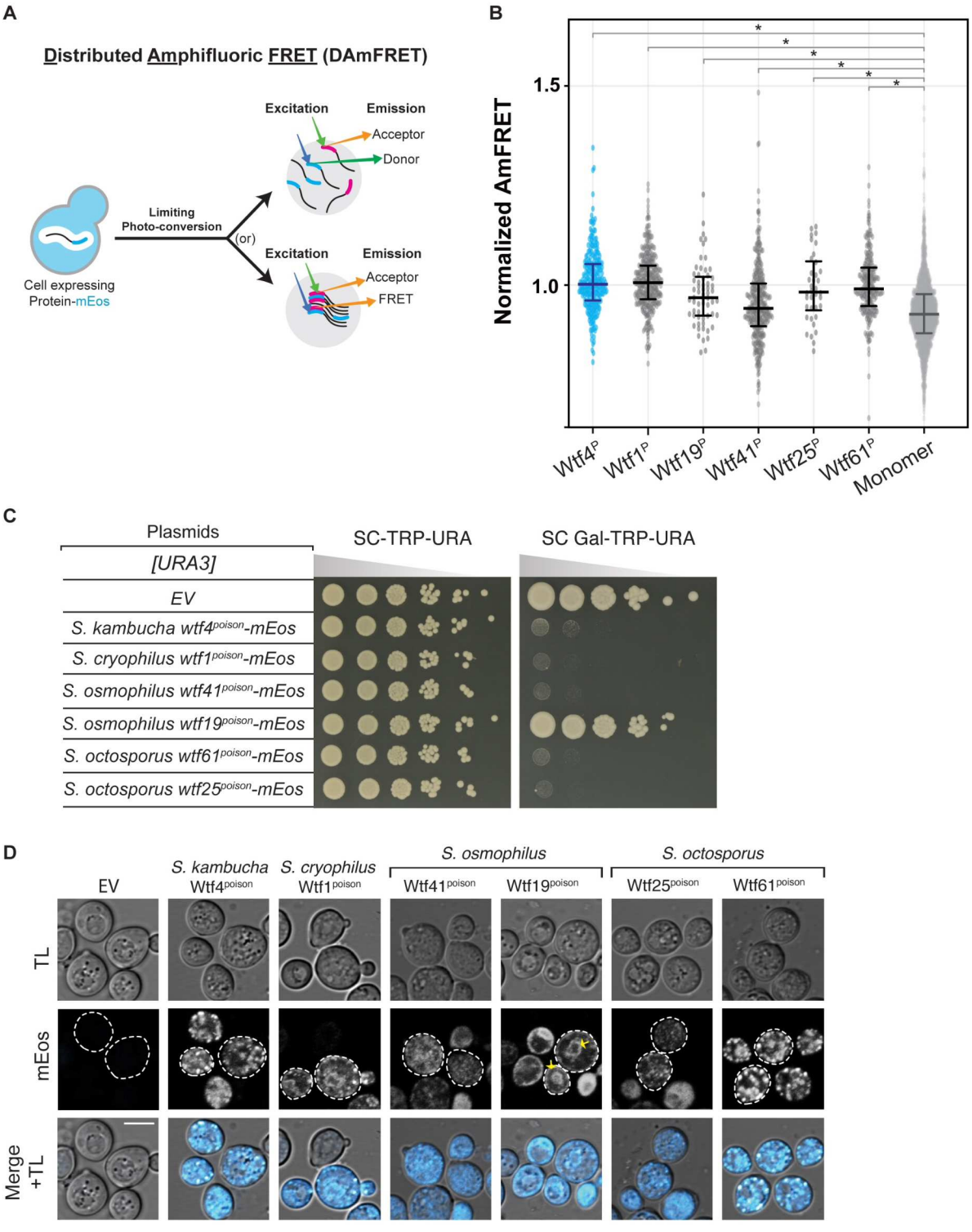
A
Distributed Amphifluoric FRET (DAmFRET)
Excitation
Emission
Acceptor
Donor
Limiting
Photo-conversion
(or)
Excitation
Emission
Acceptor
FRET
Cell expressing
Protein-mEos
B
Normalized AmFRET
1.5
1.0
Wtf4P
Wtf1P
Wtf19P
Wtf41P
Wtf25P
Wtf61P
Monomer
C
Plasmids
SC-TRP-URA
SC Gal-TRP-URA
[URA3]
EV
S. kambucha wtf4poison-mEos
S. cryophilus wtf1poison-mEos
S. osmophilus wtf41poison-mEos
S. osmophilus wtf19poison-mEos
S. octosporus wtf61poison-mEos
S. octosporus wtf25poison-mEos
D
EV
S. kambucha Wtf4poison
S. cryophilus Wtf1poison
S. osmophilus
Wtf41poison
Wtf19poison
S. octosporus
Wtf25poison
Wtf61poison
TL
mEos
Merge +TL

Figure 3

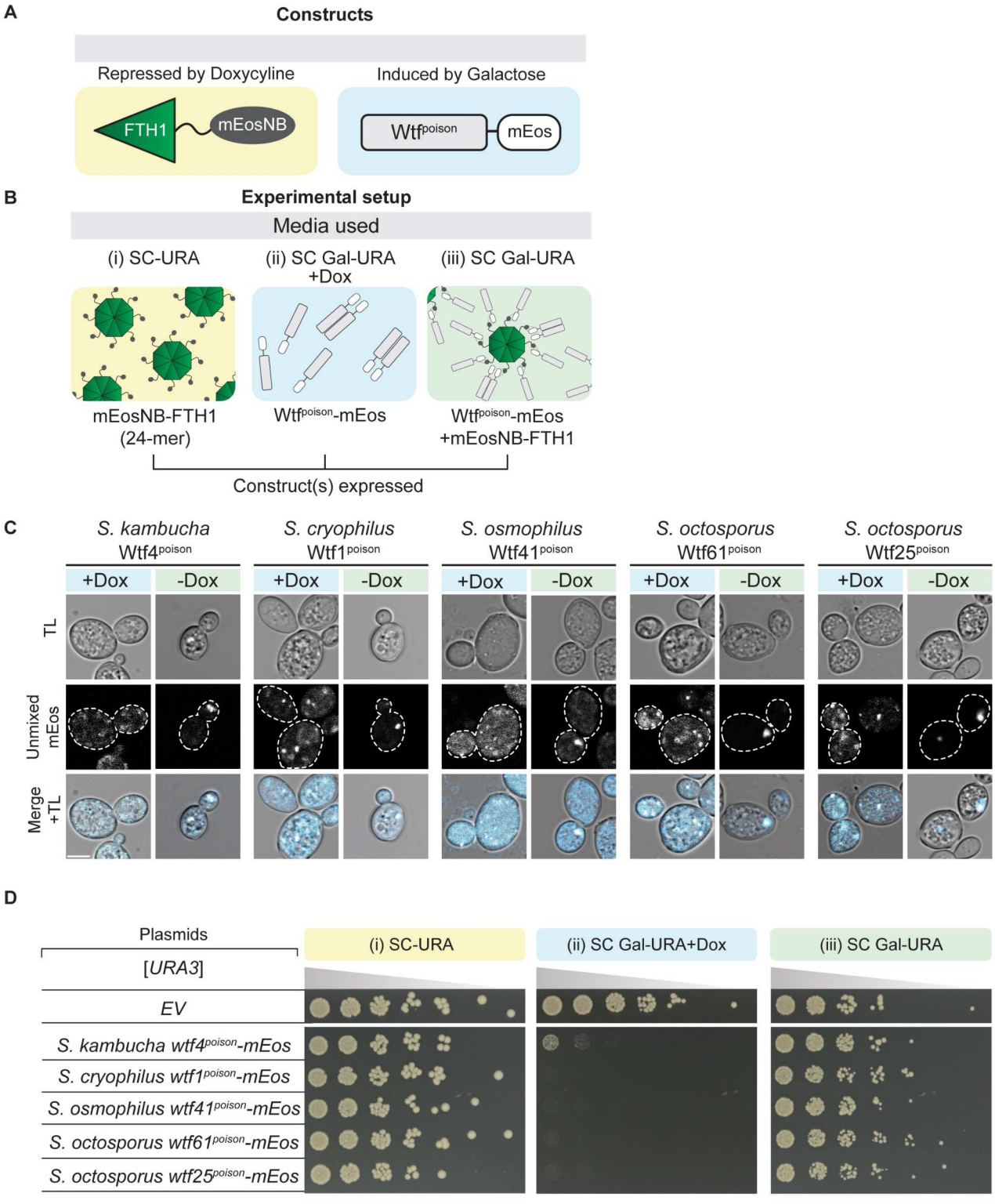
A
Constructs
Repressed by Doxycyline
Induced by Galactose
FTH1
mEosNB
Wtf poison
mEos
B
Experimental setup
Media used
(i) SC-URA
(ii) SC Gal-URA +Dox
(iii) SC Gal-URA
mEosNB-FTH1 (24-mer)
Wtf poison-mEos
Wtf poison-mEos +mEosNB-FTH1
Construct(s) expressed
C
S. kambucha Wtf4 poison
S. cryophilus Wtf1 poison
S. osmophilus Wtf41 poison
S. octosporus Wtf61 poison
S. octosporus Wtf25 poison
+Dox
-Dox
TL
Unmixed mEos
Merge +TL
D
Plasmids
[URA3]
EV
S. kambucha wtf4 poison-mEos
S. cryophilus wtf1 poison-mEos
S. osmophilus wtf41 poison-mEos
S. octosporus wtf61 poison-mEos
S. octosporus wtf25 poison-mEos
(i) SC-URA
(ii) SC Gal-URA+Dox
(iii) SC Gal-URA

Figure 4

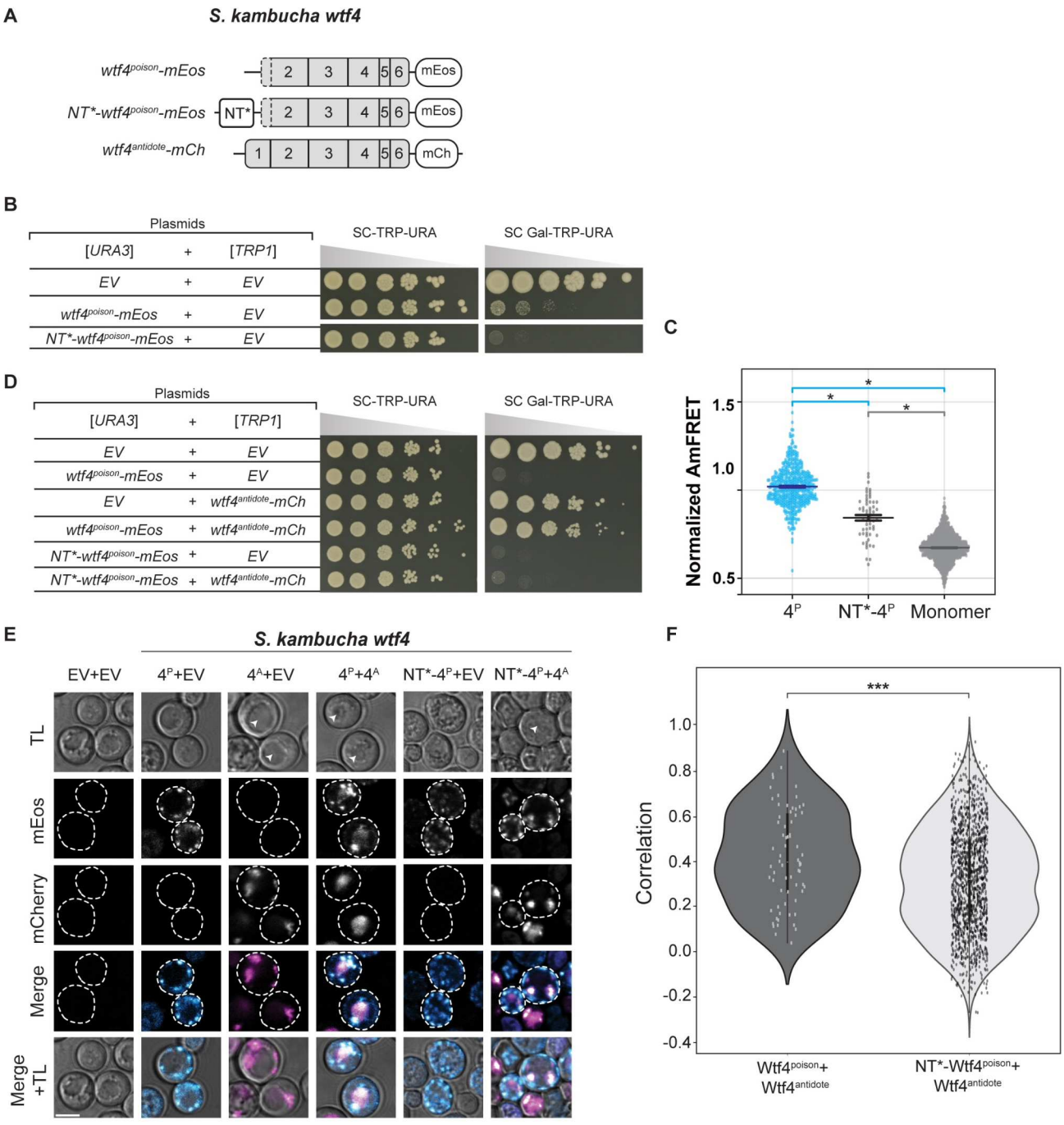
A
S. kambucha wtf4
wtf4poison-mEos
NT*-wtf4poison-mEos
wtf4antidote-mCh
NT*
1
2
3
4
5
6
mEos
mCh
B
Plasmids
[URA3] + [TRP1]
EV + EV
wtf4poison-mEos + EV
NT*-wtf4poison-mEos + EV
SC-TRP-URA
SC Gal-TRP-URA
C
Normalized AmFRET
1.5
1.0
0.5
*
4P
NT*-4P
Monomer
D
Plasmids
[URA3] + [TRP1]
EV + EV
wtf4poison-mEos + EV
EV + wtf4antidote-mCh
wtf4poison-mEos + wtf4antidote-mCh
NT*-wtf4poison-mEos + EV
NT*-wtf4poison-mEos + wtf4antidote-mCh
SC-TRP-URA
SC Gal-TRP-URA
E
S. kambucha wtf4
EV+EV
4P+EV
4A+EV
4P+4A
NT*-4P+EV
NT*-4P+4A
TL
mEos
mCherry
Merge
Merge +TL
F
Correlation
1.0
0.8
0.6
0.4
0.2
0.0
-0.2
-0.4
***
Wtf4poison+ Wtf4antidote
NT*-Wtf4poison+ Wtf4antidote

Figure 5

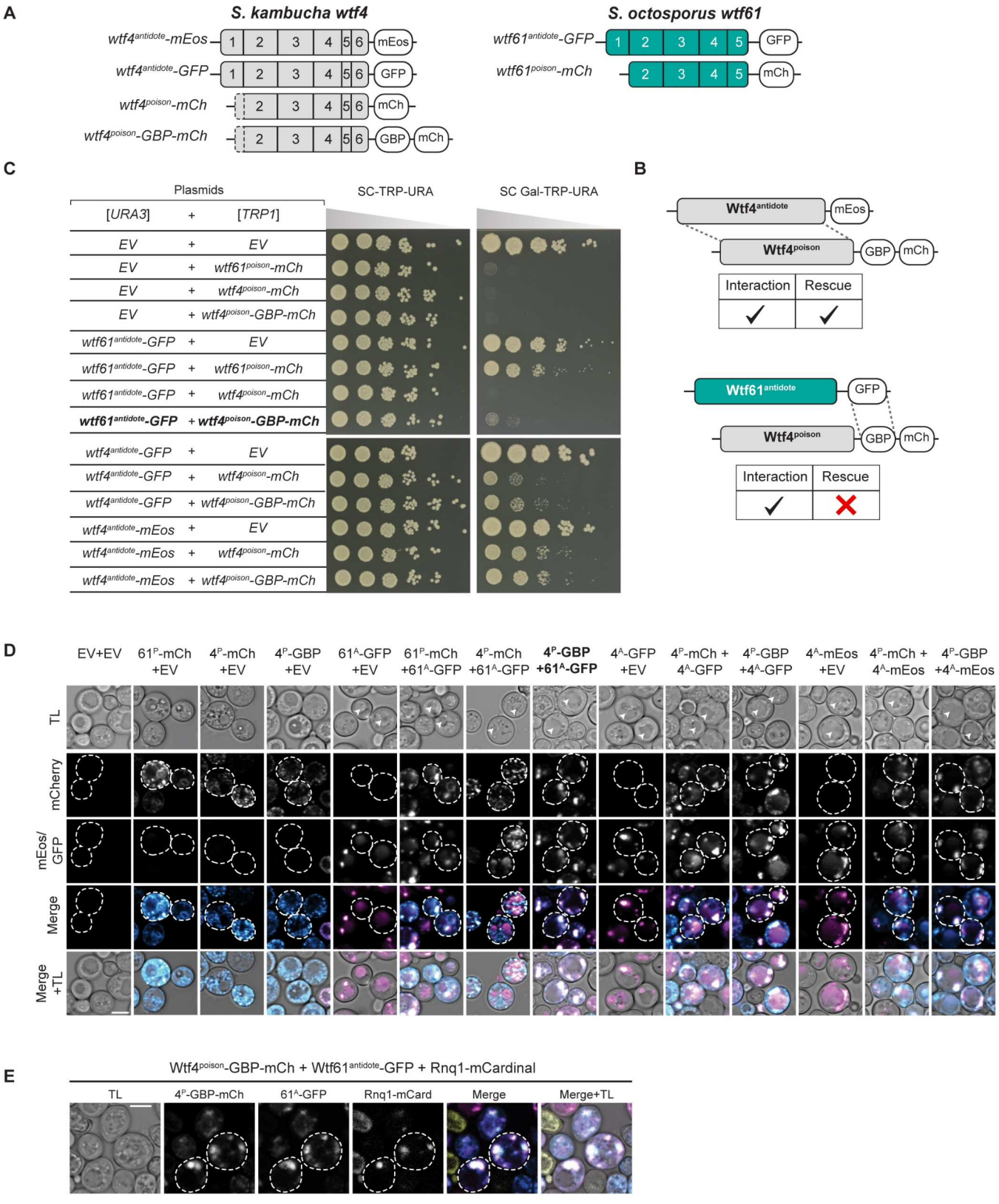
A
S. kambucha wtf4
wtf4antidote-mEos
wtf4antidote-GFP
wtf4poison-mCh
wtf4poison-GBP-mCh
1 2 3 4 5 6
mEos
GFP
mCh
GBP
S. octosporus wtf61
wtf61antidote-GFP
wtf61poison-mCh
1 2 3 4 5
C
Plasmids
[URA3] + [TRP1]
SC-TRP-URA
SC Gal-TRP-URA
EV + EV
EV + wtf61poison-mCh
EV + wtf4poison-mCh
EV + wtf4poison-GBP-mCh
wtf61antidote-GFP + EV
wtf61antidote-GFP + wtf61poison-mCh
wtf61antidote-GFP + wtf4poison-mCh
wtf61antidote-GFP + wtf4poison-GBP-mCh
wtf4antidote-GFP + EV
wtf4antidote-GFP + wtf4poison-mCh
wtf4antidote-GFP + wtf4poison-GBP-mCh
wtf4antidote-mEos + EV
wtf4antidote-mEos + wtf4poison-mCh
wtf4antidote-mEos + wtf4poison-GBP-mCh
B
Wtf4antidote
mEos
Wtf4poison
GBP
mCh
Interaction
Rescue
Wtf61antidote
GFP
Wtf4poison
GBP
mCh
Interaction
Rescue
D
EV+EV
61P-mCh +EV
4P-mCh +EV
4P-GBP +EV
61A-GFP +EV
61P-mCh +61A-GFP
4P-mCh +61A-GFP
4P-GBP +61A-GFP
4A-GFP +EV
4P-mCh + 4A-GFP
4P-GBP +4A-GFP
4A-mEos +EV
4P-mCh + 4A-mEos
4P-GBP +4A-mEos
TL
mCherry
mEos/ GFP
Merge
Merge +TL
E
Wtf4poison-GBP-mCh + Wtf61antidote-GFP + Rnq1-mCardinal
TL
4P-GBP-mCh
61A-GFP
Rnq1-mCard
Merge
Merge+TL

Figure 6

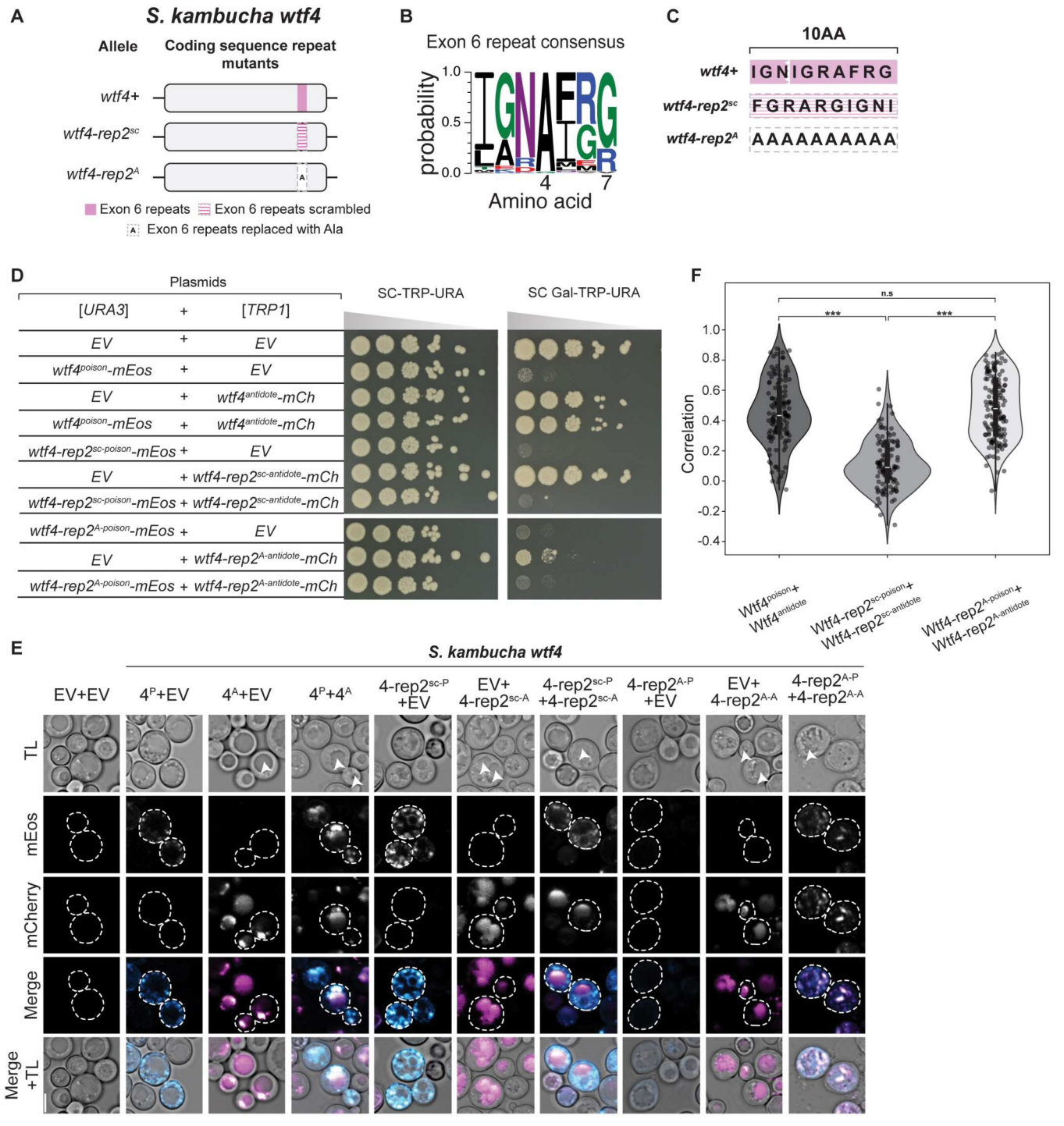
A
S. kambucha wtf4
Allele
Coding sequence repeat mutants
wtf4+
wtf4-rep2sc
wtf4-rep2A
Exon 6 repeats
Exon 6 repeats scrambled
Exon 6 repeats replaced with Ala
B
Exon 6 repeat consensus
probability
Amino acid
C
10AA
wtf4+ IGNIGRAFRG
wtf4-rep2sc FGRARGIGNI
wtf4-rep2A AAAAAAAAAA
D
Plasmids
[URA3] + [TRP1]
SC-TRP-URA
SC Gal-TRP-URA
EV + EV
wtf4poison-mEos + EV
EV + wtf4antidote-mCh
wtf4poison-mEos + wtf4antidote-mCh
wtf4-rep2sc-poison-mEos + EV
EV + wtf4-rep2sc-antidote-mCh
wtf4-rep2sc-poison-mEos + wtf4-rep2sc-antidote-mCh
wtf4-rep2A-poison-mEos + EV
EV + wtf4-rep2A-antidote-mCh
wtf4-rep2A-poison-mEos + wtf4-rep2A-antidote-mCh
F
n.s
***
***
Correlation
Wtf4poison+ Wtf4antidote
Wtf4-rep2sc-poison+ Wtf4-rep2sc-antidote
Wtf4-rep2A-poison+ Wtf4-rep2A-antidote
E
S. kambucha wtf4
EV+EV
4P+EV
4A+EV
4P+4A
4-rep2sc-P +EV
EV+ 4-rep2sc-A
4-rep2sc-P +4-rep2sc-A
4-rep2A-P +EV
EV+ 4-rep2A-A
4-rep2A-P +4-rep2A-A
TL
mEos
mCherry
Merge
Merge +TL

Figure 7

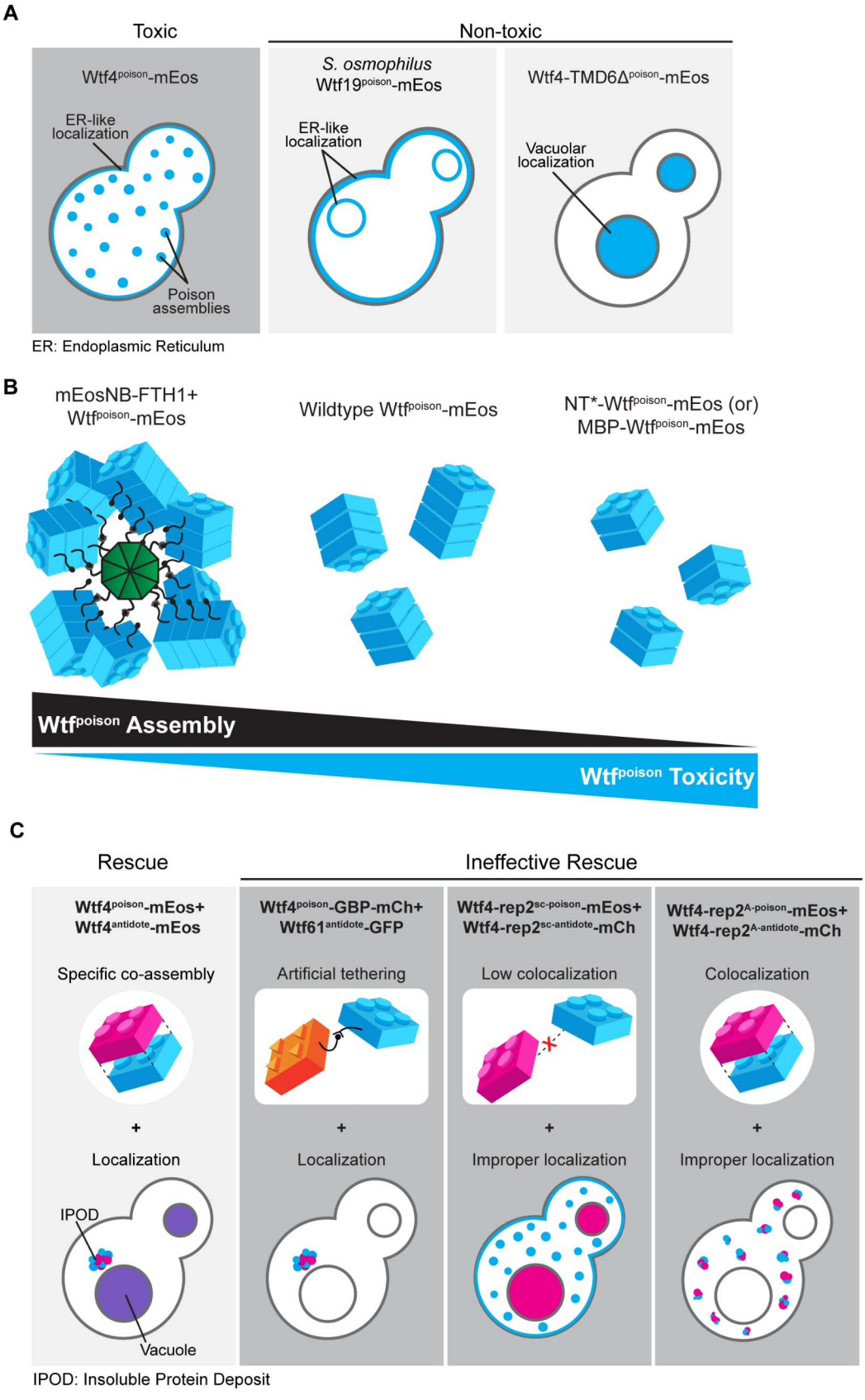
A
Toxic
Non-toxic
Wtf4poison-mEos
ER-like localization
Poison assemblies
S. osmophilus Wtf19poison-mEos
ER-like localization
Wtf4-TMD6Δpoison-mEos
Vacuolar localization
ER: Endoplasmic Reticulum
B
mEosNB-FTH1+ Wtfpoison-mEos
Wildtype Wtfpoison-mEos
NT*-Wtfpoison-mEos (or) MBP-Wtfpoison-mEos
Wtfpoison Assembly
Wtfpoison Toxicity
C
Rescue
Ineffective Rescue
Wtf4poison-mEos+ Wtf4antidote-mEos
Specific co-assembly
+
Localization
IPOD
Vacuole
Wtf4poison-GBP-mCh+ Wtf61antidote-GFP
Artificial tethering
+
Localization
Wtf4-rep2sc-poison-mEos+ Wtf4-rep2sc-antidote-mCh
Low colocalization
+
Improper localization
Wtf4-rep2A-poison-mEos+ Wtf4-rep2A-antidote-mCh
Colocalization
+
Improper localization
IPOD: Insoluble Protein Deposit

S1 Figure

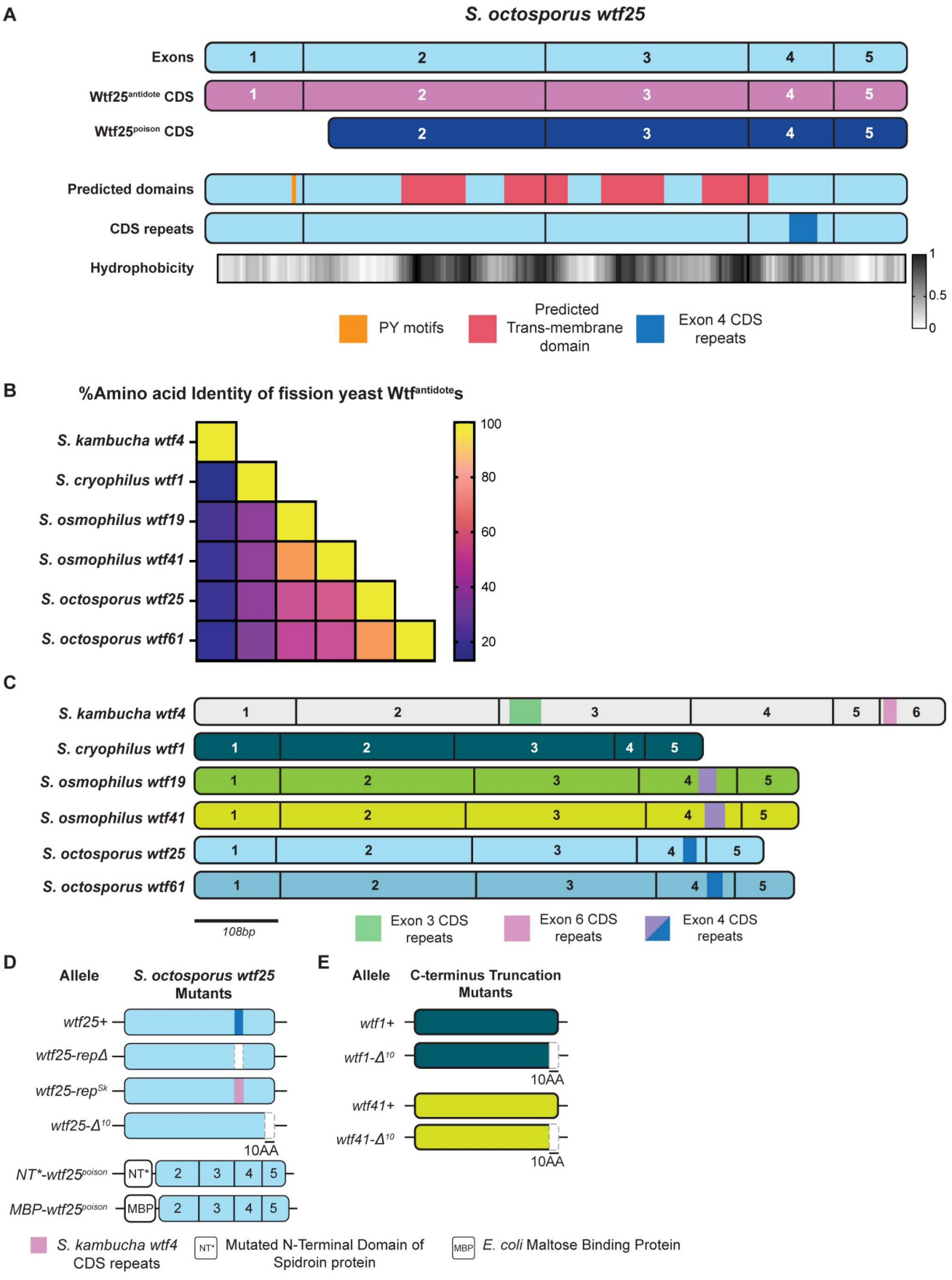
A
S. octosporus wtf25
Exons
Wtf25antidote CDS
Wtf25poison CDS
Predicted domains
CDS repeats
Hydrophobicity
1
0.5
0
PY motifs
Predicted Trans-membrane domain
Exon 4 CDS repeats
B
%Amino acid Identity of fission yeast Wtfantidotes
S. kambucha wtf4
S. cryophilus wtf1
S. osmophilus wtf19
S. osmophilus wtf41
S. octosporus wtf25
S. octosporus wtf61
100
80
60
40
20
C
S. kambucha wtf4
S. cryophilus wtf1
S. osmophilus wtf19
S. osmophilus wtf41
S. octosporus wtf25
S. octosporus wtf61
108bp
Exon 3 CDS repeats
Exon 6 CDS repeats
Exon 4 CDS repeats
D
Allele
S. octosporus wtf25 Mutants
wtf25+
wtf25-repΔ
wtf25-repSk
wtf25-Δ10
10AA
NT*-wtf25poison
MBP-wtf25poison
NT*
MBP
S. kambucha wtf4 CDS repeats
Mutated N-Terminal Domain of Spidroin protein
E. coli Maltose Binding Protein
E
Allele
C-terminus Truncation Mutants
wtf1+
wtf1-Δ10
10AA
wtf41+
wtf41-Δ10
10AA

S2 Figure

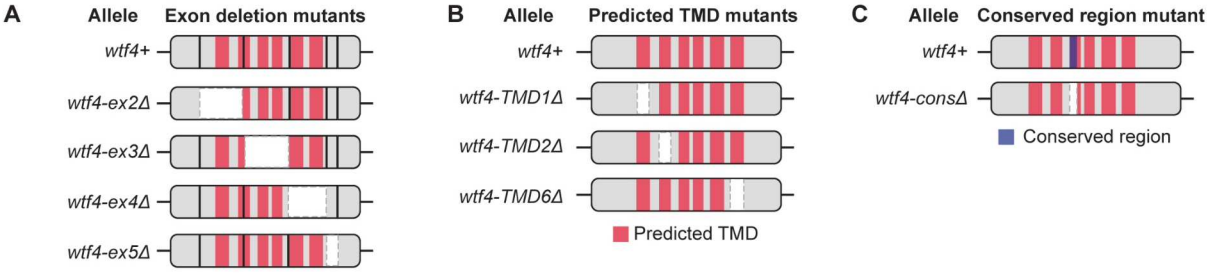
A
Allele
Exon deletion mutants
wtf4+
wtf4-ex2Δ
wtf4-ex3Δ
wtf4-ex4Δ
wtf4-ex5Δ
B
Allele
Predicted TMD mutants
wtf4+
wtf4-TMD1Δ
wtf4-TMD2Δ
wtf4-TMD6Δ
Predicted TMD
C
Allele
Conserved region mutant
wtf4+
wtf4-consΔ
Conserved region

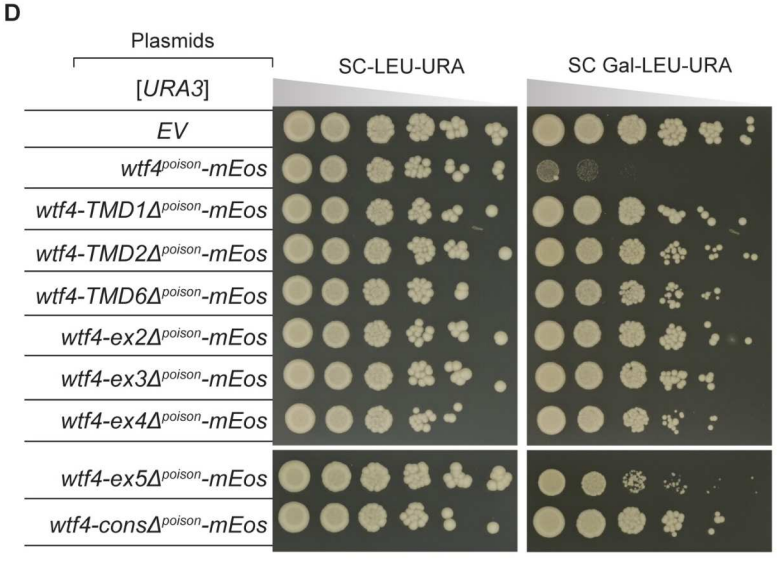
D
Plasmids
[URA3]
SC-LEU-URA
SC Gal-LEU-URA
EV
wtf4poison-mEos
wtf4-TMD1Δpoison-mEos
wtf4-TMD2Δpoison-mEos
wtf4-TMD6Δpoison-mEos
wtf4-ex2Δpoison-mEos
wtf4-ex3Δpoison-mEos
wtf4-ex4Δpoison-mEos
wtf4-ex5Δpoison-mEos
wtf4-consΔpoison-mEos

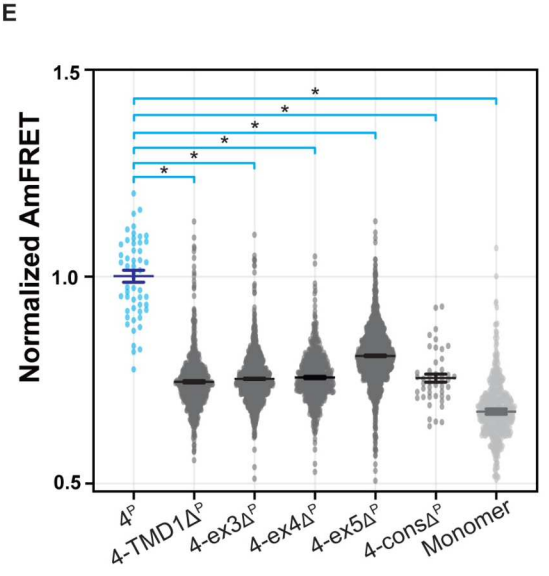
E
Normalized AmFRET
1.5
1.0
0.5
*
4P
4-TMD1ΔP
4-ex3ΔP
4-ex4ΔP
4-ex5ΔP
4-consΔP
Monomer

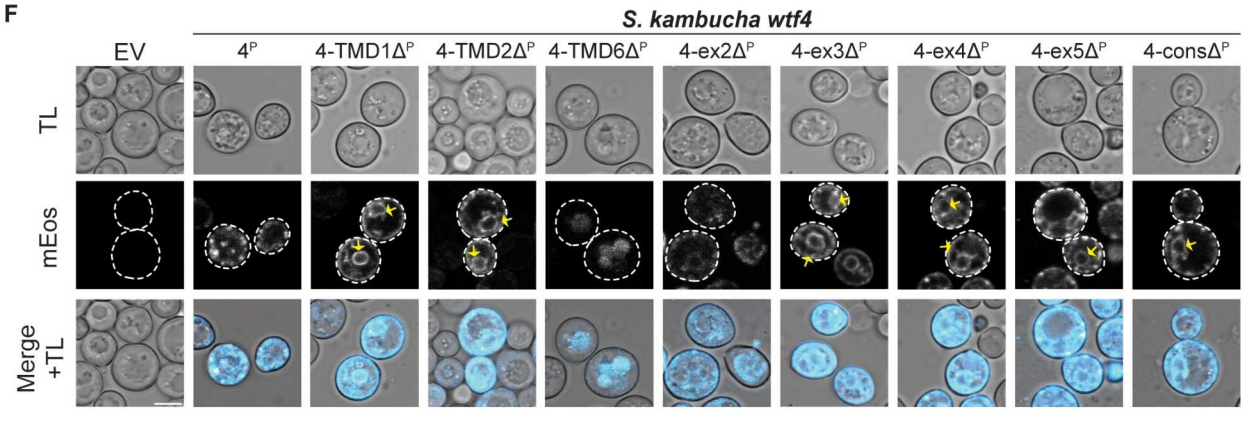
F
S. kambucha wtf4
EV
4P
4-TMD1ΔP
4-TMD2ΔP
4-TMD6ΔP
4-ex2ΔP
4-ex3ΔP
4-ex4ΔP
4-ex5ΔP
4-consΔP
TL
mEos
Merge +TL

S3 Figure

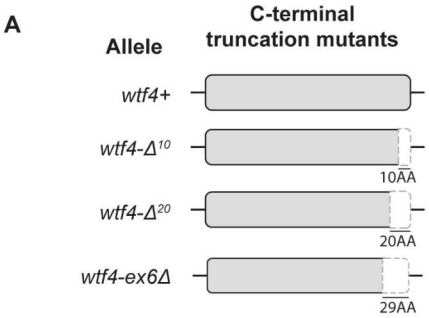
A
Allele
C-terminal truncation mutants
wtf4+
wtf4-Δ10
10AA
wtf4-Δ20
20AA
wtf4-ex6Δ
29AA

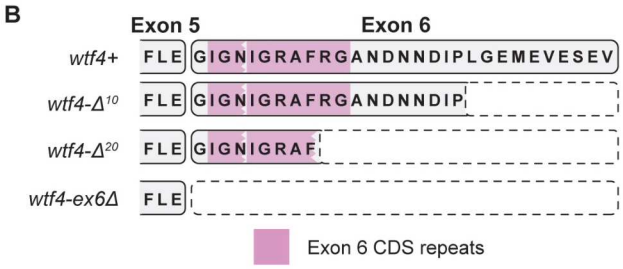
B
Exon 5
Exon 6
wtf4+
FLE
GIGNIGRAFRGANDNNDIPLGEMEVESEV
wtf4-Δ10
FLE
GIGNIGRAFRGANDNNDIP
wtf4-Δ20
FLE
GIGNIGRAF
wtf4-ex6Δ
FLE
Exon 6 CDS repeats

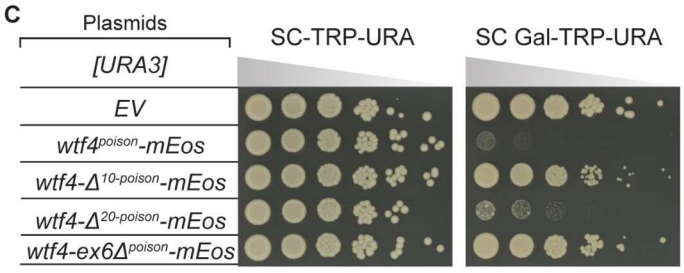
C
Plasmids
SC-TRP-URA
SC Gal-TRP-URA
[URA3]
EV
wtf4poison-mEos
wtf4-Δ10-poison-mEos
wtf4-Δ20-poison-mEos
wtf4-ex6Δpoison-mEos

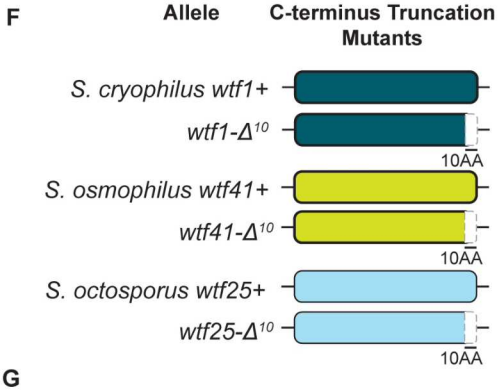
F
Allele
C-terminus Truncation Mutants
S. cryophilus wtf1+
wtf1-Δ10
10AA
S. osmophilus wtf41+
wtf41-Δ10
10AA
S. octosporus wtf25+
wtf25-Δ10
10AA

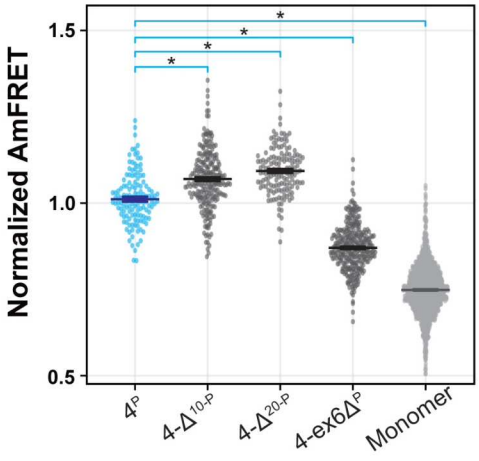
D
Normalized AmFRET
1.5
1.0
0.5
*
*
*
*
4P
4-Δ10-P
4-Δ20-P
4-ex6ΔP
Monomer

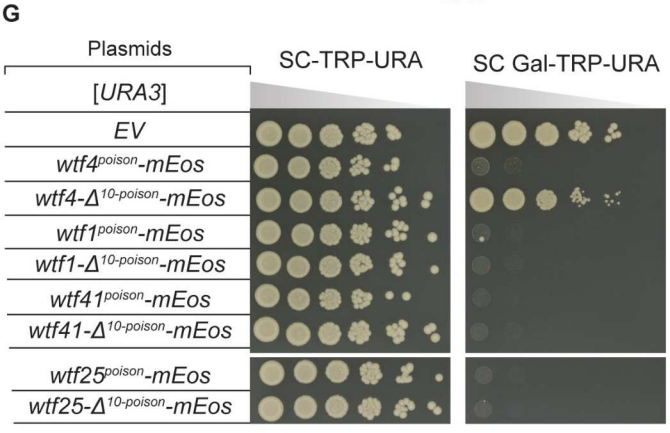
G
Plasmids
SC-TRP-URA
SC Gal-TRP-URA
[URA3]
EV
wtf4poison-mEos
wtf4-Δ10-poison-mEos
wtf1poison-mEos
wtf1-Δ10-poison-mEos
wtf41poison-mEos
wtf41-Δ10-poison-mEos
wtf25poison-mEos
wtf25-Δ10-poison-mEos

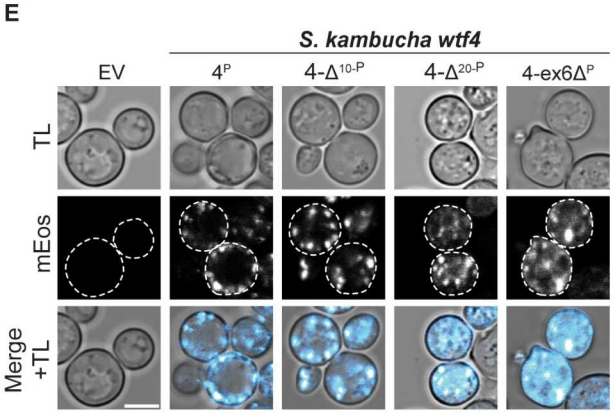
E
S. kambucha wtf4
EV
4P
4-Δ10-P
4-Δ20-P
4-ex6ΔP
TL
mEos
Merge +TL

S4 Figure

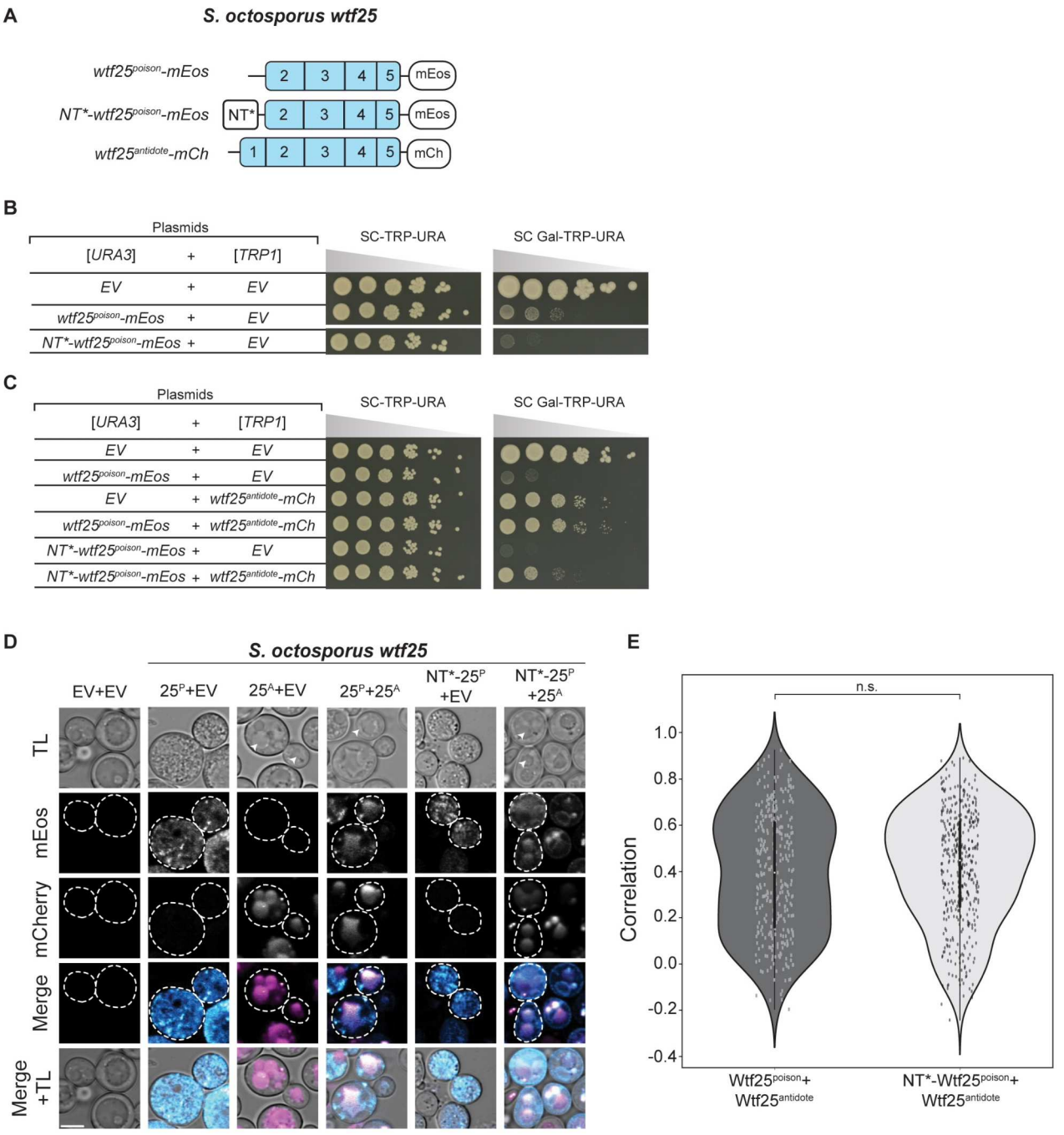
A
S. octosporus wtf25
wtf25poison-mEos
NT*-wtf25poison-mEos
wtf25antidote-mCh
NT*
1
2
3
4
5
mEos
mCh
B
Plasmids
[URA3] + [TRP1]
EV + EV
wtf25poison-mEos + EV
NT*-wtf25poison-mEos + EV
SC-TRP-URA
SC Gal-TRP-URA
C
Plasmids
[URA3] + [TRP1]
EV + EV
wtf25poison-mEos + EV
EV + wtf25antidote-mCh
wtf25poison-mEos + wtf25antidote-mCh
NT*-wtf25poison-mEos + EV
NT*-wtf25poison-mEos + wtf25antidote-mCh
SC-TRP-URA
SC Gal-TRP-URA
D
S. octosporus wtf25
EV+EV
25P+EV
25A+EV
25P+25A
NT*-25P +EV
NT*-25P +25A
TL
mEos
mCherry
Merge
Merge +TL
E
n.s.
Correlation
1.0
0.8
0.6
0.4
0.2
0.0
-0.2
-0.4
Wtf25poison+ Wtf25antidote
NT*-Wtf25poison+ Wtf25antidote

S5 Figure

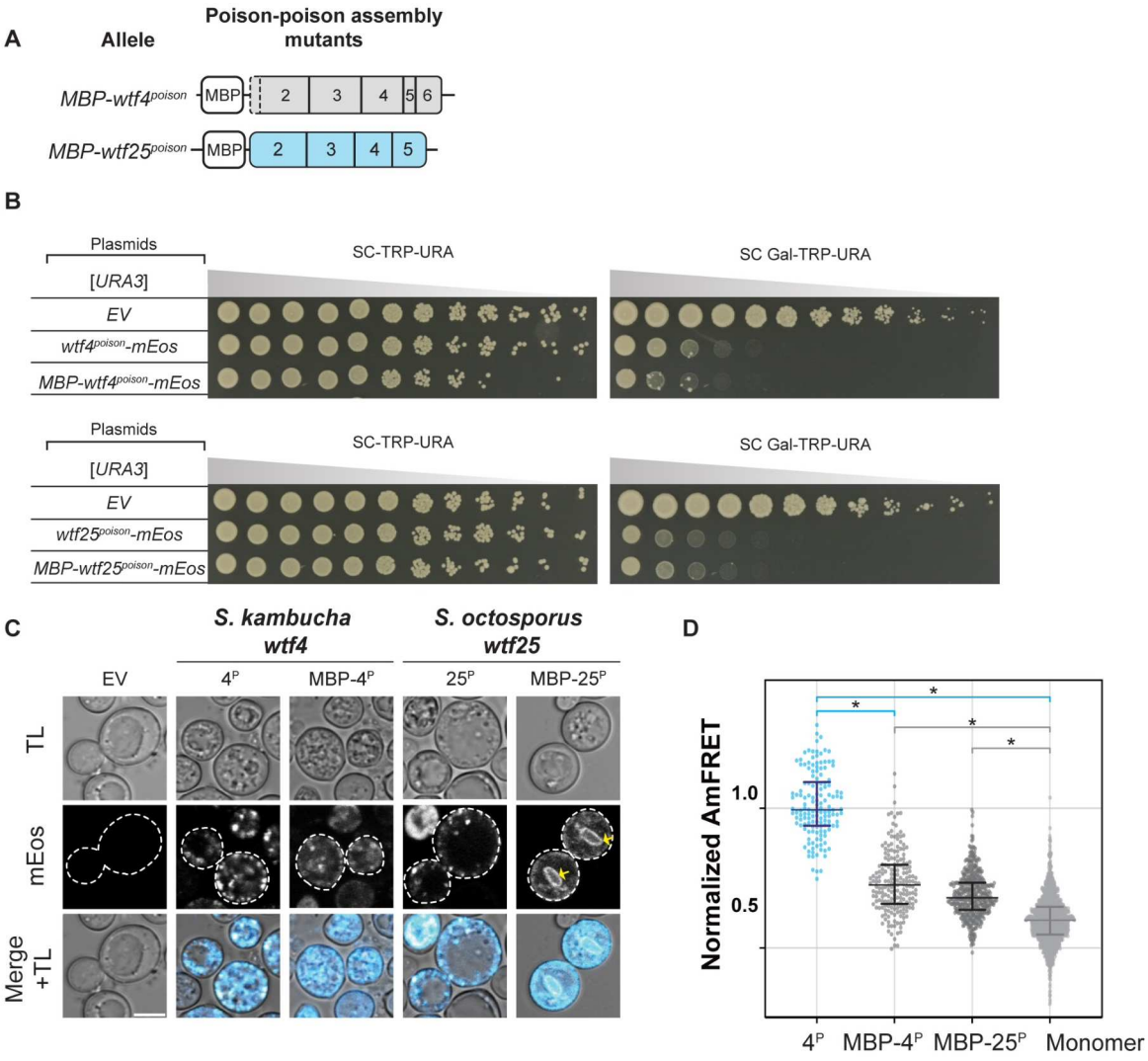
A
Allele
Poison-poison assembly mutants
MBP-wtf4poison
MBP
2
3
4
5
6
MBP-wtf25poison
MBP
2
3
4
5
B
Plasmids
[URA3]
EV
wtf4poison-mEos
MBP-wtf4poison-mEos
SC-TRP-URA
SC Gal-TRP-URA
Plasmids
[URA3]
EV
wtf25poison-mEos
MBP-wtf25poison-mEos
SC-TRP-URA
SC Gal-TRP-URA
C
S. kambucha wtf4
S. octosporus wtf25
EV
4P
MBP-4P
25P
MBP-25P
TL
mEos
Merge +TL
D
Normalized AmFRET
1.0
0.5
*
*
*
*
4P
MBP-4P
MBP-25P
Monomer

S6 Figure

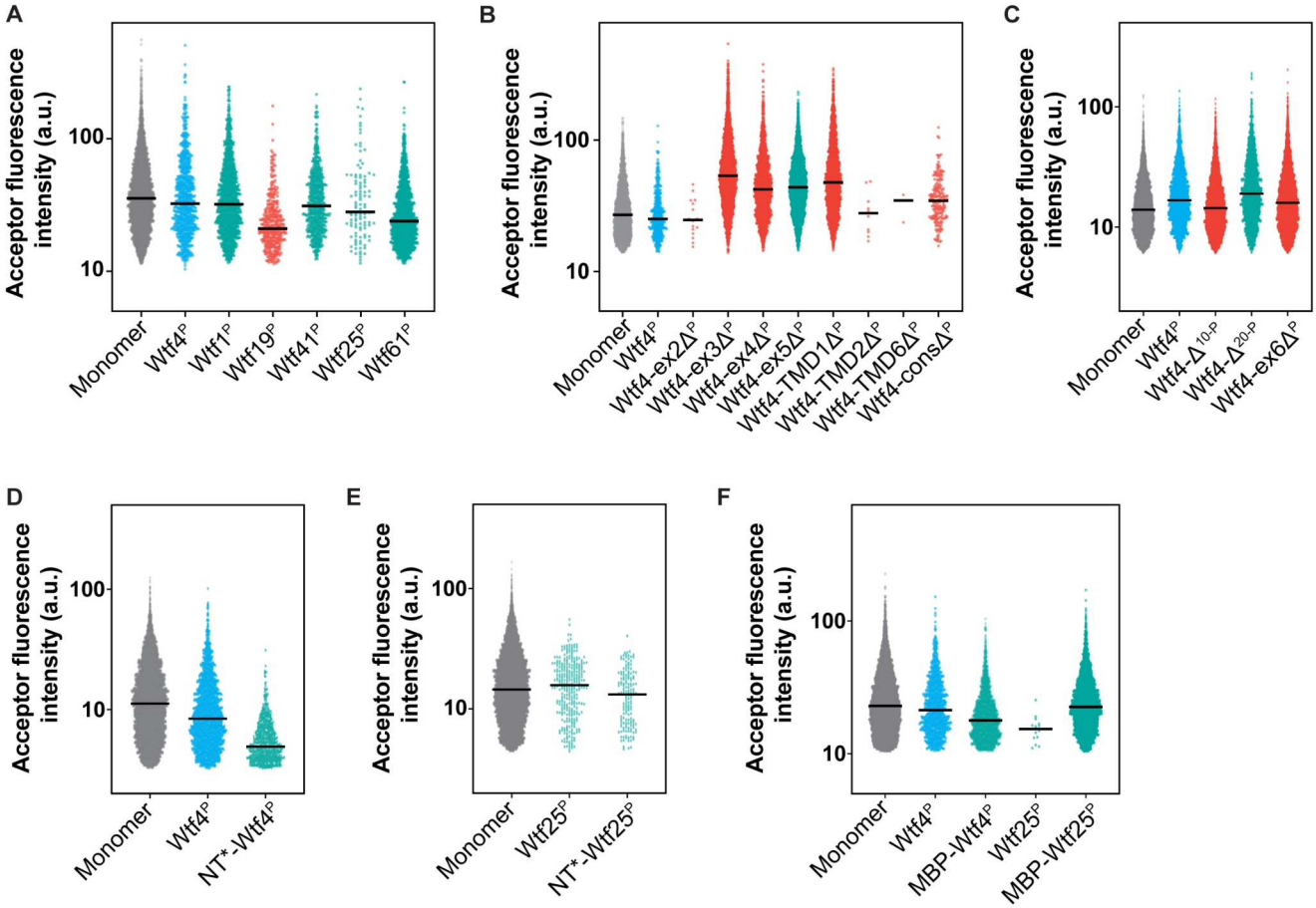
A
Acceptor fluorescence intensity (a.u.)
100
10
Monomer
Wtf4P
Wtf1P
Wtf19P
Wtf41P
Wtf25P
Wtf61P
B
Acceptor fluorescence intensity (a.u.)
100
10
Monomer
Wtf4P
Wtf4-ex2ΔP
Wtf4-ex3ΔP
Wtf4-ex4ΔP
Wtf4-ex5ΔP
Wtf4-TMD1ΔP
Wtf4-TMD2ΔP
Wtf4-TMD6ΔP
Wtf4-consΔP
C
Acceptor fluorescence intensity (a.u.)
100
10
Monomer
Wtf4P
Wtf4-Δ10-P
Wtf4-Δ20-P
Wtf4-ex6ΔP
D
Acceptor fluorescence intensity (a.u.)
100
10
Monomer
Wtf4P
NT*-Wtf4P
E
Acceptor fluorescence intensity (a.u.)
100
10
Monomer
Wtf25P
NT*-Wtf25P
F
Acceptor fluorescence intensity (a.u.)
100
10
Monomer
Wtf4P
MBP-Wtf4P
Wtf25P
MBP-Wtf25P

S7 Figure

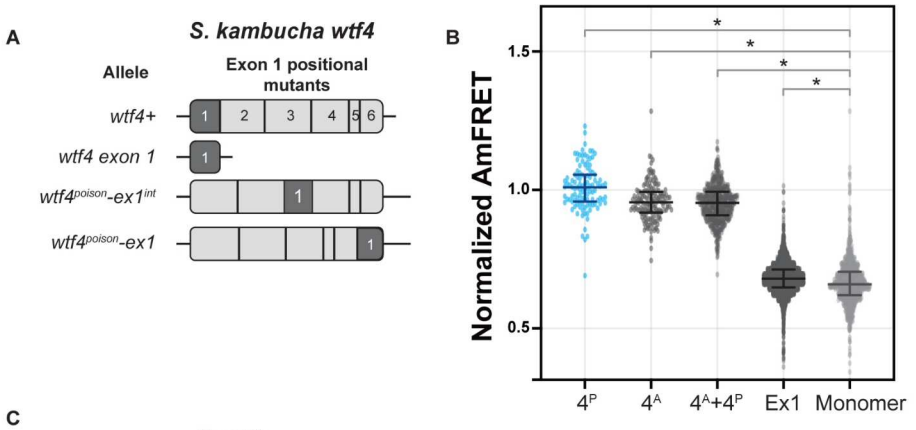

C

Plasmids [URA3]	+	[TRP1]
EV	+	EV
EV	+	wtf4poison-mCh
Ex1-mEos	+	EV
Ex1-mEos	+	wtf4poison-mCh

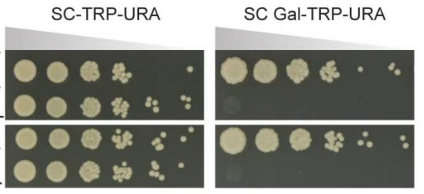

D

Plasmids [URA3]	+	[TRP1]
EV	+	EV
EV	+	wtf4poison-mCh
wtf4antidote-mEos	+	EV
wtf4antidote-mEos	+	wtf4poison-mCh
wtf4poison-ex1int-mEos	+	EV
wtf4poison-ex1int-mEos	+	wtf4poison-mCh
wtf4poison-ex1-mEos	+	EV
wtf4poison-ex1-mEos	+	wtf4poison-mCh

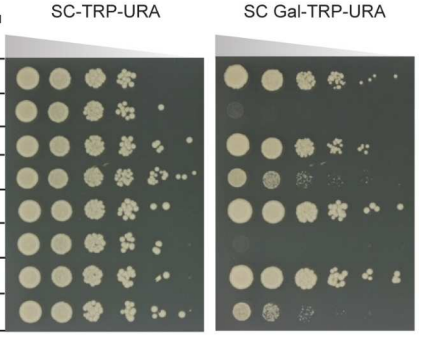

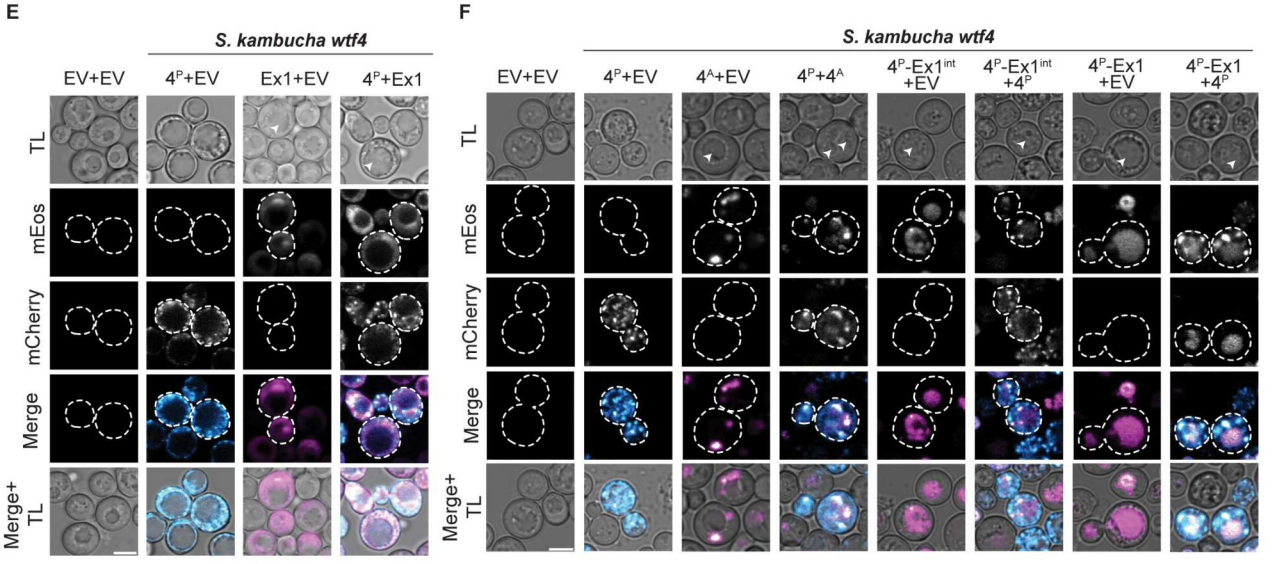

S8 Figure

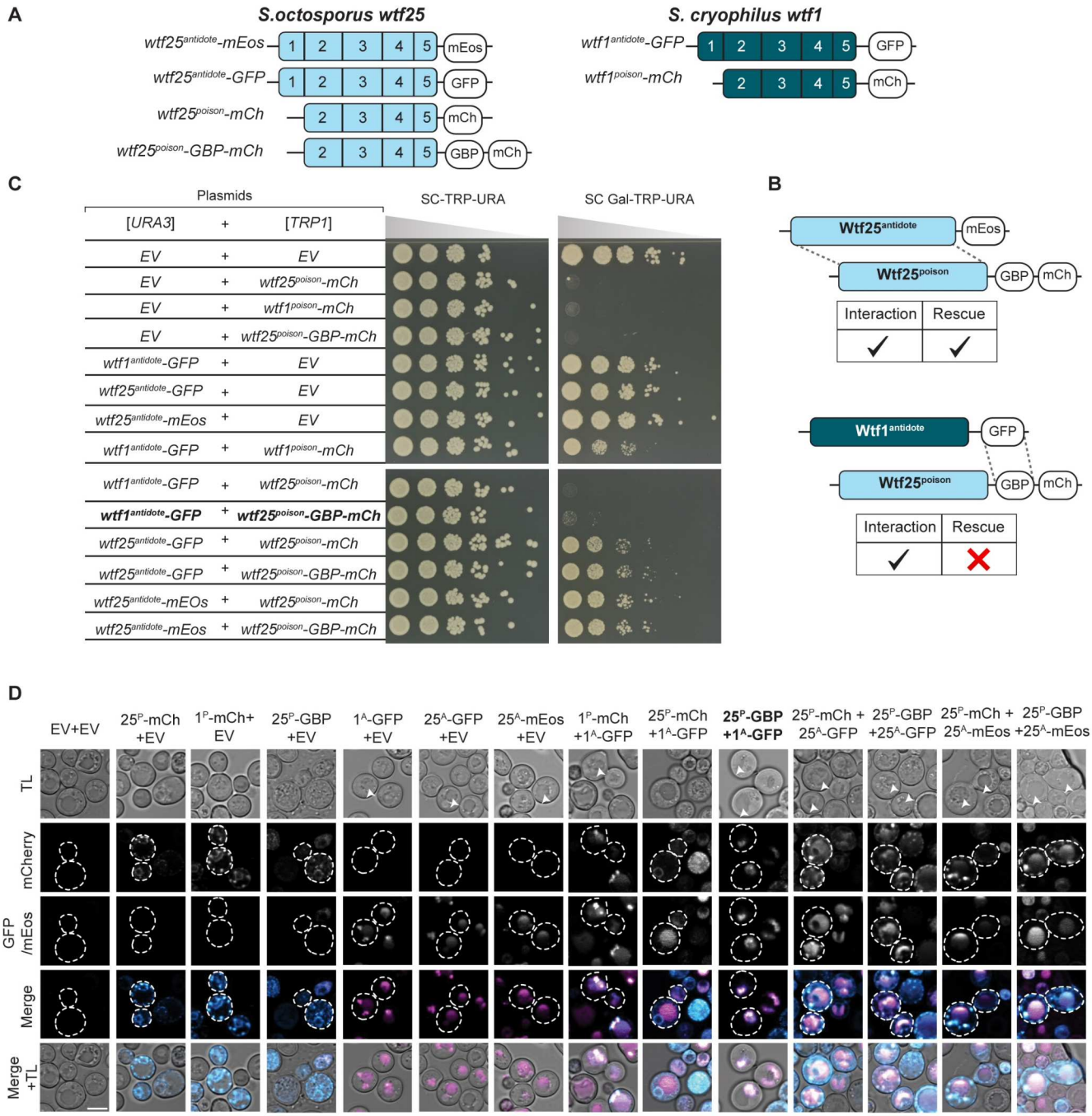
A
S.octosporus wtf25
wtf25antidote-mEos
wtf25antidote-GFP
wtf25poison-mCh
wtf25poison-GBP-mCh
1 2 3 4 5
mEos
GFP
mCh
GBP
S. cryophilus wtf1
wtf1antidote-GFP
wtf1poison-mCh
C
Plasmids
[URA3] + [TRP1]
SC-TRP-URA
SC Gal-TRP-URA
EV + EV
EV + wtf25poison-mCh
EV + wtf1poison-mCh
EV + wtf25poison-GBP-mCh
wtf1antidote-GFP + EV
wtf25antidote-GFP + EV
wtf25antidote-mEos + EV
wtf1antidote-GFP + wtf1poison-mCh
wtf1antidote-GFP + wtf25poison-mCh
wtf1antidote-GFP + wtf25poison-GBP-mCh
wtf25antidote-GFP + wtf25poison-mCh
wtf25antidote-GFP + wtf25poison-GBP-mCh
wtf25antidote-mEOs + wtf25poison-mCh
wtf25antidote-mEos + wtf25poison-GBP-mCh
B
Wtf25antidote
mEos
Wtf25poison
GBP
mCh
Interaction
Rescue
Wtf1antidote
GFP
Wtf25poison
GBP
mCh
Interaction
Rescue
D
EV+EV
25P-mCh +EV
1P-mCh+ EV
25P-GBP +EV
1A-GFP +EV
25A-GFP +EV
25A-mEos +EV
1P-mCh +1A-GFP
25P-mCh +1A-GFP
25P-GBP +1A-GFP
25P-mCh + 25A-GFP
25P-GBP +25A-GFP
25P-mCh + 25A-mEos
25P-GBP +25A-mEos
TL
mCherry
GFP /mEos
Merge
Merge +TL

S9 Figure

A

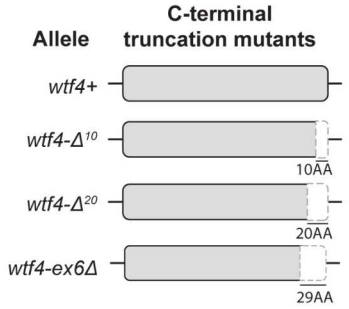

B

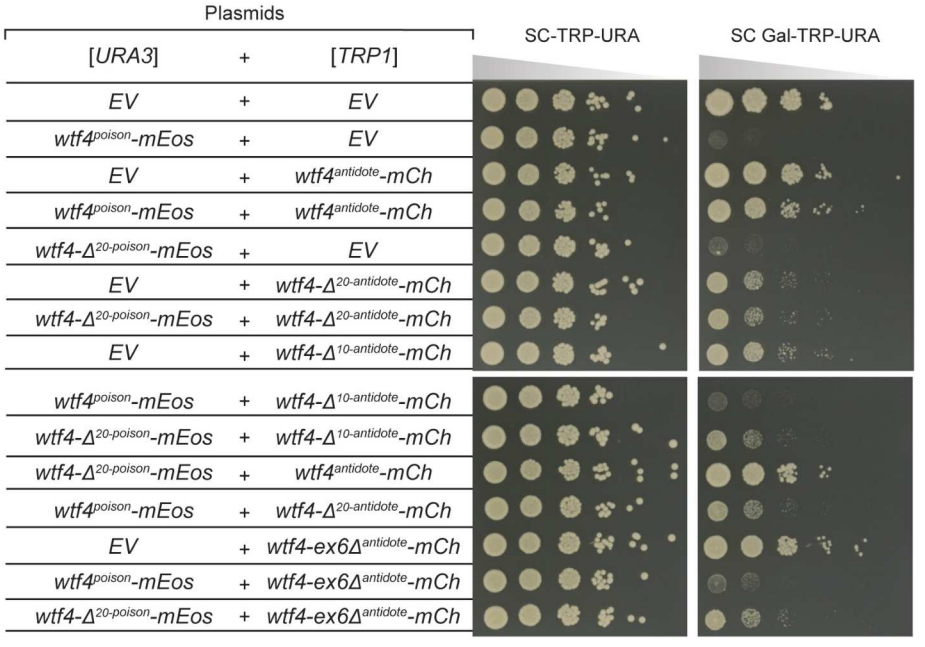

C

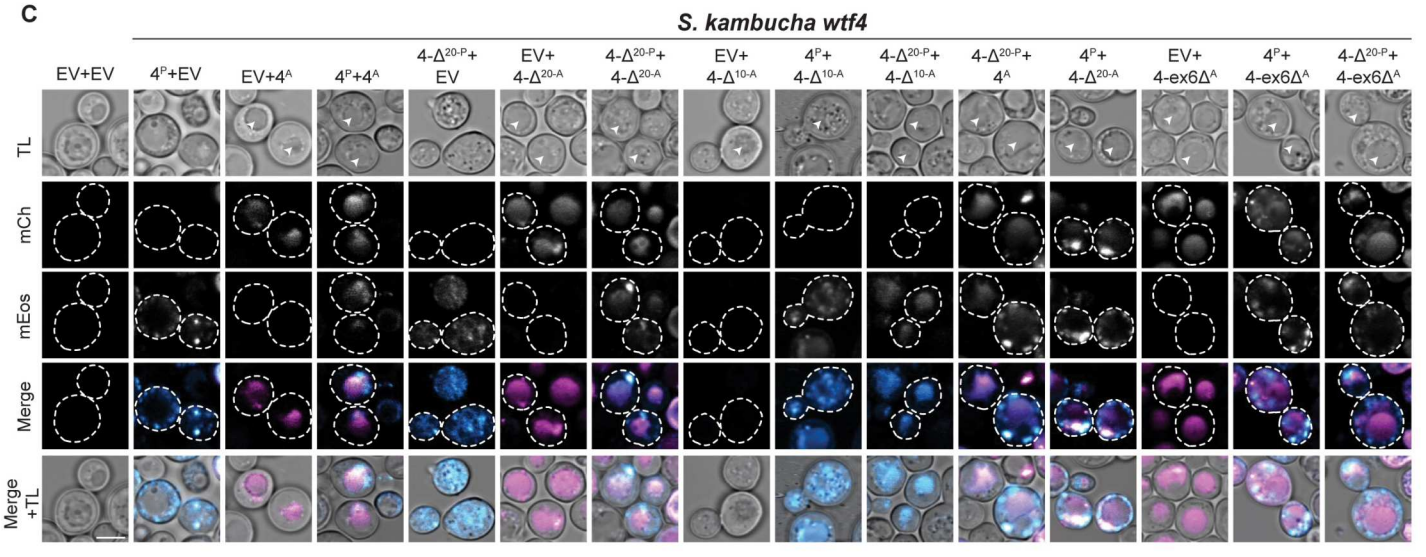

S10 Figure

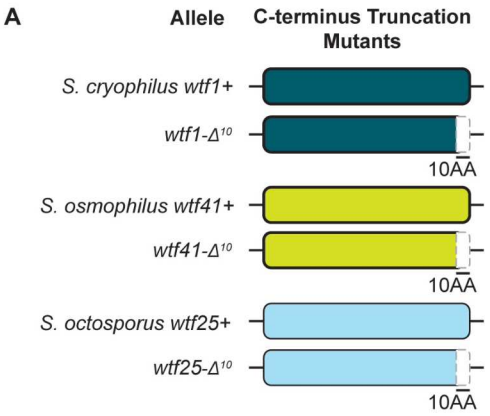
A
Allele
C-terminus Truncation Mutants
S. cryophilus wtf1+
wtf1-Δ10
10AA
S. osmophilus wtf41+
wtf41-Δ10
10AA
S. octosporus wtf25+
wtf25-Δ10
10AA

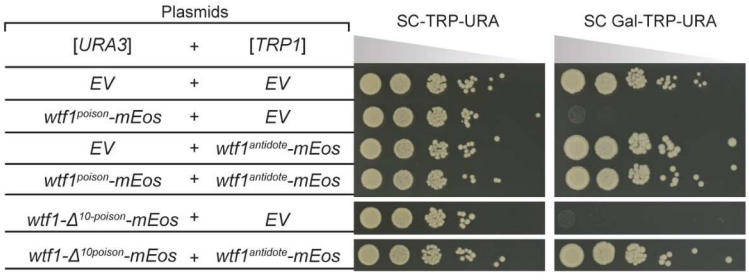
B
Plasmids
SC-TRP-URA
SC Gal-TRP-URA
[URA3] + [TRP1]
EV + EV
wtf1poison-mEos + EV
EV + wtf1antidote-mEos
wtf1poison-mEos + wtf1antidote-mEos
wtf1-Δ10-poison-mEos + EV
wtf1-Δ10poison-mEos + wtf1antidote-mEos

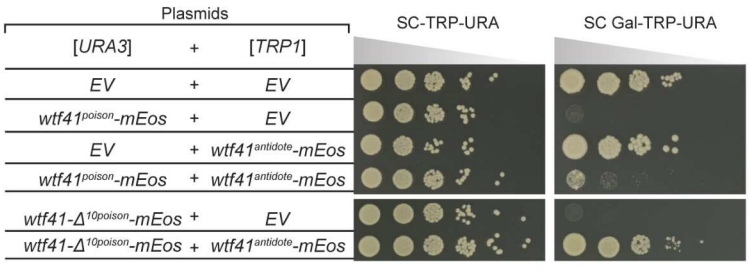
C
Plasmids
SC-TRP-URA
SC Gal-TRP-URA
[URA3] + [TRP1]
EV + EV
wtf41poison-mEos + EV
EV + wtf41antidote-mEos
wtf41poison-mEos + wtf41antidote-mEos
wtf41-Δ10poison-mEos + EV
wtf41-Δ10poison-mEos + wtf41antidote-mEos

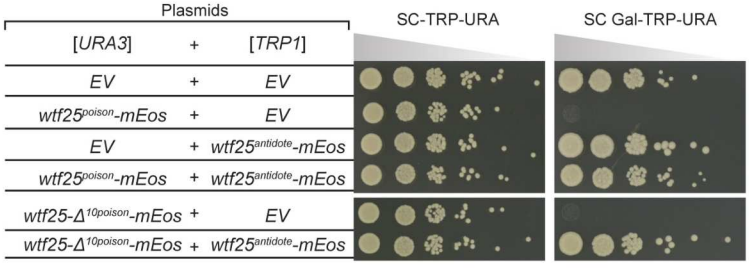
D
Plasmids
SC-TRP-URA
SC Gal-TRP-URA
[URA3] + [TRP1]
EV + EV
wtf25poison-mEos + EV
EV + wtf25antidote-mEos
wtf25poison-mEos + wtf25antidote-mEos
wtf25-Δ10poison-mEos + EV
wtf25-Δ10poison-mEos + wtf25antidote-mEos

S11 Figure

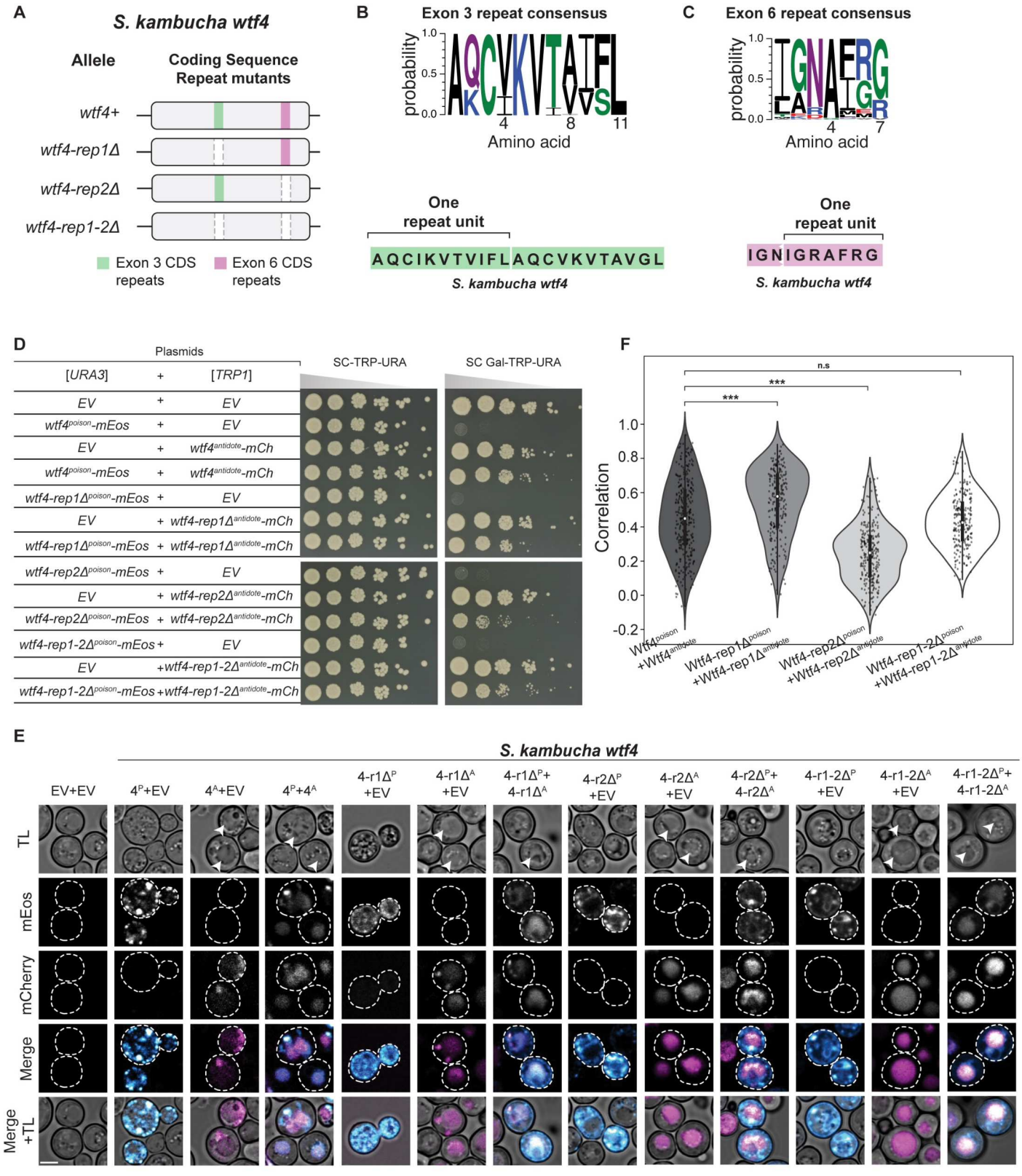
A
S. kambucha wtf4
Allele
Coding Sequence Repeat mutants
wtf4+
wtf4-rep1Δ
wtf4-rep2Δ
wtf4-rep1-2Δ
Exon 3 CDS repeats
Exon 6 CDS repeats
B
Exon 3 repeat consensus
probability
Amino acid
One repeat unit
AQCIKVTVIFLAQCVKVTAVGL
S. kambucha wtf4
C
Exon 6 repeat consensus
probability
Amino acid
One repeat unit
IGNIGRAFRG
S. kambucha wtf4
D
Plasmids
[URA3] + [TRP1]
SC-TRP-URA
SC Gal-TRP-URA
EV + EV
wtf4poison-mEos + EV
EV + wtf4antidote-mCh
wtf4poison-mEos + wtf4antidote-mCh
wtf4-rep1Δpoison-mEos + EV
EV + wtf4-rep1Δantidote-mCh
wtf4-rep1Δpoison-mEos + wtf4-rep1Δantidote-mCh
wtf4-rep2Δpoison-mEos + EV
EV + wtf4-rep2Δantidote-mCh
wtf4-rep2Δpoison-mEos + wtf4-rep2Δantidote-mCh
wtf4-rep1-2Δpoison-mEos + EV
EV + wtf4-rep1-2Δantidote-mCh
wtf4-rep1-2Δpoison-mEos + wtf4-rep1-2Δantidote-mCh
F
n.s
***
***
Correlation
Wtf4poison +Wtf4antidote
Wtf4-rep1Δpoison +Wtf4-rep1Δantidote
Wtf4-rep2Δpoison +Wtf4-rep2Δantidote
Wtf4-rep1-2Δpoison +Wtf4-rep1-2Δantidote
E
S. kambucha wtf4
EV+EV
4P+EV
4A+EV
4P+4A
4-r1ΔP +EV
4-r1ΔA +EV
4-r1ΔP+ 4-r1ΔA
4-r2ΔP +EV
4-r2ΔA +EV
4-r2ΔP+ 4-r2ΔA
4-r1-2ΔP +EV
4-r1-2ΔA +EV
4-r1-2ΔP+ 4-r1-2ΔA
TL
mEos
mCherry
Merge
Merge +TL

S12 Figure

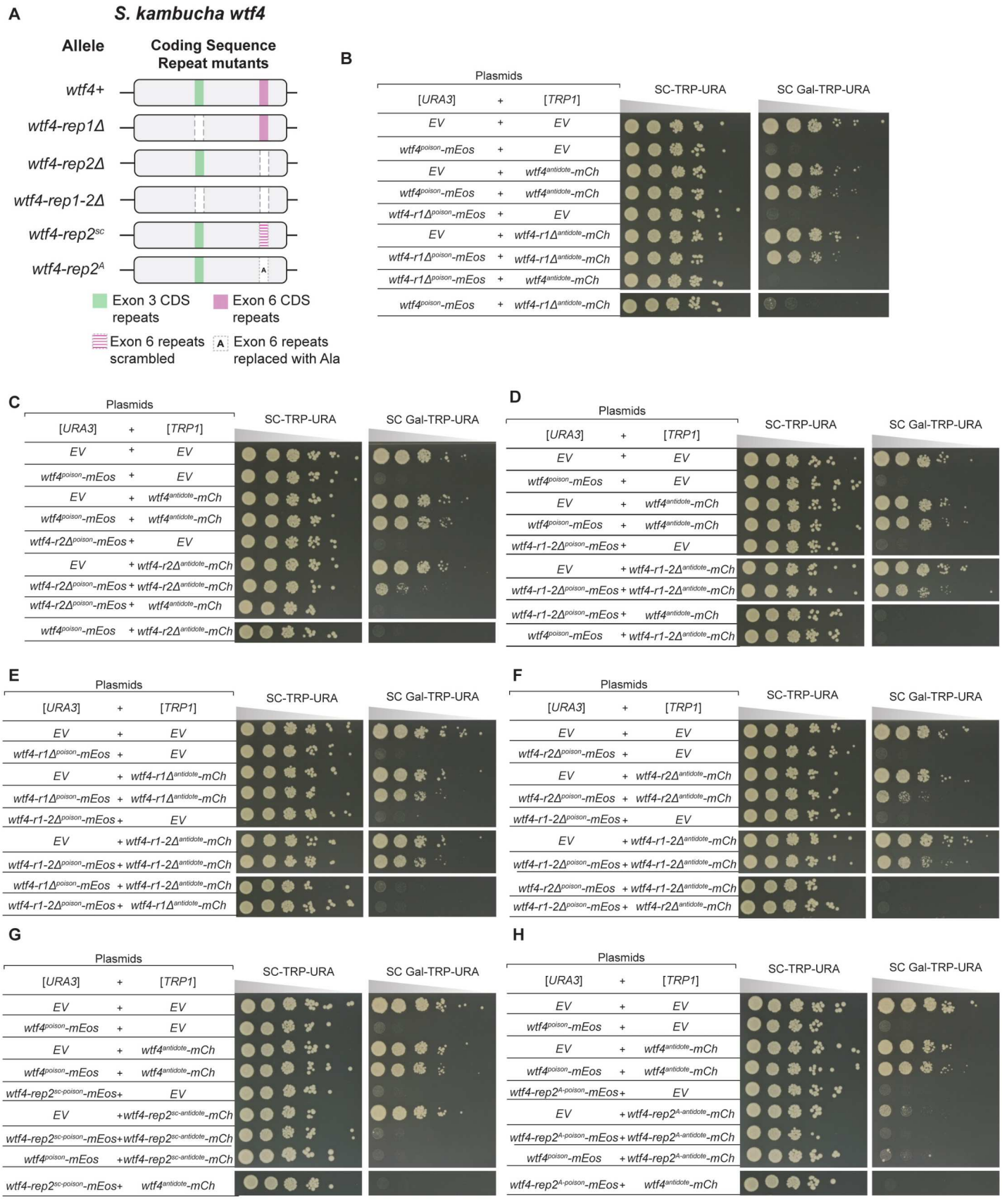
A
S. kambucha wtf4
Allele
Coding Sequence Repeat mutants
wtf4+
wtf4-rep1Δ
wtf4-rep2Δ
wtf4-rep1-2Δ
wtf4-rep2sc
wtf4-rep2A
Exon 3 CDS repeats
Exon 6 CDS repeats
Exon 6 repeats scrambled
Exon 6 repeats replaced with Ala
B
Plasmids
[URA3] + [TRP1]
SC-TRP-URA
SC Gal-TRP-URA
EV + EV
wtf4poison-mEos + EV
EV + wtf4antidote-mCh
wtf4poison-mEos + wtf4antidote-mCh
wtf4-r1Δpoison-mEos + EV
EV + wtf4-r1Δantidote-mCh
wtf4-r1Δpoison-mEos + wtf4-r1Δantidote-mCh
wtf4-r1Δpoison-mEos + wtf4antidote-mCh
wtf4poison-mEos + wtf4-r1Δantidote-mCh
C
Plasmids
[URA3] + [TRP1]
SC-TRP-URA
SC Gal-TRP-URA
EV + EV
wtf4poison-mEos + EV
EV + wtf4antidote-mCh
wtf4poison-mEos + wtf4antidote-mCh
wtf4-r2Δpoison-mEos + EV
EV + wtf4-r2Δantidote-mCh
wtf4-r2Δpoison-mEos + wtf4-r2Δantidote-mCh
wtf4-r2Δpoison-mEos + wtf4antidote-mCh
wtf4poison-mEos + wtf4-r2Δantidote-mCh
D
Plasmids
[URA3] + [TRP1]
SC-TRP-URA
SC Gal-TRP-URA
EV + EV
wtf4poison-mEos + EV
EV + wtf4antidote-mCh
wtf4poison-mEos + wtf4antidote-mCh
wtf4-r1-2Δpoison-mEos + EV
EV + wtf4-r1-2Δantidote-mCh
wtf4-r1-2Δpoison-mEos + wtf4-r1-2Δantidote-mCh
wtf4-r1-2Δpoison-mEos + wtf4antidote-mCh
wtf4poison-mEos + wtf4-r1-2Δantidote-mCh
E
Plasmids
[URA3] + [TRP1]
SC-TRP-URA
SC Gal-TRP-URA
EV + EV
wtf4-r1Δpoison-mEos + EV
EV + wtf4-r1Δantidote-mCh
wtf4-r1Δpoison-mEos + wtf4-r1Δantidote-mCh
wtf4-r1-2Δpoison-mEos + EV
EV + wtf4-r1-2Δantidote-mCh
wtf4-r1-2Δpoison-mEos + wtf4-r1-2Δantidote-mCh
wtf4-r1Δpoison-mEos + wtf4-r1-2Δantidote-mCh
wtf4-r1-2Δpoison-mEos + wtf4-r1Δantidote-mCh
F
Plasmids
[URA3] + [TRP1]
SC-TRP-URA
SC Gal-TRP-URA
EV + EV
wtf4-r2Δpoison-mEos + EV
EV + wtf4-r2Δantidote-mCh
wtf4-r2Δpoison-mEos + wtf4-r2Δantidote-mCh
wtf4-r1-2Δpoison-mEos + EV
EV + wtf4-r1-2Δantidote-mCh
wtf4-r1-2Δpoison-mEos + wtf4-r1-2Δantidote-mCh
wtf4-r2Δpoison-mEos + wtf4-r1-2Δantidote-mCh
wtf4-r1-2Δpoison-mEos + wtf4-r2Δantidote-mCh
G
Plasmids
[URA3] + [TRP1]
SC-TRP-URA
SC Gal-TRP-URA
EV + EV
wtf4poison-mEos + EV
EV + wtf4antidote-mCh
wtf4poison-mEos + wtf4antidote-mCh
wtf4-rep2sc-poison-mEos + EV
EV + wtf4-rep2sc-antidote-mCh
wtf4-rep2sc-poison-mEos + wtf4-rep2sc-antidote-mCh
wtf4poison-mEos + wtf4-rep2sc-antidote-mCh
wtf4-rep2sc-poison-mEos + wtf4antidote-mCh
H
Plasmids
[URA3] + [TRP1]
SC-TRP-URA
SC Gal-TRP-URA
EV + EV
wtf4poison-mEos + EV
EV + wtf4antidote-mCh
wtf4poison-mEos + wtf4antidote-mCh
wtf4-rep2A-poison-mEos + EV
EV + wtf4-rep2A-antidote-mCh
wtf4-rep2A-poison-mEos + wtf4-rep2A-antidote-mCh
wtf4poison-mEos + wtf4-rep2A-antidote-mCh
wtf4-rep2A-poison-mEos + wtf4antidote-mCh

S13 Figure

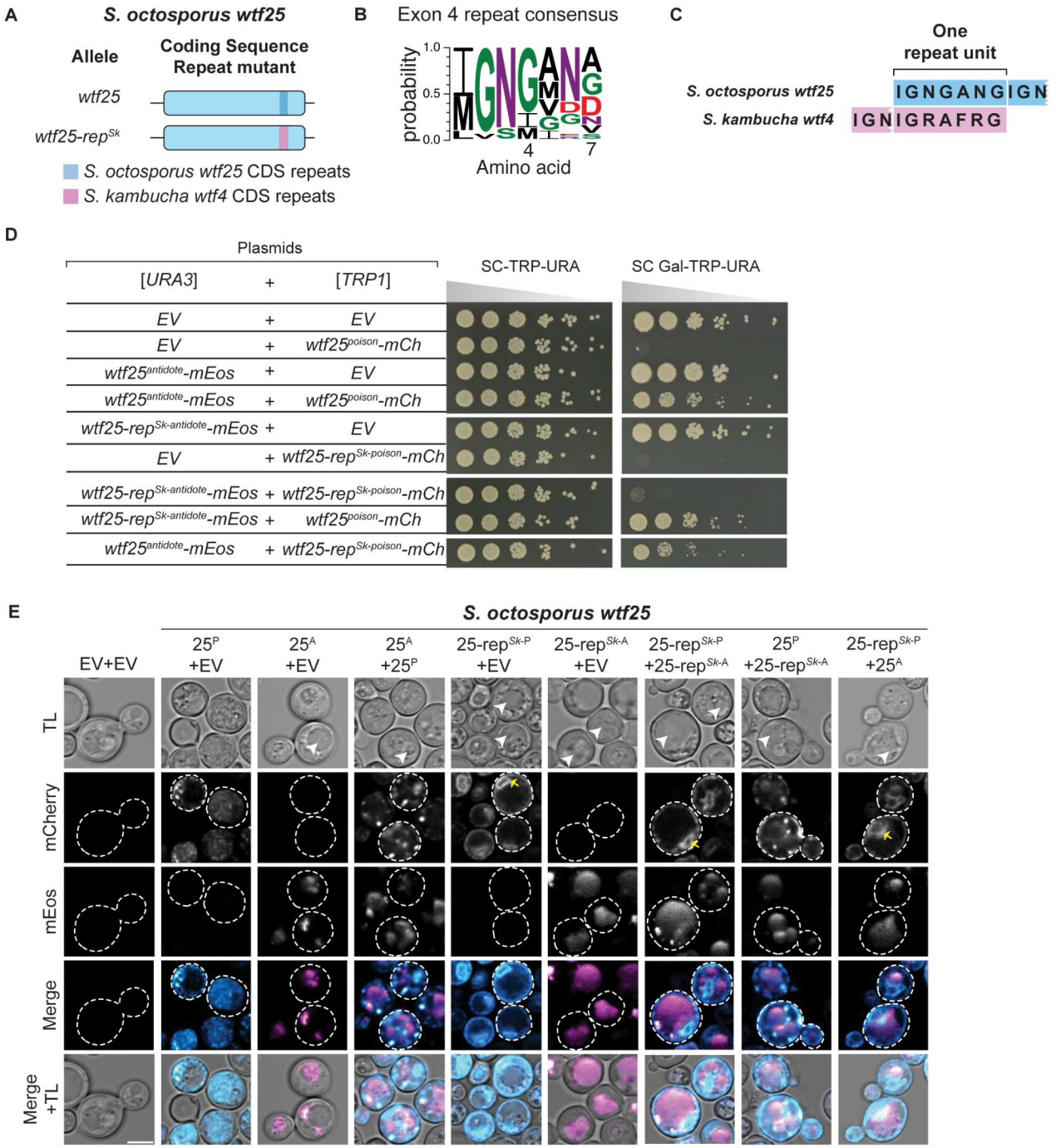
A
S. octosporus wtf25
Allele
Coding Sequence Repeat mutant
wtf25
wtf25-repSk
S. octosporus wtf25 CDS repeats
S. kambucha wtf4 CDS repeats
B
Exon 4 repeat consensus
probability
1.0
0.5
0.0
4
7
Amino acid
C
One repeat unit
S. octosporus wtf25
IGNGANGIGN
S. kambucha wtf4
IGNIGRAFRG
D
Plasmids
[URA3] + [TRP1]
SC-TRP-URA
SC Gal-TRP-URA
EV + EV
EV + wtf25poison-mCh
wtf25antidote-mEos + EV
wtf25antidote-mEos + wtf25poison-mCh
wtf25-repSk-antidote-mEos + EV
EV + wtf25-repSk-poison-mCh
wtf25-repSk-antidote-mEos + wtf25-repSk-poison-mCh
wtf25-repSk-antidote-mEos + wtf25poison-mCh
wtf25antidote-mEos + wtf25-repSk-poison-mCh
E
S. octosporus wtf25
EV+EV
25P +EV
25A +EV
25A +25P
25-repSk-P +EV
25-repSk-A +EV
25-repSk-P +25-repSk-A
25P +25-repSk-A
25-repSk-P +25A
TL
mCherry
mEos
Merge
Merge +TL

S14 Figure

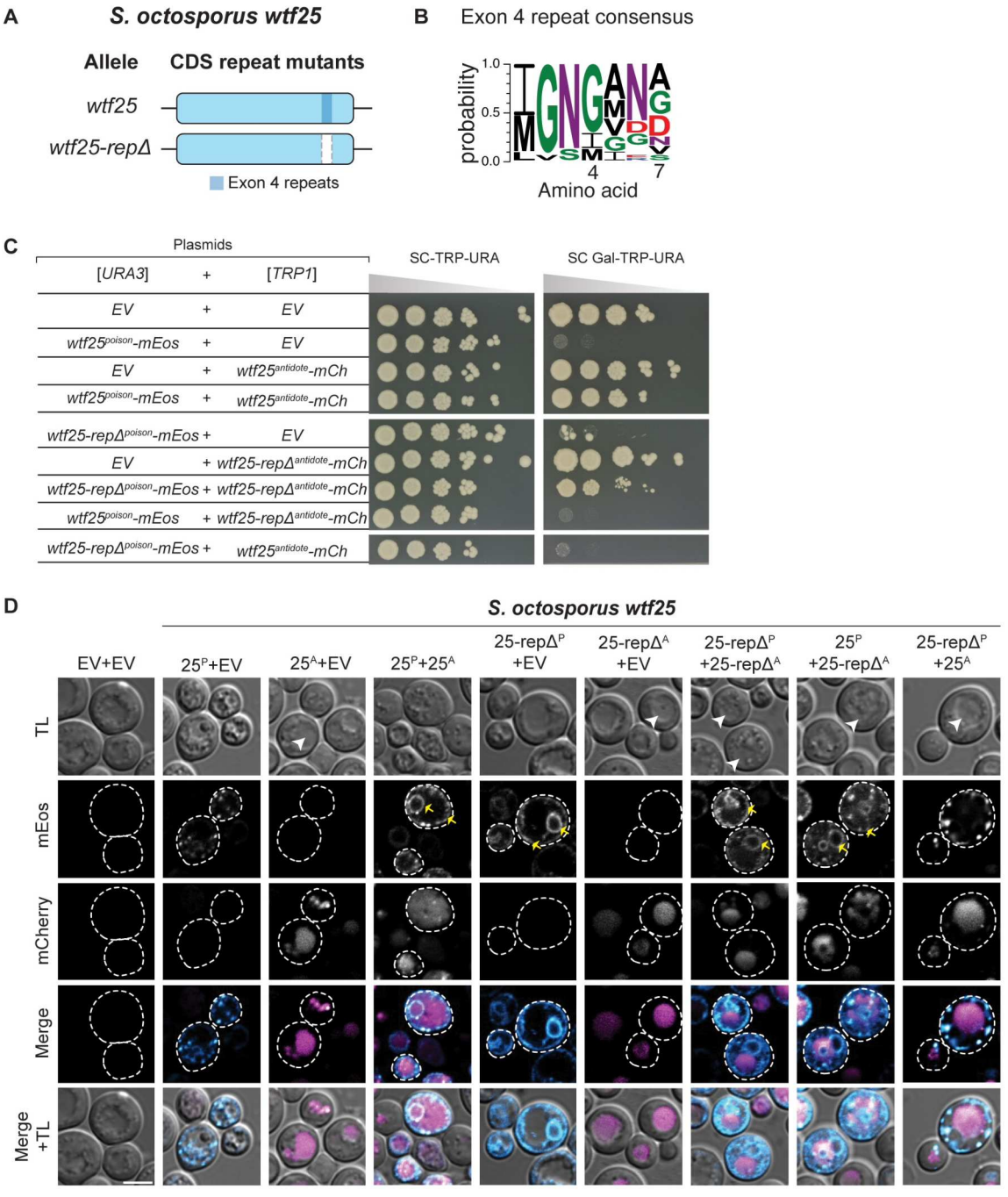
A
S. octosporus wtf25
Allele
CDS repeat mutants
wtf25
wtf25-repΔ
Exon 4 repeats
B
Exon 4 repeat consensus
probability
1.0
0.5
0.0
4
7
Amino acid
C
Plasmids
[URA3] + [TRP1]
SC-TRP-URA
SC Gal-TRP-URA
EV + EV
wtf25poison-mEos + EV
EV + wtf25antidote-mCh
wtf25poison-mEos + wtf25antidote-mCh
wtf25-repΔpoison-mEos + EV
EV + wtf25-repΔantidote-mCh
wtf25-repΔpoison-mEos + wtf25-repΔantidote-mCh
wtf25poison-mEos + wtf25-repΔantidote-mCh
wtf25-repΔpoison-mEos + wtf25antidote-mCh
D
S. octosporus wtf25
EV+EV
25P+EV
25A+EV
25P+25A
25-repΔP +EV
25-repΔA +EV
25-repΔP +25-repΔA
25P +25-repΔA
25-repΔP +25A
TL
mEos
mCherry
Merge
Merge +TL